5-16-2008

Synthesis and Characterization of Novel Nanoparticles for Use as Photocatalytic Probes and Radiotracers

Anindya Pradhan
University of New Orleans

Synthesis and Characterization of Novel Nanoparticles for Use as Photocatalytic Probes and Radiotracers

A Dissertation

Submitted to the Graduate Faculty of the
University of New Orleans
in partial fulfillment of the
requirements for the degree of

Doctor of Philosophy
in
Chemistry

by

Anindya Pradhan

M.B.A. Viswabharati University (India), 2001
M.S. University of New Orleans, 2006

May, 2008

DEDICATION

Dedicated to my parents, family and Ms. Rajni Ekta Soharu who all have been my inspirations and motivating factor in my life.

ACKNOWLEDGEMENT

Many people have inspired, guided, and helped me, in the course of my PhD at University of New Orleans and I would like to thank them all for a great graduate school experience. First and foremost I would like to thank my advisor, Dr. Matthew A. Tarr, for his perceptive supervision as my advisor throughout the duration of my research and while I was writing the dissertation. I also want to thank him for his help, support, advice, and freedom that he gave me, to pursue all directions and interests in different research areas. Without his insightful guidance, many of the results presented here would not have been possible.

I would also like to thank Dr. Richard B. Cole, Dr. John B. Wiley and Dr. Pierre F. P. Poudeu for being a part of my committee and for giving me their precious time, valuable suggestions and undivided support.

I must acknowledge as well the many friends and colleagues, who assisted and supported me, during my research and studies over the years. My special thanks go to my friends Weixi Zheng, Sandra Lochhead, Sourav Chakraborty, Chanel Fortier, Curt Jarand and specially Brittany Oliva. Furthermore I am deeply indebted to Rajni Ekta Soharu, Assistant Registrar of Technology at UNO for her help and express my deepest gratitude for her continued support throughout.

My family has been a motivating factor to me. Their love, support and confidence in me has given me strength to go on, even in the hardest and the toughest situations. In recognition of all

their efforts, I would like to dedicate this thesis to my family who always had faith in me and gave me their love and support.

TABLE OF CONTENTS

List of Figures xi

List of Tables xvi

Abstract xvii

1. Introduction 1

1.1 General Perspective 1

1.2 Nanoparticles 1

1.3 Nanotechnology 2

1.4 Synthesis of Nanoparticles 3

1.4.1 Gas Phase Synthesis 3

1.4.2 Sol Gel Processing 3

1.4.3 Sonochemical Synthesis 3

1.4.4 Cavitation Processing 4

1.4.5 Micoemulsion Processing 4

1.4.6 High Energy Ball Milling 4

1.5 Characterization of Nanoparticles 5

1.5.1 Transmission Electron Microscope 6

1.5.2 Inductively Coupled Plasma 8

1.5.3 Energy Dispersive Spectra 10

1.5.4 X-ray Diffraction Spectrometer 12

1.6 References 14

2 Applications of Nanoparticles and Previous Research 19

2.1 Medicine 19

2.2 Drug Delivery 19
2.3 Tissue Engineering 20
2.4 Diagnostics 20
2.5 Chemistry and Environment 21
2.6 Catalysis 21
2.7 Filtration 21
2.8 Energy 22
2.9 Reduction of Energy Consumption 22
2.10 Increase the Efficiency of Energy Production 23
2.11 The Use of More Environment Friendly Energy System 23
2.12 Recycling of Batteries 24
2.13 Information and Communication 24
2.14 Novel Optoelectronic Devices 24
2.15 Displays 25
2.16 Consumer Goods 25
2.17 Previous Research on Magnetic Nanoparticles 27
2.18 References 31
3 Synthesis and Characterization of Gold-Magnetite Nanoparticles 38
3.1 Abstract 38
3.2 Introduction 39
3.3 Experimental Procedure 44
3.4 Experimental Procedure of Sonochemical Synthesis 45
3.5 Results and Discussion 47

3.5.1 Separation Process 47
3.5.2 TEM Images 48
3.5.3 EDS Data 51
3.5.4 Magnetic Measurements 52
3.5.5 Absorbance Data 58
3.6 Experimental Procedure for UV Radiation Synthesis 59
3.6.1 Time Based Experiment 59
3.6.2 Concentration Based Experiment 59
3.7 Results and Discussion 61
3.7.1 TEM Images 61
3.7.2 EDS Spectra 65
3.8 Conclusion 67
3.9 References 68
4 Synthesis and Characterization of Gold-Titania-Magnetite Nanoparticles 70
4.1 Abstract 70
4.2 Introduction 71
4.3 Experimental Procedure 74
4.4 Results and Discussions 76
4.4.1 TEM Images 76
4.4.2 EDS Spectra 79
4.4.3 Absorbance Data 80
4.4.4 Magnetic Measurements 82
4.4.5 XRD Data 84

4.5 Conclusion 85
4.6 References 87
5 Photocatalytic Activity of Nanoparticles 90
5.1 Abstract 90
5.2 Introduction 91
5.3 Experimental Procedure 94
5.3.1 Degradation Study of Bisphenol A 94
5.3.2 Reuse of the Photocatalytic Au@TiO_2@Fe_3O_4 Particles 95
5.4 Results and Discussion 96
5.5 Conclusion 101
5.6 References 102
6 Synthesis of Indium Doped Magnetite Nanoparticles for Radiotracer Studies 104
6.1 Abstract 104
6.2 Introduction 105
6.3 Chemicals and Instruments Used 107
6.4 Experimental Procedure 108
6.5 Results and Discussion 110
6.5.1 TEM Images 110
6.5.2 EDS Data 114
6.5.3 Indium Loading in Particles 116
6.5.4 XRD Data 117
6.5.5 Magnetic Measurements 120
6.5.5.1 Hysterisis Loop 120

6.5.5.2 ZFC-FC Graph 124
6.6 Conclusions 127
6.7 References.....128
7 Vita.....133

LIST OF FIGURES

Figure 1.1. Schematic of Transmission Electron Microscope 6

Figure 1.2. Schematic of Inductively Coupled Plasma 8

Figure 1.3. Schematic of Energy Dispersive Spectra.....10

Figure 1.4. Schematic of XRD Instrument 12

Figure 3.1. Schematic of Sonochemical Process 42

Figure 3.2. Gold magnetite nanocomposite materials suspended in ethanol prior to (a) and after (b) magnetic separation.....47

Figure 3.3. TEM image of gold-magnetite nanocomposite material formed by sonication of magnetite in aqueous $HAuCl_4$ with added methanol.....48

Figure 3.4. TEM image of gold-magnetite nanocomposite formed with diethylene glycol additive 49

Figure 3.5. TEM image of gold-magnetite nanocomposite formed with oleic acid additive.....49

Figure 3.6. EDS spectrum of composite particles depicted in Figure 3.3.....51

Figure 3.7. EDS Spectra for Au-magnetite nanocomposites in DEG 51

Figure 3.8. Magnetization vs. temperature for magnetite nanoparticles (a) and gold-magnetite nanocomposite material (MeOH) (b) 52

Figure 3.9. Magnetization vs. temperature for gold magnetite nanocomposite material with DEG in 100 Oe 53

Figure 3.10. Magnetization vs. temperature for gold magnetite nanocomposite material with Oleic Acid in 100 Oe Field. 54

Figure 3.11. Hysteresis loops for untreated magnetite (a) and gold-magnetite nanocomposite material (b).....55

Figure 3.12. Hysteresis loop for gold-magnetite nanocomposite material in DEG at 5K 56

Figure 3.13. Hysteresis loop for gold-magnetite nanocomposite material in Oleic Acid.....56

Figure 3.14. The absorbance spectra of the different types of gold magnetite nanocomposites suspended in ethanol 58

Figure 3.15. TEM image of gold-magnetite nanoparticles irradiated with UV light for 60 min in 0.05 mM $HAuCl_4$.....61

Figure 3.16. TEM image of gold-magnetite nanoparticles irradiated with UV light for 60 min in 0.1 mM $HAuCl_4$.....62

Figure 3.17. TEM image of gold-magnetite nanoparticles irradiated with UV light for 60 min in 0.2 mM $HAuCl_4$.....62

Figure 3.18. TEM image of gold-magnetite nanoparticles irradiated with UV light for 30 min in 0.1 mM $HAuCl_4$.....63

Figure 3.19. TEM image of gold-magnetite nanoparticles irradiated with UV light for 45 min in 0.1 mM $HAuCl_4$.....63

Figure 3.20. TEM image of gold-magnetite nanoparticles irradiated with UV light for 60 min in 0.1 mM $HAuCl_4$.....64

Figure 3.21. EDS spectrum of nanoparticles depicted in Figure 3.16 65

Figure 3.22 EDS spectrum of nanoparticles depicted in Figure 3.20 66

Figure 4.1. TEM image of Fe_3O_4–TiO_2–Au nanocomposite formed by irradiating Fe_3O_4–TiO_2 suspended in 0.1 mM $HAuCl_4$ (aq with 2% EtOH); irradiated with 254 nm lamps for 30 min. 77

Figure 4.2. TEM image of Fe_3O_4–TiO_2–Au nanocomposite formed by irradiating Fe_3O_4–TiO_2 suspended in 0.5 mM $HAuCl_4$ (aq with 2% EtOH); irradiated with 254 nm lamps for 45 min.....78

Figure 4.3. EDS spectrum from particles in Fig. 4.1. 79

Figure 4.4. Absorbance spectra of particles made with varying concentrations of $HAuCl_4$ as indicated on the graph. Fe_3O_4–TiO_2–Au formed by irradiating Fe_3O_4–TiO_2 suspended in aqueous $HAuCl_4$ with 2% EtOH; irradiated with 254 nm lamps for 45 min.....80

Figure 4.5 Wavelength of maximum absorbance versus [$HAuCl_4$] used in preparation of particles.....81

Figure 4.6. Fe_3O_4–TiO_2–Au nanocomposite magnetic properties: (a) hysteresis loop at 5 K and (b) ZFC/FC curves at an applied field strength.....82

Figure 4.7. XRD data for Fe_3O_4–TiO_2–Au nanocomposite pictured in Fig. 4.1: (*) Fe_3O_4 and (+) Au.....84

Figure 5.1. Degradation of 0.05 mM Bisphenol A solution for different amounts of time in 254 nm lamps.....96

Figure 5.2. Degradation of 0.05 mM Bisphenol A solution for different amounts of time in 300 nm lamps.....97

Figure 5.3. Degradation of 0.05 mM Bisphenol A solution for different amounts of time in 350 nm lamps.....98

Figure 5.2. Different amounts of Fe_3O_4@TiO_2@Au nanoparticles used to degrade of 0.05 mM Bisphenol A solution for 30 min.....99

Figure 5.3. Separate Bisphenol A samples were degraded for 30 min using 100mL of Fe_3O_4@TiO_2@Au nanoparticles with magnetic separation between exposures.....100

Figure 6.1. TEM image of 2% indium doped magnetite nanoparticles after magnetic separation and washing.....110

Figure 6.2. TEM image of 5% indium doped magnetite nanoparticles after magnetic separation and washing.....111

Figure 6.3. TEM image of 10% indium doped magnetite nanoparticles after magnetic separation and washing.....111

Figure 6.4. TEM image of 15% indium doped magnetite nanoparticles after magnetic separation and washing.....112

Figure 6.5. TEM image of 50% indium doped magnetite nanoparticles after magnetic separation and washing.....112

Figure 6.6. EDS pattern for water dispersible indium doped magnetite nanoparticles (5 mol % [A] and 15 mol % [B]).....114

Figure 6.7. X-ray powder diffraction pattern for water dispersible indium doped (2 mol % [A] & 5 mol % [B]) magnetite nanoparticles.....117

Figure 6.8. X-ray powder diffraction pattern for water dispersible indium doped (10 mol % [A] and 15 mol % [B]) magnetite nanoparticles.....118

Figure 6.9. SQUID measurements for 5% Indium doped magnetite particles. Magnetic moment vs Field at 5 K (FIGURE A) and 300 K (FIGURE B).....120

Figure 6.10. SQUID measurements for 10% Indium doped magnetite particles. Magnetic moment vs Field at 5 K (FIGURE A) and 300 K (FIGURE B).....121

Figure 6.11. SQUID measurements for 15% Indium doped magnetite particles. Magnetic moment vs Field at 5 K (FIGURE A) and 300 K (FIGURE B).....122

Figure 6.12. Zero Field Cooled – Field Cooled graph for 5% Indium doped magnetite particles 124

Figure 6.12. Zero Field Cooled – Field Cooled graph for 10% Indium doped magnetite particles 124

Figure 6.12. Zero Field Cooled – Field Cooled graph for 15% Indium doped magnetite particles 124

LIST OF TABLES

Table 3.1. The ratios of the Au and Fe in the samples with MeOH, DEG and Oleic acid. Data obtained from the ICP.....50

Table 6.1. Different amounts of $FeCl_3.6H_2O$ and $InCl_3.4H_2O$ used for different reactions.....109

Table 6.2. Indium loading of the magnetic nanoparticles.....116

Table 6.3. Coercivity change for 5%, 10% and 15% Indium magnetite particles.....123

ABSTRACT

Two novel synthetic routes to formation of gold-magnetite nanoparticles have been designed. Treatment of preformed magnetite nanoparticles with ultrasound in aqueous media with dissolved tetrachloroauric acid resulted in the formation of gold-magnetite nanocomposite materials. The other route involved irradiation of preformed magnetite nanoparticles by UV light in aqueous media with dissolved tetrachloroauric acid. This method resulted in the formation of gold-magnetite nanocomposite materials. These materials maintained the morphology of the original magnetite particles. The morphology of the gold particles could be controlled by adjusting experimental parameters, like addition of small amounts of solvent modifiers such as methanol, diethylene glycol, and oleic acid as well as variation of the concentration of the tetrachloroauric acid solution and time of the reaction. The nanocomposite materials were magnetic and exhibited optical properties similar to gold nanoparticles.

Since we were not able to directly synthesize core shell gold magnetite nanoparticles, TiO_2 was used as a bridging material. TiO_2 nanoparticles with embedded magnetite were suspended in aqueous $HAuCl_4$ and irradiated with ultraviolet light to photodeposit gold. The degree of gold coating and the wavelength of absorbance could be controlled by adjusting concentration of $HAuCl_4$. Absorbance maxima were between 540-590 nm. Particles exhibited superparamagnetic properties (blocking temperature ~170 K) whether or not coated with gold. These particles have potential applications as drug delivery agents, magnetic imaging contrast agents, and magnetically separatable photocatalysts with unique surface properties.

Another goal was to synthesize and characterize indium doped magnetite nanoparticles for application as radiotracers for *in vivo* fate studies. The labeled particles will be useful for determination of pharmacological behavior in biological systems. Indium doped magnetite particles with varying size and surface chemistry were synthesized with wet chemical techniques. The synthesized nanoparticles were characterized in terms of the size and shape with the help of TEM, the elemental composition by ICP and EDS, the crystal structure by XRD and magnetic properties by SQUID measurements. It was found that the indium loading could be controlled even though the magnetic properties were similar to undoped magnetite.

Keywords: magnetite nanoparticles, gold magnetite nanocomposites, TiO_2 nanoparticles, indium magnetite nanocomposites, radiotracers

Chapter 1. Introduction

1.1 General Perspective

Scientists around the world are storming the nanoscience and nanotechnology field. Researchers aim to revolutionize the world in which we live with radical breakthroughs in areas such as materials and manufacturing, electronics,[1-3] medicine and healthcare[4], biotechnology[4-6], agriculture and environment,[7,8] computation and information technology as well as chemical[9-12] and pharmaceutical areas.[13-17] Nanotechnology is combining all areas of science and technology.

1.2 Nanoparticles

The question still remains, what are nanoparticles? There is no particular definition for nanoparticles. The internationally accepted definition is that any particle which has at least one dimension less than 100nm is called a nanoparticle. Nano actually comes from the Greek word "nanos" which means dwarf or extremely small in size. It can be used as a prefix for any unit to mean a billionth of that unit.

Nanoparticles are larger than individual atoms and molecules but are smaller than the bulk material. Since there is a size variation they do not obey the absolute quantum chemistry nor the laws of classical physics and have properties that are very different from that of the bulk material. This makes the size of the particles or the scale of its features the most important attribute of nanoparticles.

Ever since it was recognized that the particles on the nanoscale have very different and interesting properties,[18-22] scientists have been looking at how they may be applied for their own

purposes. There is no strict dividing line between nanoparticles and non-nanoparticles. The size at which materials display different properties to the bulk material and are less than hundred nanometers are generally defined as nanoparticles.

1.3 Nanotechnology

Nanotechnology refers broadly to a field of applied science and technology whose unifying theme is the control of matter on the molecular level on scales smaller than 1 µm and the fabrication of devices within that size range. Nanotechnology can be viewed as a combination of the existing sciences into the nanoscale science. It is a new field of study, and the fate of nanoparticles[23-25] in biological and environmental systems is in general still unknown. There are several approaches for manufacturing nanoparticles,[26-28] but two main approaches are generally dominant. One is the bottom up approach in which the materials are built from their atomic or molecular counterparts which assemble themselves chemically and physically by the principles of particular molecular recognition. The other approach is the top-down one where the nanoparticles are constructed from larger entities without atomic level control. Examples of nanotechnology in the modern day world are designing of computer chip layouts based on surface science as well as manufacturing of biosensors and drug delivery devices. Nowadays nanoparticles are being used in real commercial applications such as suntan lotion, cosmetics, protective coatings and stain resistant clothes.

1.4 Synthesis of Nanoparticles

Nanoparticles are synthesized in various methods like gas phase[29-31] and sol-gel processing[32-36], sonochemical synthesis,[37-39] cavitation processing, microemulsion processing[40-42] and high-energy ball milling.

The characteristics of different synthesis are as follows:

1.4.1 Gas phase synthesis

- Consistent crystal structures
- Diameters ranging from 1 – 10 nm
- Nucleation and growth
- Use of inert gas atmosphere

1.4.2 Sol-gel processing

- High degree of monodispersity
- Surface modification
- Consistent particle shape
- Can be manipulated by dopant, surfactant, and capping agents

1.4.3 Sonochemical synthesis

- Generates transient localized hot zone
- High gradient of temperature and pressure
- Formation of hydroxyl radical and hydrogen atom
- Sonochemical precursor
- Can be used for large quantity manufacturing

1.4.4 Cavitation processing

- Creation and generation of gas bubbles
- Supercritical drying chamber
- Nucleation, growth and quenching of nanoparticles
- Particle size controlled by pressure and retention time

1.4.5 Microemulsion Processing

- Synthesis of metallic, silica, semiconductor and magnetic nanoparticles
- Use of surfactants to control size
- No need for significant mechanical agitation
- Large scale production
- Simple and inexpensive hardware

1.4.6 High energy ball milling

- Used as a commercial technique
- Large particle to smaller versions
- Generation of magnetic nanoparticles
- Contamination problem
- Low surface areas
- Highly polydisperse size distribution

1.5. Characterization of Nanoparticles

Nanoparticles are generally characterized by the following techniques:

- Transmission Electron Microscope (TEM)
- Aerosol Mass Spectroscopy (Aerosol MS)
- Laser Light Diffraction or Static Light Scattering
- Light Microscopy or Optical Imaging
- Condensation Nucleus Counter (CNC)
- Microelectrophoresis
- Differential Mobility Analysis (DMA)
- Scanning Electron Microscopy (SEM)
- Electrical Zone Sensing (Coulter Counting)
- Sieving
- Gas Adsorption Surface Area Analysis (e.g. BET)
- X-ray Diffraction (XRD)
- Dynamic Light Scattering (DLS)
- Inductively Coupled Plasma (ICP)
- Superconducting Quantum Interference Device (SQUID) Magnetometry

There are several other techniques but the above mentioned ones are the most common. Scientists use a combination of the listed methods to characterize and illustrate the physical and chemical properties of the nanoparticles. Some of the techniques are qualitative and some are quantitative but a combination of these techniques can always give a clear picture of the shape, size and morphology of the nanomaterials. Some of the techniques that have been used in the research are described below.

Transmission Electron Microscope (TEM)

Transmission electron microscopy (TEM) is an imaging technique whereby a filament (Tungsten or LaB6) is heated to produce a beam of electrons. The voltages generally range from 100 to 200kV. The sample that is being observed is held in a high-vacuum object chamber that can be reached from outside through an inside chamber[43,44]. The electron beam is focused with the help

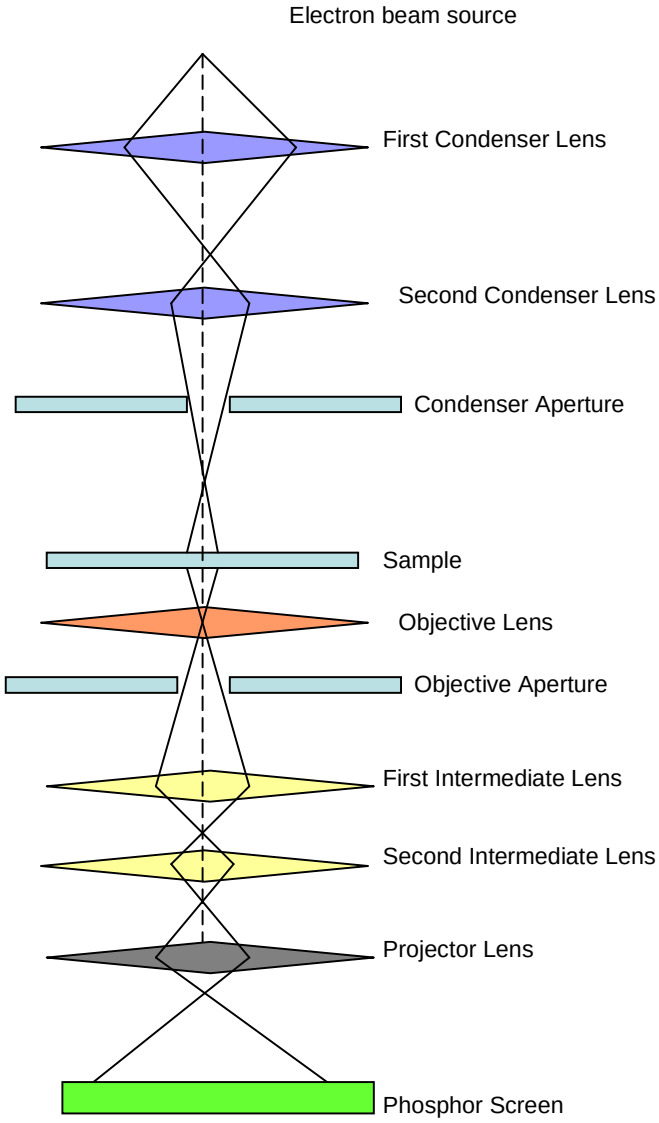

Fig 1.1. Schematic of Transmission Electron Microscope

of the first and second condenser lenses which are user selectable and allowed to focus on the sample. Most of the times the sample has to be thin enough so that the electrons can pass through them to form the image[44,47]. The electrons interact with the sample and only those that go past unobstructed hit the phosphor screen at the end. The image is then imposed on a photographic film or detected by a sensor such as a CCD camera[44].

The darker areas of an image represent those areas of the sample that fewer electrons were transmitted through (they are thicker or denser). The lighter areas of the image represent those areas of the sample that more electrons were transmitted through (they are thinner or less dense). The advantages of TEM are small sample loading, less preparation time and moreover the ability to see nanometer range particles.

Inductively Coupled Plasma (ICP)

Inductively coupled plasma (ICP) is a type of emission spectroscopy that uses a plasma to produce excited atoms that emit electromagnetic radiation at a wavelength characteristic of a particular element.[44,45] The intensity of this emission is indicative of the concentration of the element within the sample. This is a technique that is used primarily for the determination of trace concentrations of metals.

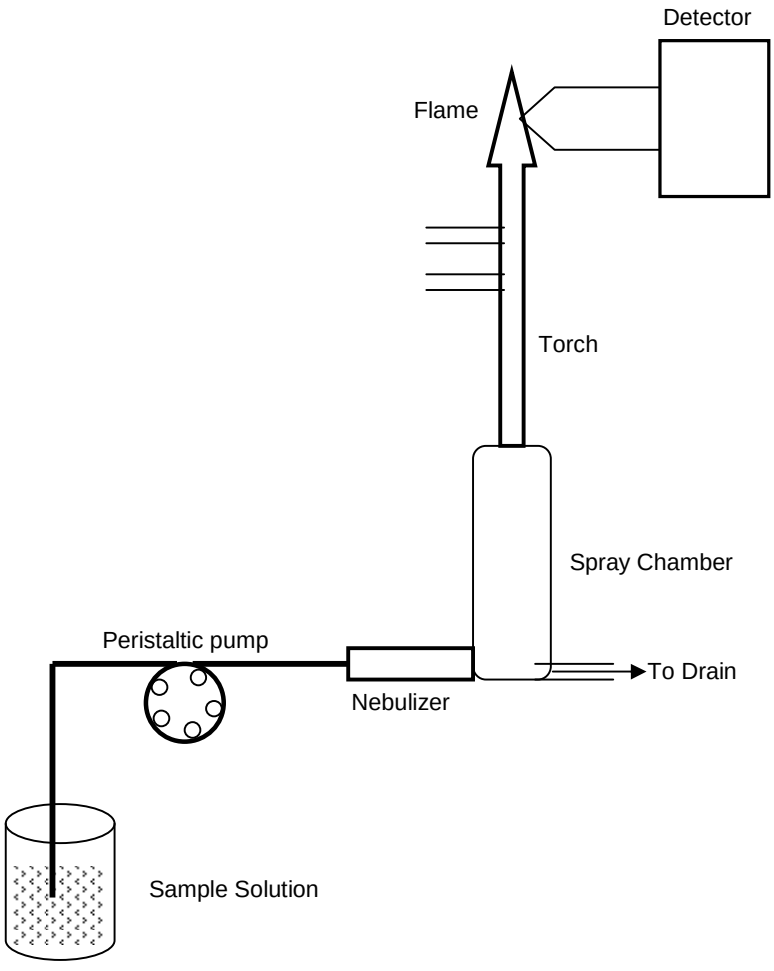

Fig 1.2. Schematic of Inductively coupled plasma

The fluid sample is pumped into the nebulizer via the peristaltic pump. The nebulizer generates an aerosol mist and injects humidified Ar gas into the chamber along with the sample. This mist accumulates in the spray chamber, where the largest portion settles out as waste and the finest particles are subsequently swept into the torch assembly.[45-47] Approximately 1% of the total solution eventually enters the torch as a mist, whereas the remainder is pumped away as waste. The fine aerosol mist containing Ar gas and sample is injected vertically up the length of the torch assembly into the plasma. The plasma, which is as hot as 10,000 K[45-46], excites the electrons. The electrons emitted are particular to the sample's elemental composition. Light emitted from the plasma is focused into the spectrometer. The detector (photomultiplier tube) is fixed in space at the far end of the spectrometer.

The largest advantage of employing an ICP when performing quantitative analysis is the fact that multielemental analysis can be accomplished, and quite rapidly. Another advantage is the detection limit which in general is really low for almost all the elements.

Energy Dispersive Spectra

Interaction of an electron beam with a sample target produces a variety of emissions, including x-rays. An energy-dispersive (EDS) detector is used to separate the characteristic x-rays of different elements into an energy spectrum, and EDS system software is used to analyze the energy spectrum in order to determine the abundance of specific elements. EDS can be used to find the chemical composition of materials. EDS capabilities provide fundamental compositional information for a wide variety of materials[46, 48].

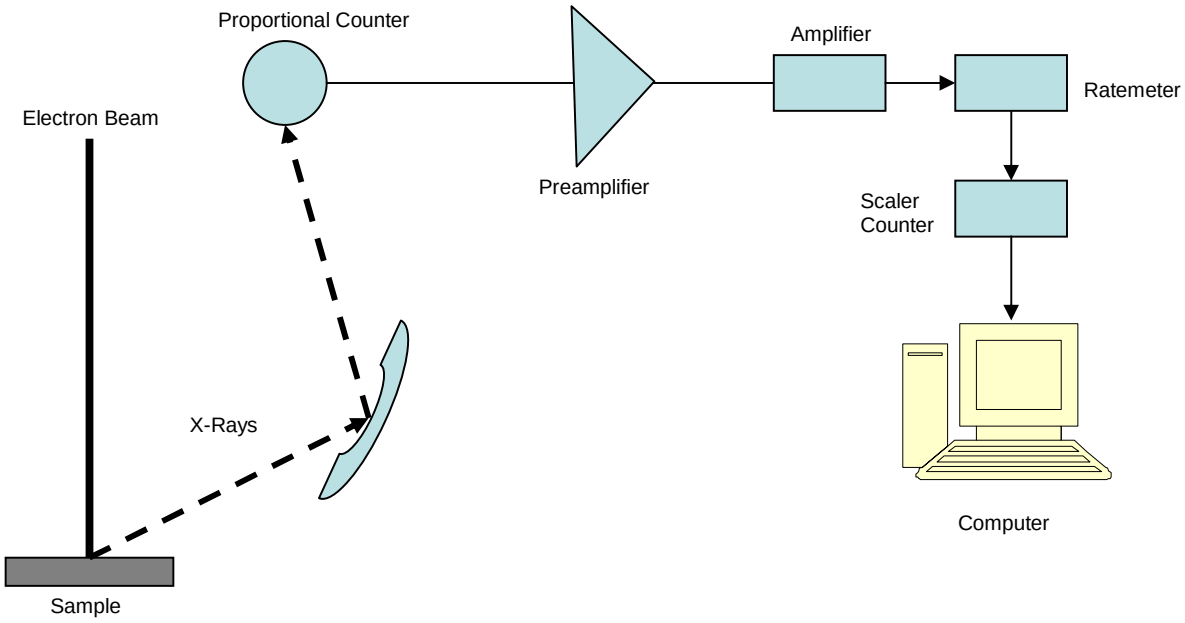

Fig 1.3. Schematic of Energy Dispersive Spectra instrument

EDS systems are typically integrated with either a scanning electron microscope or transmission electron microscope instruments. EDS systems include a sensitive x-ray detector, a liquid nitrogen chamber for cooling, and software to collect and analyze energy spectra. The detector is mounted in the sample chamber of the main instrument. An EDS detector contains a crystal that absorbs the energy of incoming x-rays by ionization, yielding free electrons in the

crystal that become conductive and produce an electrical charge bias. The x-ray absorption thus converts the energy of individual x-rays into electrical voltages of proportional size; the electrical pulses correspond to the characteristic x-rays of the element.[46, 48, 50]

The advantages of EDS Spectra are a user can acquire a full elemental spectrum in only a few seconds. Supporting software makes it possible to readily identify peaks, which makes EDS a great survey tool to quickly identify unknown phases prior to quantitative analysis.

X-ray Diffraction Spectrometer

X-ray Diffraction (XRD) is a powerful non-destructive technique for characterizing crystalline materials. It provides information on structures, phases, preferred crystal orientations and other structural parameters such as average grain size, crystallinity and crystal defects. The X-ray diffraction pattern is the fingerprint of periodic atomic arrangements in a given material.[45,47-51]

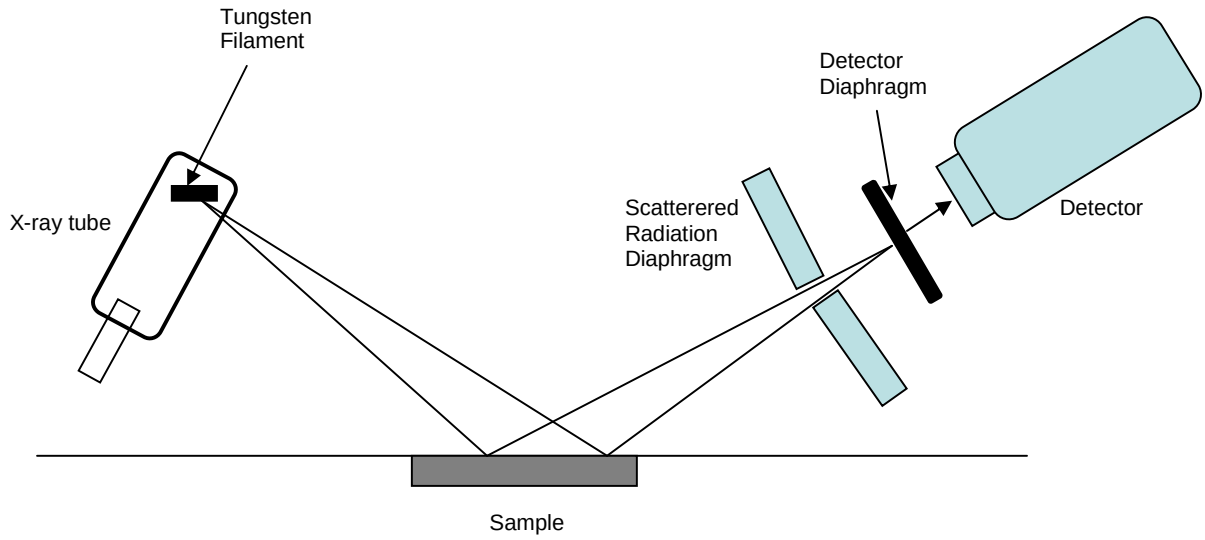

Fig 1.4. Schematic of XRD instrument

When electrons strike a metal anode with sufficient energy, X-rays are produced. This process is typically accomplished using a sealed x-ray tube, which consists of a metal target (often copper metal) and a tungsten metal filament, which can be heated by passing a current through it resulting in the emission of electrons from the tungsten filament.[49,50] These electrons are accelerated from the tungsten filament to the metal target by an applied voltage. The collision between these energetic electrons and electrons in the target atoms results in electron from target atoms being excited out of their core-level orbitals, placing the atom in a short-lived excited

state. The atom returns to its ground state by having electrons from lower binding energy levels making transitions to the empty core levels. The difference in energy between these lower and higher binding energy levels is radiated in the form of X-rays. This process results in the production of characteristic X-rays.[47-51] X-ray powder diffractometers record all reflections using a detector. The pattern of diffracted X-rays is unique for a particular structure type and can be used as a fingerprint to identify the structure type.

The main types of applications for the characterization of solid particles are

• Determination of phase contents of particles

• Measurement of average crystallite size

1.6 References

1. Mulvaney, Paul; *Nanoscale Materials in Chemistry*, **2001**, 121-167
2. Mishra, Rahul; Rajanna, K; *Sensors and Materials*, **2005**, 17(8), 433-440.
3. Nishihara, Hiroshi; Kanaizuka, Katsuhiko; Nishimori, Yoshihiko; Yamanoi, Yoshinori; *Coordination Chemistry Reviews*, **2007**, 251(21-24), 2674-2687.
4. Jain Kewal K; *Drug discovery today*, **2005**, 10(21), 1435-42
5. Pope-Harman, Amy; Cheng, Mark Ming-Cheng; Robertson, Fredika; Sakamoto, Jason; Ferrari, Mauro; *Medical Clinics of North America*, **2007**, 91(5), 899-927
6. Li, Guangyong; Xi, Ning; Wang, Donna H; *Medical Clinics of North America*, **2007**, 91(5), 929-936
7. Moore, M. N; *Environment International*, **2006**, 32(8), 967-976
8. Fulekar, M. H; *Environment Science & Engineering*, **2007**, 5(2), 65-75.
9. Caruntu, Daniela; Caruntu, Gabriel; O'Connor, Charles J.; *Journal of Physics D: Applied Physics*, **2007**, 40(19), 5801-5809.
10. Njoki, Peter N.; Lim, I-Im S.; Mott, Derrick; Park, Hye-Young; Khan, Bilal; Mishra, Suprav; Sujakumar, Ravishanker; Luo, Jin; Zhong, Chuan-Jian; *Journal of Physical Chemistry C*, **2007**, 111(40), 14664-14669.
11. He, Qiuxing; Tu, Weiping; Hu, Jianqing; *Journal of Materials Science*, **2007**, 42(19), 8292-8297
12. Lim, Dong Chan; Lopez-Salido, Ignacio; Dietsche, Rainer; Bubek, Moritz; Kim, Young Dok; *Chemical Physics*, **2006**, 330(3), 441-448.

13. Chen, Haiyan; Gu, Yueqing; Hu, Yuzhu; Qian, Zhiyu; *PDA Journal of Pharmaceutical Science and Technology*, **2007**, 61(4), 303-313
14. Liu, Kuang-Kai; Cheng, Chi-Liang; Chang, Chia-Ching; Chao, Jui-I.; *Nanotechnology*, **2007**, 18(32), 325102/1-325102/10.
15. Urry, Dan W.; Woods, T. Copper; Hayes, Larry C.; Xu, Jie; McPherson, David T.; Parker, Timothy M.; Iwama, Masamichi; Furutan, Masakazu; Hayashi, Toshio; Murata, Mitsuhiro; *Tissue Engineering and Novel Delivery Systems*, **2004**, 31-54.
16. Leuschner, Carola; Kumar, Challa; *Nanofabrication towards Biomedical Applications*, **2005**, 289-326.
17. Nahar, Manoj; Dutta, Tathagata; Murugesan, Senthilkumar; Asthana, Abhay; Mishra, Dinesh; Rajkumar, Vijayaraj; Tare, Manoj; Saraf, Surbhi; Jain, Narendra Kumar; *Critical Reviews in Therapeutic Drug Carrier Systems*, **2006**, 23(4), 259-318.
18. Hao, F.; Nordlander, P.; *Chemical Physics Letters*, **2007**, 446(1-3), 115-118.
19. Hanemann, T.; Boehm, J.; Henzi, P.; Honnef, K.; Litfin, K.; Ritzhaupt-Kleissl, E.; Hausselt, J.; *Nanobiotechnology*, **2004**, 151(4), 167-172.
20. Manova, Elina; Kunev, Boris; Paneva, Daniela; Mitov, Ivan; Petrov, Lachezar; Estournes, Claude; D'Orleans, Celine; Rehspringer, Jean-Luc; Kurmoo, Mohamedally; *Chemistry of Materials*, **2004**, 16(26), 5689-5696.
21. Ogawa, Tomoyuki; Takahashi, Yasuhiro; Yang, Haitao; Kimura, Kaori; Sakurai, Masatoshi; Takahashi, Migaku; *Nanotechnology*, **2006**, 17(22), 5539-5543.
22. Knecht, Marc R.; Garcia-Martinez, Joaquin C.; Crooks, Richard M.; *Langmuir*, **2005**, 21(25), 11981-11986.

23. Bertholon Isabelle; Hommel Hubert; Labarre Denis; Vauthier Christine; *Langmuir*, **2006**, 22(12), 5485-90.
24. Deng, X.; Jia, G.; Wang, H.; Sun, H.; Wang, X.; Yang, S.; Wang, T.; Liu, Y.; *Carbon*, **2007**, 45(7), 1419-1424.
25. Borm, Paul; Klaessig, Frederick C.; Landry, Timothy D.; Moudgil, Brij; Pauluhn, Juergen; Thomas, Karluss; Trottier, Remi; Wood, Stewart; *Toxicological Sciences*, **2006**, 90(1), 23-32.
26. Premkumar, T.; Geckeler, Kurt E; *Journal of Physics and Chemistry of Solids*, **2006**, 67(7), 1451-1456.
27. Amiens, C.; Chaudret, B; *Modern Physics Letters B*, **2007**, 21(18), 1133-1141.
28. Mukherjee, B.; Ravishankar, N; *Nanotechnology*, **2007**, 18(2), 025603/1-025603/9.
29. Choi, Mansoo; *Thermal Science and Engineering*, **2005**, 13(2), 7-11.
30. Wegner, Karsten; Pratsinis, Sotiris E; *Powder Technology*, **2005**, 150(2), 117-122.
31. Pickett, Nigel L.; Riddell, Frank. G.; Foster, Douglas F.; Cole-Hamilton, David J.; Fryer, John R; *Journal of Materials Chemistry*, **1997**, 7(9), 1855-1865.
32. Long, Qi; Cai, Mei; Rogers, Jerry D.; Rong, Huilin; Li, Jinru; Jiang, Long; *Nanotechnology*, **2007**, 18(35), 355601/1-355601/6.
33. Moncada, E.; Quijada, R.; Retuert, J; *Nanotechnology*, **2007**, 18(33), 335606/1-335606/7.
34. Zhou, J.; Wu, W.; Caruntu, D.; Yu, M. H.; Martin, A.; Chen, J. F.; O'Connor, C. J.; Zhou, W. L; *Journal of Physical Chemistry C*, **2007,** 111(35), 13028-13032.
35. Krishnan, Venkata; Bottaro, Gregorio; Gross, Silvia; Armelao, Lidia; Tondello, Eugenio; Bertagnolli, Helmut; *Journal of Materials Chemistry*, **2005**, 15(20), 2020-2027.

36. Park, S. M.; Ki, W.; Yu, J.; Du, H; *Journal of Materials Research*, **2005**, 20(11), 3094-3101.
37. Mizukoshi, Yoshiteru; Seino, Satoshi; Okitsu, Kenji; Kinoshita, Takuya; Otome, Yohei; Nakagawa, Takashi; Yamamoto, Takao A.; *Ultrasonics Sonochemistry*, **2005**, 12(3), 191-195.
38. Okitsu, Kenji; Ashokkumar, Muthupandian; Grieser, Franz; *Journal of Physical Chemistry B*, **2005**, 109(44), 20673-20675.
39. Basnayake, Rukma; Li, Zhengrong; Katar, Srilakshmi; Zhou, Wei; Rivera, Harry; Smotkin, Eugene S.; Casadonte, Dominick J., Jr.; Korzeniewski, Carol; *Langmuir*, **2006**, 22(25), 10446-10450.
40. Yang, Yunhua; Jing, Lihong; Yu, Xiaolan; Yan, Dadong; Gao, Mingyuan; *Chemistry of Materials*, **2007**, 19(17), 4123-4128.
41. Zhang, K.; Chew, C. H.; Xu, G. Q.; Wang, J.; Gan, L. M.; *Langmuir*, **1999**, 15(9), 3056-3061.
42. Lopez Perez, J. A.; Lopez Quintela, M. A.; Mira, J.; Rivas, J.; Charles, S. W.; *Journal of Physical Chemistry B*, **1997**, 101(41), 8045-8047.
43. Egerton, R. F., *Physical principles of electron microscopy : An introduction to TEM, SEM, and AEM, New York : Springer Science & Business Media*, **2005**
44. David B. Williams and C. Barry Carter, *Transmission Electron Microscopy: A Textbook for Materials Science, Kluwer Academic/Plenum Publishers*, **1996**
45. Taylor, Larry, Richard Papp, Bruce Pollard; *Instrumental methods for determining elements, VCH*, **1994**
46. Galen Wood Ewing; *Analytical Instrumentation Handbook, Marcel Dekker*, **1997**

47. Settle, Frank A.; *Handbook of instrumental techniques for analytical chemistry, Prentice Hall PTR*, **1997**
48. Strobel, Howard A., Heinmann, William R.; *Chemical Instrumentation: A Systematic Approach, Wiley Inrescience*, **1989**
49. Pungor, E.; *A practical guide to instrumental analysis, CRC Press*, **1995**
50. Skoog, Douglas A; *Principles of instrumental analysis, Holt, Rinehart and Winston*, **1971**
51. Delahay, Paul; *Instrumental analysis, Macmillan*, **1957**

Chapter 2. Applications of Nanoparticles and Previous Research

Materials on the nanoscale exhibit unique properties that, while in it's very early days yet, are potentially useful for various applications. The applications of these particles range from the research areas to the real world. Titanium dioxide nanoparticles have been used in sunscreen, cosmetics and some food products; silver nanoparticles in food packaging, clothing, disinfectants and household appliances; zinc oxide nanoparticles in sunscreens and cosmetics, surface coatings, paints and outdoor furniture varnishes; and cerium oxide nanoparticles as a fuel catalyst. Various fields where nanotechnology can and have been used are discussed below.

2.1 Medicine

Due to their exclusive properties, nanomaterials have been extensively used in biological and medical fields. They have been used as contrast agents for cell imaging[1-3] and therapeutics for curing cancer[4]. This hybrid between nanotechnology and medicinal studies has been called by various names as medical nanotechnology, nanomedicine or bionanotechnology.

2.2 Drug delivery

According to the census in 2006, 47 million people in the US live without health insurance. There is an urgent need to reduce the cost of public health care so that more people can be accommodated in the system. Drug consumption and side-effects can be drastically lowered by depositing the active agent in the morbid region only and in no higher dose than needed. This highly selective approach reduces costs and human suffering. An example can be found in dendrimers and nanoporous materials. These materials can hold small drug molecules,

transporting them to the desired location. Some potentially important applications include cancer treatment with iron nanoparticles or gold nanoshells.

Nanotechnology has also helped in the implantable delivery systems, which are often preferable to the use of injectable drugs[5] because the latter frequently display first-order kinetics (the blood concentration goes up rapidly, but drops exponentially over time). This rapid rise may cause difficulties with toxicity, and drug efficacy can diminish as the drug concentration falls below the targeted range.

2.3 Tissue engineering

When nanotechnology is also used for repairing and reproducing damaged tissue, it is called tissue engineering.[6-8] Tissue engineering uses artificially simulated cell propagation by making use of nanomaterials-based scaffolds and growth factors. On one hand, scientists believe that tissue engineering is a boon and can substitute for conventional treatment methods like organ transplants or artificial implants. On the other hand it also involves the ethical dilemma of human stem cells and its implications.

2.4 Diagnostics

Nanotechnology-on-a-chip is one more dimension of lab-on-a-chip technology. Biological tests measuring the presence or activity of selected substances become quicker, more sensitive and more flexible when certain nanoscale particles are put to work as tags or labels. Magnetic nanoparticles, bound to a suitable antibody, are used to label specific molecules, structures or microorganisms. Gold nanoparticles tagged with short segments of DNA can be used for detection of the genetic sequence[9,10] in a sample. Multicolor optical coding for

biological assays[11,12] has been achieved by embedding different-sized quantum dots into polymeric microbeads. Nanopore technology for analysis of nucleic acids[13-16] converts strings of nucleotides directly into electronic signatures.

2.5 Chemistry and Environment

Nanotechnology is used in many areas in chemistry but it is mainly used in chemical catalysis[16,17] and filtration techniques.[18] Nanoscale synthesis results in novel materials which have certain customized features and chemical properties. In a short-term perspective, chemistry will provide novel "nanomaterials" and in the long run, superior processes such as "self-assembly" will enable energy and time preserving strategies. Nanomaterials with unique chemical surroundings (ligands) or precise optical properties are a few examples.

2.6 Catalysis

Due to the high surface to volume ratio in nanomaterials, they are highly beneficial in chemical catalysis. Though catalysis is most important in the manufacturing of chemicals, it also has a large range of other applications, from fuel cells[19,20] to catalytic converters and photocatalytic devices.

2.7 Filtration

A strong influence of nanochemistry on waste-water treatment, air purification and energy storage devices is to be expected. Mechanical or chemical methods can be used for effective filtration techniques. One class of filtration techniques is based on the use of membranes with suitable pore sizes, whereby the liquid is pressed through the membrane.

Nanoporous membranes are suitable for mechanical filtration with extremely small pores of less than 10 nm ("nanofiltration") and may be composed of nanotubes[21]. On a larger scale, the membrane filtration technique is named ultrafiltration, which works down to between 10 and 100 nm. One important field of application for ultrafiltration is medical purposes as can be found in renal dialysis.

Magnetic nanoparticles offer an effective and reliable method to remove heavy metal contaminants from waste water by making use of magnetic separation techniques. Using nanoscale particles increases the efficiency to absorb the contaminants and is relatively inexpensive compared to traditional precipitation and filtration methods.

2.8 Energy

Nanotechnology taps on various aspects of energy, but the most advanced and beneficial projects are related to the storage, conversion, and manufacturing improvements of energy. The manufacturing improvements are achieved by reducing materials and process rates. This results in energy savings by better thermal insulations and enhanced renewable energy sources.

2.9 Reduction of energy consumption

The energy crisis in the world is a major concern for all. Scientists have been extensively researching new technologies to reduce energy consumption. Nanotechnological methods like light-emitting diodes (LED)[22] or quantum caged atoms (QCAs)[23] could lead to a reduction in energy consumption for illumination, as compared to the currently used light bulbs which convert very little of the electrical energy into light.

2.10 Increasing the efficiency of energy production

Due to the energy crisis in the world, we have to tap into various forms of energy sources. One of the cleanest sources of energy in the world is solar energy. Today's best solar cells have layers of many different semiconductors stacked together to absorb light at different energies, but they are still not able to efficiently absorb all the energy available. They only make use of 40% of the sun's energy. Nanotechnology can help in increasing the efficiency of light conversion by using nanostructures with a continuum of bandgaps. Nanotechnology could improve combustion by designing specific catalysts with maximized surface area. Scientists have recently developed tetrad-shaped nanoparticles that, when applied to a surface, instantly transform it into a solar collector. [24]

2.11 The use of more environment friendly energy systems

An example for an environmentally friendly form of energy is the use of fuel cells[19-22] powered by hydrogen, which is ideally produced by renewable energies. Probably the most prominent nanostructured material in fuel cells is the catalyst consisting of carbon supported noble metal particles with diameters of 1- 5 nm. Suitable materials for hydrogen storage contain a large number of small nanosized pores. Therefore many nanostructured materials like nanotubes, zeolites or alanates are under investigation.[21,22]

Nanotechnology can contribute to the further reduction of combustion engine pollutants by nanoporous filters, which can clean the exhaust mechanically, by catalytic converters based on nanoscale noble metal particles or by catalytic coatings on cylinder walls and catalytic nanoparticles as additive for fuels.

2.12 Recycling of Batteries

In today's world, batteries have become a very integral part of our daily lives. Batteries have a very low energy density and therefore have a very short operating time. Consequently, they must be replaced or recharged very often. The huge consumption and disposal of batteries can pose a threat to the environment. Nanotechnology can create high energy batteries[22,23] which can also be recharged. Thus use of these high energy and rechargeable batteries or supercapacitors[25] will be helpful in reducing the disposal problem.

2.13 Information and communication

Information technology has been utilizing nanotechnology without any formal introduction of this science. The critical length scale of integrated circuits is already at the nanoscale (50 nm and below) in regards to the gate length of transistors in CPUs. The high-technology production processes which are based on conventional top down strategies, already make use of nanotechnology.

2.14 Novel optoelectronic devices

In modern communication technology, traditional analog electrical devices are increasingly replaced by optical or optoelectronic[26] devices due to their enormous bandwidth and capacity. Two promising examples are photonic crystals and quantum dots.

Quantum dots are nanoscaled objects, which can be used, among many other things, for the construction of lasers. The advantage of a quantum dot laser[27] over the traditional semiconductor laser is that their emitted wavelength depends on the diameter of the dot. Quantum dot lasers are cheaper and offer a higher beam quality than conventional laser diodes.

2.15 Displays

Displays have become a major part of advertising industry. There is a need for creating displays with low energy consumption, and this goal can be attained by using carbon nanotubes[28,29] (CNT). Carbon nanotubes are electrically conductive, and because of their small diameter (~ several nanometers), they can be used as field emitters with extremely high efficiency for field emission displays[29-31] (FED). This method is close to the cathode ray tube but it is on a much smaller length scale.

2.16 Consumer goods

Consumer goods are becoming more user friendly and easy to use. Nanotechnology is making an impact in this field by providing consumers with easy-to-clean and scratch-resistant products. Textiles made with nanotechnology are wrinkle-resistant and stain-repellent and are gradually becoming “smart”. Products made with nanoparticles are increasingly hitting the consumer market, especially in the fields of cosmetics.

Foods

Nanotechnology has been extensively and routinely used in the food production,[32] processing, safety[32] and packing.[32,33] The nanocomposite coating process improves the food packaging by placing anti-microbial agents on the surface of coated film. Research is being performed to apply nanotechnology to the detection of chemical and biological substances for sensing biochemical changes in foods. [32,33] Nanocomposites can drastically increase and decrease gas permeability of the various fillers as they are required for the various products.

Household

"Self-cleaning"[33] or "easy to clean" surfaces[34,35] in a household can reduce the extent of household chores. Nanotechnology has made that possible by providing us such materials in the form of ceramics and glasses. It has also improved the smoothness and heat resistance of common household equipment such as the flat iron which provides better results.

Optics

Sunglasses save our eyes from the harmful UV rays. Sunglasses which are now available on the market, with protective and antireflective ultrathin polymer coatings make them close to impenetrable. Nanotechnology has also helped in providing scratch resistant surface coatings[36] based on nanocomposites for a longer life of the sunglasses. The most significant application of nanotechnology in optics is the increased precision in pupil repair and other types of laser eye surgery.

Textiles

Nanoparticles have also played a very important role in the textile industry. In today's world, a need for wrinkle-free, stain-repellent and water-repellent cloth is satisfied by nanofibers.[37] This has made the use of nanofibers in the manufacturing of cloth inimitable. Furthermore, textiles manufactured with nanotechnological finishes are created in such a way that they require less washing and can be washed at lower temperatures. The latest application of nanoparticles is in military applications as camouflage. In these applications nanocameras along with nanodisplays are incorporated in the textile material and this could create an "invisibility coat" acting as a skin like a chameleon.

Cosmetics

In the present world of cosmetic preference and cancer awareness, it is required to produce effective products which can be used on a long-term basis. Sunscreens[38] are one of the most used products in the market. In earlier days, sunscreens were made out of traditional chemicals that absorbed UV radiation. However, these compounds suffer from poor long-term stability. Whereas, sunscreens made out of mineral nanoparticles such as titanium oxide are more durable and have a comparable UV protection property.[39,40] Furthermore, nanoparticle sized oxides decrease the cosmetically undesirable white color as the particle size decreases.

2.17 Previous Research on Magnetic Nanoparticles

Magnetic nanoparticles have been a key area of research in biomedical applications of nanomaterials. In many cases, the properties and characteristics of the bulk materials are well understood, but when materials are transformed into the nanoscale region their behavior changes dramatically and cannot be easily predicted. Consequently, efforts to understand biological responses to nanomaterials has been of interest to researchers for many years.

There are two reasons why magnetic nanoparticles or magnetic nanocomposites have attracted scientists so much. First, magnetic nanoparticles can be controlled externally to the body by application of magnetic fields. Second, magnetite can be combined with gold, silica or other materials and thus the surface properties of the magnetic nanomaterials can be modified according to the necessity of their application.

Previous research has shown that magnetic nanocomposites not only have their application in the medical field but also it can be used in the household uses. There have been advances in the handling and manipulation of magnetic particles in microfluidic systems[41,42].

Starting from the properties of magnetic nanoparticles and microparticles, they have been used in magnetic separation[43], immunoassays, magnetic resonance imaging[44-48], drug delivery[49-53], and hyperthermia[54,55]. Magnetic nanoparticles that are applied as markers for the specific analysis of biomolecules have the advantage that they are stable, mostly non-toxic and can be used for *in vitro* as well as *in vivo* experiments.

Magnetic nanoparticles, sometimes with their surfaces modified by polymers or different noble metals, have been also used for treatment of water[56,57]. Moreover surface-modified magnetic nanoparticles synthesized for cellular interactions have shown improved biological applications. Bifunctional nanomaterials have been used for detection of very low concentrations of bacteria[58] and also to probe pathogenic bacteria[59].

Scientists have reviewed some relevant aspects of the magnetic properties of metallic nanoparticles of different shapes and sizes and how they differ from their bulk counterpart. The magnetic properties of nanoparticles enable them to be used as storage devices and for targeted drug delivery systems[49-53]. Moreover they are also used for targeted heating of cancerous cells and tumors[60-63]. Serial heat treatments were possible without repeated injection of magnetic fluid. The popularity and practicality of nanoparticle materials create a need for a synthesis method that produces quality particles in sizable quantities.

To further the application of nanoparticles in disease diagnosis and therapy, it is important that the systems are stable, capable of being functionalized, biocompatible, and directed to specific target sites in the body after systemic administration. For this reason the magnetic nanoparticles need to be coated or made core shell so that they are not toxic and are not easily oxidized. The surface modification helps the nanoparticles to be evenly dispersed and stable in aqueous medium.

Lee *et al.* have capped the surface of monodispersed maghemite (γ-Fe_2O_3) to increase the stability of the particles in polar solvents.[64] Interfacial ligand exchange of the capping molecules was done to make the particle surface more hydrophilic. The maghemite particles showed enhanced miscibility and short-term stability in water after interfacial ligand exchange. Gajdosikova *et al.* have been able to reduce the acute toxicity of magnetite nanoparticles by coating them with poly (D,L) lactide.[65] Olle and coworkers observed enhancement of oxygen mass transfer in the presence of colloidal dispersions of magnetite nanoparticles coated with oleic acid and a polymerizable surfactant.[66] These fluids improved gas-liquid oxygen mass transfer up to six fold in an agitated, sparged, cell-free reactor and showed remarkable stability in high-ionic strength media over a wide pH range. Nishiya and research group coated the magnetic nanoparticles with hydroxyapatite[67] which is not only an important material for bone and tooth implants, but is also commonly used in protein purification. These particles could be directly and readily used in biomedical applications. Moreover, they showed that these particles could be controlled by an external magnet.

Feng *et al.* synthesized HSA-coated magnetic nanoparticles labeled with rhenium-188 for the purpose of regional target therapy.[68] These radioactive Re doped magnetite particles are used for the γ-imaging technique. To investigate the different magnetic properties scientists have doped the magnetite particles with various other metals like tin[69,70], zinc[71], cobalt[72,73] or nickel[74,75].

One other important area of research was attaching or coating magnetite particles with noble metals like gold. This not only makes the magnetite particles less susceptible to oxidation but also helps in attaching a linker to the surface of gold. Gold surfaces are very readily modified using sulfide linkages and thus antibodies could be subsequently attached to gold and used for

targeted drug delivery. Sun *et al.* were able to synthesize dumbbell shaped bifunctional gold magnetite nanoparticles[76], and Caruntu and coworkers were able to attach gold nanograins on larger magnetite particles using different wet chemical methods of synthesis.[77] Kawaguchi and his group have prepared gold/iron-oxide composite nanoparticles by a unique laser process in an aqueous medium[78].

Scientists have used different approaches for synthesizing the nanoparticles, with one of the most amazing techniques being sonochemistry. Polycrystalline iron phosphide coated iron oxide and hollow iron phosphide nanoparticles were synthesized by sonochemistry[79]. Moreover it has already been proven that scientists can control the shape and size of the noble metals by adjusting the parameters in sonochemical processes[80]. Researchers were also able to produce coated or bare magnetite particles of desired size and morphology[80-83].

The nanocomposites produced in various different ways can be used in biomedicine, drug delivery, MRI contrast agents and in household applications. Though the research area is in its early stages, scientists have successfully shown that some of the nanoparticles can be used in fields ranging from targeted cancer therapy to textile industry. So it can be seen that the use of nanoparticles are widely varied and thus have become an important area of scientific research.

2.18 References

1. Xu, Fang; Mukhopadhyay, Somshuvra; Sehgal, Pravin B; *American Journal of Physiology*, **2007**, 293(4), C1374-C1382.
2. Li, Qian; Chang, Young-Tae; *Nature Protocols*, **2006**), 1(6), 2922-2932.
3. Andresen, Martin; Schmitz-Salue, Rita; Jakobs, Stefan; Molecular *Biology of the Cell*, **2004**, 15(12), 5616-5622.
4. Larson, Timothy A.; Bankson, James; Aaron, Jesse; Sokolov, Konstantin; *Nanotechnology*, **2007**, 18(32), 325101/1-325101/8.
5. Sendo, T.; Teshima, D.; Makino, K.; Mishima, K.; Itoh, Y.; Oishi, R; *Journal of Clinical Pharmacy and Therapeutics*, **2002**, 27(2), 79-84.
6. Kaufman, Jessica; Wong, Joyce Y.; Klapperich, Catherine; *Biomaterials*, **2007**, 10/1-10/14.
7. Boccaccini, Aldo R.; Blaker, Jonny J.; Maquet, Veronique; Chung, Wendy; Jerome, Robert; Nazhat, Showan N; *Journal of Materials Science*, **2006**, 41(13), 3999-4008.
8. Ito, Akira; Ino, Kousuke; Hayashida, Masao; Kobayashi, Takeshi; Matsunuma, Hiroshi; Kagami, Hideaki; Ueda, Minoru; Honda, Hiroyuki; *Tissue Engineering*, **2005**, 11(9/10), 1553-1561.
9. Wu, Zai-Sheng; Jiang, Jian-Hui; Fu, Li; Shen, Guo-Li; Yu, Ru-Qin; *Analytical Biochemistry*, **2006**, 353(1), 22-29.
10. Li, Huixiang; Rothberg, Lewis J; *Analytical Chemistry*, **2004**, 76(18), 5414-5417.
11. Han M; Gao X; Su J Z; Nie S; *Nature biotechnology*, **2001**, 19(7), 631-5.
12. Mattheakis Larry C; Dias Jennifer M; Choi Yun-Jung; Gong Jing; Bruchez Marcel P; Liu Jianquan; Wang Eugene; *Analytical Biochemistry*, **2004**, 327(2), 200-8.

13. Beidler, John L.; Hilliard, Peter R.; Rill, Randolph L.; *Analytical Biochemistry*, **1982**, 126(2), 374-80.
14. Wang, Joseph; Gruendler, Peter; Flechsig, Gerd-Uwe; Jasinski, Markus; Rivas, Gustavo; Sahlin, Eskil; Lopez Paz, Jose Luis; *Analytical Chemistry*, **2000**, 72(16), 3752-3756.
15. Bilitewski Ursula; Genrich Meike; Kadow Sabine; Mersal Gaber; *Analytical and bioanalytical chemistry*, **2003**, 377(3), 556-69.
16. Zheng, Nanfeng; Stucky, Galen D.; *Journal of the American Chemical Society*, **2006**, 128(44), 14278-14280.
17. Kim, Nam Seo; Lee, Yun Tack; Park, Jeunghee; Ryu, Hyun; Lee, Hwack Joo; Choi, Seung Yeol; Choo, Jaebum; *Journal of Physical Chemistry B*, **2002**, 106(36), 9286-9290.
18. Sato, Shintaro; Chen, Da-Ren; Pui, David Y. H.; *Aerosol and Air Quality Research*, **2007**, 7(3), 278-303.
19. Mu, Shichun; Wang, Xiaoen; Tang, Haolin; Li, Peigang; Lei, Ming; Pan, Mu; Yuan, Run Zhang; *Journal of the Electrochemical Society*, **2006**, 153(10), A1868-A1872.
20. Tu, Hung-Chi; Wang, Wen-Lin; Wan, Chi-Chao; Wang, Yung-Yun; *Journal of Physical Chem. B*, **2006**, 110(32), 15988-15993.
21. Theron J, Walker JA, Cloete TE; *Critical Reviews in Microbiology*, **2008**, 34(1), 43-69
22. Kwak, Joon Seop; Song, J.-O.; Seong, T.-Y.; Kim, B. I.; Cho, J.; Sone, C.; Park, Y.; *Journal of Nanoscience and Nanotechnology*, **2006**, 6(11), 3547-3550.
23. Han-Chang Liu and Shiow-Kang Yen; *Journal of Power Sources*, **2007**, 166(2), 478-484
24. Lopez-Luke T; Wolcott A; Xu LP; Chen SW; Wen ZH; Li JH; De LR; Zhang JZ; *Journal of Physical Chem. C*, **2008**, 112(4), 1282-1292

25. Ying Zheng, Jun Yang, Jiulin Wang and Yanna NuLi; *Electrochimica Acta*, **2007**, 52(19), 5863-5867
26. K.M. Begam and S.R.S. Prabaharan; *Journal of Power Sources*, **2006**, 159(1), 319-322
27. Domink Heiss, Miro Kroutvar, Jonathan J. Finley and Gerhard Abstreiter; *Solid State Communications*, **2005**, 135(9), 591-601
28. L. Gavrila Florescu, C. Fleaca, I. Voicu, I. Morjan, L. Stamatin and Ioan Stamatin; *Applied Surface Science*, **2007**, 253(31), 7729-7732
29. Axel Schindler, Jochen Brill, Norbert Fruehauf, James P. Novak and Zvi Yaniv; *Physica E: Low-dimensional Systems and Nanostructures*, **2007**, 37(1) 119-123
30. Fan-Guang Zeng, Chang-Chun Zhu, Weihua Liu and Xinghui Liu; *Microelectronics Journal*, **2006**, 37(6), 495-499
31. Zhejuan Zhang, Z. Sun and Yiwei Chen; *Applied Surface Science*, **2007**, 253(6), 3292-3297
32. Liu Xinghui, Zhu Changchun, Liu Weihua, Zeng Fanguang and Tian Changhui; *Materials Chemistry and Physics*, **2005**, 93(3), 473-477
33. Peerasak Sanguansri and Mary Ann Augustin; *Trends in Food Science & Technology*, **2006**, 17(10), 547-556
34. D.A. Pereira de Abreu, P. Paseiro Losada, I. Angulo and J.M. Cruz; *European Polymer Journal*, **2007**, 43(6), 2229-2243
35. Eric Puzenat and Pierre Pichat; *Journal of Photochemistry and Photobiology A: Chemistry*, **2003**, 160(1-2), 127-133
36. J.O. Carneiro, V. Teixeira, A. Portinha, A. Magalhães, P. Coutinho, C.J. Tavares and R. Newton; *Materials Science and Engineering: B*, **2007**, 138(2), 144-150

37. T. Yuranova, D. Laub and J. Kiwi; *Catalysis Today*, **2007**, 122(1-2), 109-117

38. Ronan Tartivel, Emmanuelle Reynaud, Fabien Grasset, Jean-Christophe Sangleboeuf and Tanguy Rouxel; *Journal of Non-Crystalline Solids*, **2007**, 353(1), 108-110

39. A. Bozzi, T. Yuranova and J. Kiwi; *Journal of Photochemistry and Photobiology A: Chemistry*, **2005**, 172(1), 27-34

40. Mariana Sincai, Diana Argherie, Diana Ganga, Doina Bica and Ladislau Vekas; *Journal of Magnetism and Magnetic Materials*, **2007**, 311(1), 363-366

41. J.R. Villalobos-Hernández and C.C. Müller-Goymann; *International Journal of Pharmaceutics*, **2006**, 322(1-2), 161-170

42. Chunjin Song and Shuangxi Liu; *International Journal of Biological Macromolecules*, **2005**, 36(1) 116-119

43. Elisabeth Galopin, Maxime Beaugeois, Bernard Pinchemel, Jean-Christophe Camart, Mohamed Bouazaoui and Vincent Thomy; *Biosensors and Bioelectronics*, **2007**, 23(5), 746-750

44. Gregory T. Roman and Robert T. Kennedy; *Journal of Chromatography A*, **2007**, 1168, (1), 170-188

45. Nadja Schultz, Christoph Syldatk, Matthias Franzreb and Timothy John Hobley; *Journal of Biotechnology*, **2007**, 132(2), 202-208

46. Lin, A. W. H.; Lewinski, N. A.; West, J. L.; Halas, N. J.; Drezek, R. A.; *J. Biomed. Opt.*, **2005**, 10, 064035/1-064035/10

47. Sokolov, K.; Follen, Mi.; Aaron, J.; Pavlova, I.; Malpica, A.; Lotan, R.; Richards-Kortum, R.; *Cancer Res.*, **2004**, 63, 1999-2004.

48. Arbab, A. S.; Liu, W.; Frank, J. A.; *Expert Rev. Med. Devices*, **2006**, 3, 427-439.

49. Sun, C.; Sze, R.; Zhang, M.; *J. Biomed. Mat. Res., Part A,* **2006**, 78(A), 550-557.

50. Frias, J. C.; Ma, Y.; Williams, K. J.; Fayad, Z. A.; Fisher, E. A.; *Nano Lett.*, **2006**, 6, 1752-1756.

51. Niidome, T.; Yamagata, M.; Okamoto, Y.; Akiyama, Y.; Takahashi, H.; Kawano, T.; Katayama, Y.; Niidome, Y.; *J. Controlled Release*, **2006**, 114, 343-347.

52. Astete, C. E.; Sabliov, C. M.; *Particulate Sci. Technol.*, **2006**, 24, 321-328.

53. Bertram, J.; *Curr. Pharm. Biotechnol.*, **2006**, 7, 277-285.

54. Wu, W.; DeCoster, M. A.; Daniel, B. M.; Chen, J. F.; Yu, M. H.; Cruntu, D.; O'Connor, C. J.; Zhou, W. L.; *J. Appl. Phys.*, **2006**, 99, 08H104/1-08H104/3.

55. Zhou, W.; Gao, P.; Shao, L.; Caruntu, D.; Yu, M.; Chen, J.; O'Connor, C. J.; *Nanomed.*, **2005**, 1, 233-237.

56. E. Pollert, K. Knížek, M. Maryško, P. Kašpar, S. Vasseur and E. Duguet; Journal *of Magnetism and Magnetic Materials*, **2007**, 316(2), 122-125

57. Akira Ito, Yuko Kuga, Hiroyuki Honda, Hiroyuki Kikkawa, Atsushi Horiuchi, Yuji Watanabe and Takeshi Kobayashi; *Cancer Letters*, **2004**, 212(2), 167-175

58. Yinhui Xu and Dongye Zhao; *Water Research*, **2007**, 41(10), 2101-2108

59. L. Lhomme, S. Brosillon and D. Wolbert; *Chemosphere*, **2007**, 70(3), 381-386

60. Madhukar Varshney, Yanbin Li, Balaji Srinivasan and Steve Tung; *Sensors and Actuators B: Chemical*, **2007**, 128(1), 99-107

61. Tsai, Pei-Jane; Lin, Ya-Shiuan; Chen, Yu-Chie; *Analytical Chemistry*, **2004**, 76(24), 7162-7168

62. Manfred Johannsen, Uwe Gneveckow, Burghard Thiesen, Kasra Taymoorian, Chie Hee Cho, Norbert Waldöfner, Regina Scholz, Andreas Jordan, Stefan A. Loening and Peter Wust; *European Urology*, **2007**, 52(6), 1653-1662
63. Akira Ito, Masashige Shinkai, Hiroyuki Honda and Takeshi Kobayashi; *Journal of Bioscience and Bioengineering*, **2005**, 100(1), 1-11
64. Lee, SY; Harris MT; *Journal of Colloid and Interface Science*, **2006**, 293(2), 401-408
65. Gajdosikova A, Gajdosik A, Koneracka M; *Neuroendocrinology Letters*, **2006**, 27(2), 96-99
66. Olle, B.; Bromberg, L.; Hatton, T. A.; Wang, D.; *Industrial and Engineering Chemistry Research*, **2006**, 45(12), 4355-4363
67. Ingrid Hilger, Rudolf Hergt and Werner A. Kaiser; *Journal of Magnetism and Magnetic Materials*, **2005**, 293(1), 314-319
68. Andreas Jordan, Regina Scholz, Peter Wust, Horst Fähling and Roland Felix; *Journal of Magnetism and Magnetic Materials*, **1999**, 201(3), 413-419
69. Yan-Wu Lu, Qin-Sheng Zhu and Fang-Xin Liu; *Physics Letters A*, **2006**, 359(1), 66-69
70. Frank J. Berry, Örn Helgason, Kristjan Jónsson and Stephen J. Skinner; *Journal of Solid State Chemistry*, **1996**, 122(2), 353-357
71. Monica Sorescu, L. Diamandescu, D. Tarabasanu-Mihaila and V. Teodorescu; *Materials Chemistry and Physics*, **2007**, 106(2-3), 273-278
72. M. F. F. Lelis, A. O. Porto, C. M. Gonçalves and J. D. Fabris; *Journal of Magnetism and Magnetic Materials*, **2004**, 278(1-2), 263-269
73. Monica Sorescu, A. Grabias, R. A. Brand, J. Voss, D. Tarabasanu-Mihaila and L. Diamandescu; *Journal of Magnetism and Magnetic Materials*, **2002**, 246(3), 399-403

74. M. Mohapatra, Brajesh Pandey, Chandan Upadhyay, S. Anand, R.P. Das and H.C. Verma; *Journal of Magnetism and Magnetic Materials*, **2006**, 295(1), 44-50

75. Tatsuo Ishikawa, Hiroshi Nakazaki, Akemi Yasukawa, Kazuhiko Kandori and Makoto Seto; *Materials Research Bulletin*, **1998**, 33(11), 1609-1619

76. Yu, H.; Chen, M.; Rice, P. M.; Wang, S. X.; White, R. L.; Sun, S.; *Nanoletters*, **2005**, 5, 379-382.

77. Caruntu, D.; Remond, Y.; Chou, N.H.; Jun, M.; Caruntu, G.; He, J.; Goloverda, G.; O'Connor, C.; Kolesnichenko, V, *Inorg. Chem*, **2002**, 41, 6137-6146.

78. Kenji Kawaguchia, K; Jaworskib, J; Ishikawaa, Y; Sasakia, T; Koshizaki, N; *Journal of Magnetism and Magnetic Materials*, **2007**, 310(2)(3), 2369-2371

79. C.G. Hu, Y. Li, J.P. Liu, Y.Y. Zhang, G. Bao, B. Buchine and Z.L. Wang; *Chemical Physics Letters*, **2006**, 428(4-6), 343-347

80. Jong-Eun Park, Mahito Atobe and Toshio Fuchigami; *Ultrasonics Sonochemistry*, **2006**, 13(3), 237-241

81. R. Abu Mukh-Qasem and A. Gedanken; *Journal of Colloid and Interface Science*, **2005**, 284(2), 489-494

82. Eun Hee Kim, Hyo Sook Lee, Byung Kook Kwak and Byung-Kee Kim; *Journal of Magnetism and Magnetic Materials*, **2005**, 289, 328-330

83. Hui Wang, Shu Xu, Xiao-Ning Zhao, Jun-Jie Zhu and Xin-Quan Xin; *Materials Science and Engineering B*, **2002**, 96(1), 60-64

Chapter 3: Synthesis and Characterization of Gold- Magnetite Nanoparticles

3.1 Abstract

Two novel synthetic routes to formation of gold-magnetite nanoparticles have been designed. The first method involved treatment of preformed magnetite nanoparticles with ultrasound in aqueous media with dissolved tetrachloroauric acid. The other route involved irradiation of preformed magnetite nanoparticles by UV radiation in aqueous media with dissolved tetrachloroauric acid. Both the methods resulted in the formation of gold-magnetite nanocomposite materials. These materials maintained the morphology of the original magnetite particles. The morphology of the gold particles could be controlled by adjusting experimental parameters, like addition of small amounts of solvent modifiers such as methanol, diethylene glycol, and oleic acid as well as variation of the concentration of the tetrachloroauric acid solution and time of the reaction. The nanocomposite materials were magnetic and exhibited optical properties similar to gold nanoparticles.

3.2 Introduction

Nanoparticles are small crystalline particles with sizes in the range of 1-100 nm, located in the transition region between molecules and microscopic (micron-size) structures. There are various types of nanoparticles synthesized, such as insulating (ceramics), metallic and semiconductor. Recently, hollow nanocrystals have also been synthesized which are spherical shells on the nanoscale[1].

Surface modification of nanometer sized inorganic-core particles with a different inorganic shell material to form core/shell type nanostructures has become an important route to functional nanomaterials. Such modification has brought about interesting physical and chemical properties of nanostructured materials that have shown important technological applications[2-4].

Monodisperse particles (i.e. particles of uniform size) dispersed in a fluid are achievable and this is one of the reasons for the increased interest in nanoparticles in recent times[6]. Nanosize particles have a tendency to stick to surfaces and in some cases to each other, forming clusters of particles. This is caused by the relatively large electromagnetic forces, i.e., when particles carry a net charge there is a strong electrostatic repulsion between them, by Coulomb's law, and they stick strongly to oppositely charged particles, or uncharged polarizable surfaces. Nanoparticles of ferroelectric or ferromagnetic materials demonstrate a strong dipole-dipole interaction while nonpolar particles polarize and interact through van der Waals forces. Nanoparticles can be self-assembled, which is another reason for interest in them.

Nanoparticles have been produced and used for a very long time. They are usually used as pigments in inks, paints and glazes[7]. They are also an essential ingredient in sun protection lotions, and in other cosmetics. Nanoparticle applications can be separated into different categories according to the role played by the particles. The simplest case is where their size,

shape, surface chemistry, or other physical properties, affect their immediate environment. They have also been recognized to function as catalysts for carbon nanotube growth. Another application is where the particles communicate information on the local environment or modify some local physical property in a way that can be detected in real-time.

The finite size and surface effects gives rise to some noteworthy phenomena of magnetic nanoparticles including superparamagnetism, high field irreversibility and high saturation field[8]. The fact that particles of a ferromagnetic material below a critical size (<15 nm) would consist of a single magnetic domain was evident from the work of the researchers.[9] The particles show an atomic paramagnetic behavior (superparamagnetism) and have an extremely large magnetic moment above a certain temperature called the blocking temperature.

Applications such as medical diagnosis and curative therapy require these particles to be stable at physiological pH and salinity conditions. The particle size is a key issue since the precipitation due to gravity can be avoided with smaller particles. On the other, hand steric and coulombic repulsions can also be of importance with respect to charge and surface chemistry.

It is necessary to coat these magnetic nanoparticles with a biocompatible polymer during or after synthesis to prevent formation of large aggregation and biodegradation in systems for in vivo applications[10]. Among the range of magnetically responsive components (from magnetite to summarium-cobalt systems) magnetite and its oxidized form (γ-Fe_2O_3) are most commonly employed. Nickel and cobalt are susceptible to oxidation and have alarming toxicity. So they are of little or no interest for in vivo application. Thus for in vivo biological applications the magnetic particles must be synthesized from non-toxic, non-immunogenic material with small particle size to maintain after-injection circulation through the capillary systems of organs and tissues. Furthermore it is also necessary to have a higher magnetization for the particles so that

their movement can be controlled by an external magnetic field and can be immobilized to the targeted pathogenic tissue[11].

For in vitro applications, restrictions are a bit relaxed with respect to sizes. Superparamagnetic nanocrystals dispersed in submicrometric diamagnetic particles with long sedimentation times can be used. The advantage appears in the functionality of the nanoparticles. For all applications, the size, shape, and surface chemistry of the particles as well as their magnetic properties are always of prime importance.

Recently many attempts have been made to develop processes and techniques that would yield core shell uniform nanoparticles with controlled size and shape. Developments in nanotechnology demand building blocks with increasing structural and compositional complexity, which can be reproducibly self-assembled into functional materials. In this regard, nanoparticles with core-shell morphologies represent a new type of construction unit consisting of two dissimilar compositional and structural domains. Such materials should have enhanced physical and chemical properties and a broader range of applications than their single-component counterparts.[12-15]

During the last several years, interest in the study of nanostructured materials has been increasing at an accelerating rate, stimulated by recent advances in materials synthesis and characterization techniques and the realization that these materials exhibit many unique and interesting physical and chemical properties with a number of potential technological applications. As never before, magnetic materials are the key to the future of the storage industry.

Preparation of gold-magnetite nanocomposites, especially those with a core-shell structure[12], has been a topic of much interest. Magnetic nanoparticles have a wide range of

potential applications[13], including uses as medical diagnostic tools[13], drug delivery systems[13-15], and biosensors[13,14] as well as molecular sensors[16]. Effective use of magnetic nanoparticles for these purposes requires several characteristics such as uniform and controllable particle size, shape, and morphology, substantial and reliable magnetic properties[17,18], low toxicity, stability in biological or environmental systems[13,14], and readily functionalizable surfaces to allow chemical and biological selectivity[19]. Gold coated magnetite has been proposed as an effective material that would meet these requirements. It has been well established that gold can be functionalized with thiolated organic molecules[20] and via amide coupling chemistry[21]. Researchers have successfully bound thiol modified DNA and various other enzymes to gold particles[22].

Obtaining novel materials with controlled size or shape[23,24] under mild conditions and with safe precursors is an issue that has engaged many researchers. Sonic energy has been routinely used in the field of materials science for many years. Its chemical effects have recently come under investigation for the acceleration of chemical reactions[25,26] and for the synthesis of

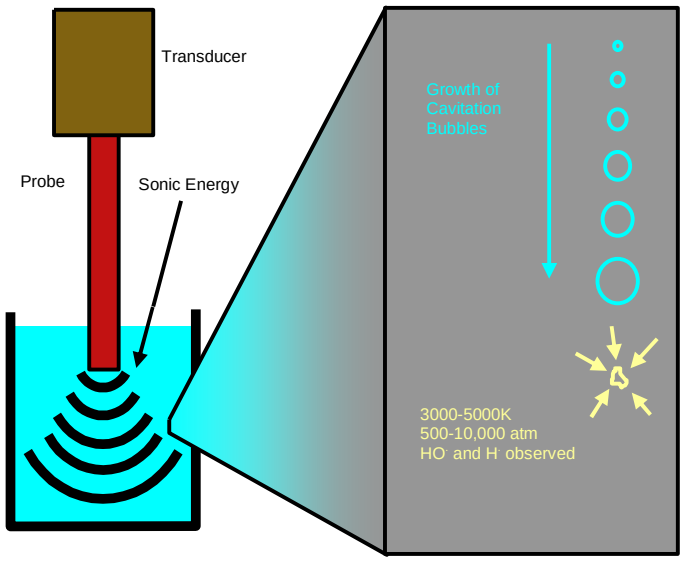

Figure 3.1. Schematic of Sonochemical Process

new materials[25], as well as for the generation of novel materials with unusual properties[26]. Many reactions which are normally sluggish can be accelerated by application of ultrasound. The acceleration is due to either physical or chemical effects of cavitation. Physical effects can enhance the reactivity of a catalyst by enlarging the surface area or by improving mass transport[26]. Chemical effects of ultrasound enhancement of reaction rates occur through high temperature, high pressure, and highly reactive radical species formed during cavitation[26].

Cavitation in a liquid occurs due to the stresses induced in the liquid by the passing of a sound wave through the liquid[25]. A sound wave consists of compression and decompression/rarefaction cycles. If the pressure during the decompression cycle is low enough, the liquid can be torn apart to leave small bubbles[25,26]. These cavitation bubbles grow during subsequent decompression phases, and contract during compression phases. Because of an imbalance between growth and contraction, the bubbles increase in size until they are no longer stable. At this point the bubbles implode violently during the next compression. During implosion temperatures can reach an estimated 5000°C, pressures can reach several hundreds of atmospheres, and solvent molecules can be homolytically cleaved to form species such as hydroxyl radical and hydrogen atoms[26]. Formation of gold nanoparticles during sonication has been previously reported, and the mechanism was proposed to occur through hydrogen atom reduction of dissolved gold[27].

3.3 Experimental Procedure

In our study we have introduced two new approaches of synthesizing magnetic nanoparticles. They are

1. Sonochemical synthesis of gold magnetite nanoparticles with various surfactants.

2. Synthesis of gold magnetite nanocomposites by UV radiation (variation of time and variation of concentration)

Hydrogen tetrachloroaurate trihydrate ($HAuCl_4.3H_2O$), methanol, ethanol, diethylene glycol, and oleic acid were obtained from Aldrich. Purified water was obtained by using NANOpureUV water system (Barnstead) with a distilled water feed.

Magnetite was prepared as reported[29,30,31] by dissolving $FeCl_2.4H_2O$ and $FeCl_3.6H_2O$ in diethylene glycol in a Schlenk flask under protection with argon. Separately, NaOH was dissolved in diethylene glycol. The solution of NaOH was added to the solution of metal chlorides while stirring at room temperature causing an immediate color change. The temperature of the resulting solution was raised during 1-1.5 h to 210-220 ^oC and then kept constant for 0.5-1 h. As the solution turned turbid, the reaction was terminated by adding oleic acid dissolved in DEG. This addition caused immediate precipitation of solids. The mixture was cooled to room temperature and then centrifuged. The precipitate was washed with methanol and redissolved in toluene. The resulting solution was centrifuged and mixed with 1-2 volumes of methanol. The precipitate was separated by centrifuging, washed with methanol, then stored in methanol.

3.4 Experimental Procedure of Sonochemical Synthesis

In this study, sonochemical methods were utilize to produce gold-magnetite nanocomposite materials. A stock solution of 0.1 mM $HAuCl_4$ (aq) was prepared. An aliquot (50 mL) of this solution was sparged with argon for 20 min. Methanol (100 μL), diethylene glycol (100 μL), or oleic acid (100 μL) was added and sparging was continued for another 5 min. Magnetite nanoparticles[25] (1 mg suspended in 100 μL of methanol) were added to the above solution and sparging continued for another 10 min. The sample was then sonicated in a jacketed, water cooled (20°C) reaction vessel under an argon atmosphere for 10 min at 50% amplitude using an ultrasonic processor (600W, ACE Glass, Vineland, NJ). The solution turned pink/purple during sonication. The resulting solution was then transferred into a test-tube and kept in front of a magnet for at least one day until the whole solution became clear and colorless as the gold-magnetite nanocomposite material was pulled against the wall of the test tube by the magnet. The transparent solution was carefully removed from the test tube while the particles were kept against the test tube wall with the magnet. The material was washed with water and re-separated twice before the nanocomposite particles were dispersed in 2 ml of ethanol and stored in capped tubes.

Portions of the ethanol suspensions were put onto copper transmission electron microscope (TEM) grids, and the solvent was allowed to evaporate prior to TEM analysis with a JEOL Model 2010 TEM, including energy dispersive spectroscopy (EDS) to determine particle composition. Additional portions of the materials were digested using aqua regia and were subsequently analyzed by inductively coupled plasma (ICP) atomic emission spectroscopy in order to determine elemental composition. For these determinations, multiple batches of

nanocomposite materials were prepared and pooled. A small aliquot of the pooled material was sampled and analyzed by ICP. Therefore, the ICP data were representative of the bulk nanocomposite material. Absorbance of the nanoparticles was measured with a Cary 5E absorbance spectrometer (Varian, Inc., Palo Alto, CA) using ethanol suspensions. Magnetic characterization was performed with a Quantum Design MPMS-5S superconducting quantum interference device (SQUID) magnetometer.

3.5 Results and Discussions

3.5.1 Magnetic Separation of Au-magnetite Nanocomposites

Sonication of magnetite nanoparticles in the absence of $HAuCl_4$ did not cause any observable changes in the TEM images of the magnetite particles. In the presence of $HAuCl_4$,

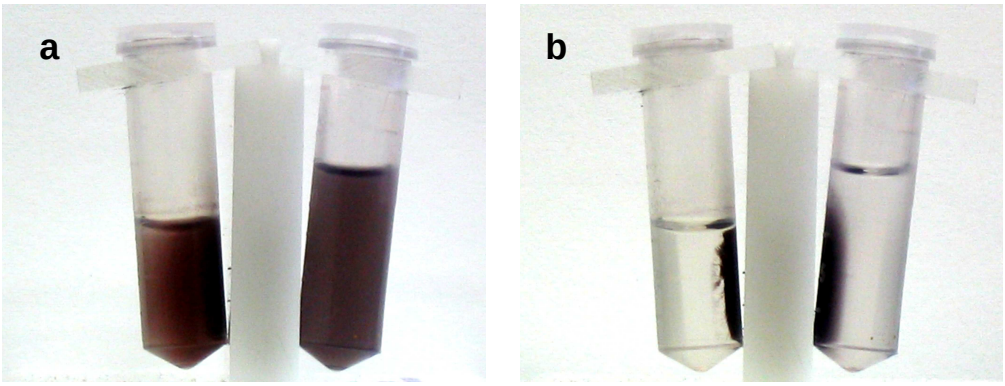

Figure 3.2. Gold magnetite nanocomposite materials suspended in ethanol prior to (a) and after (b) magnetic separation. The reddish-brown/purple color is from gold nanoparticles. Note that all the color is removed after separation, indicating that the gold was attached to magnetite

sonication resulted in the appearance of a red or purple coloration of the particles, as depicted in Figure 3.2. Exposing these materials to a magnetic field resulted in removal of all colored material from the liquid. This result indicates that the gold particles must be physically or chemically attached to the magnetite. This attachment is at least strong enough to cause the suspended gold particles to migrate with the magnetite in a magnetic field.

3.5.2 TEM Images

TEM images of these particles revealed the presence of both gold and magnetite forming a nanocomposite material. Observation of the particles in Figure 3.3 suggests a high degree of agglomeration between magnetite particles. This degree of agglomeration is likely due to the

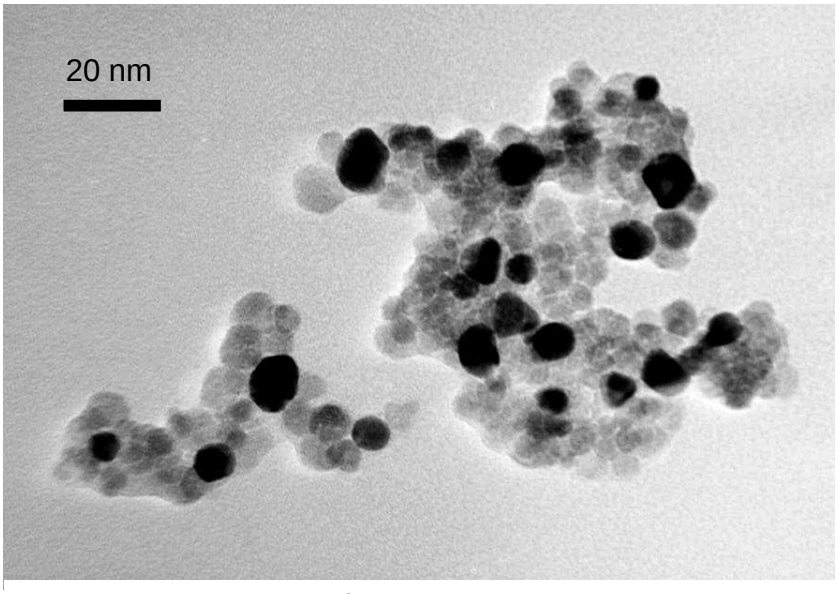

Figure 3.3. TEM image of gold-magnetite nanocomposite material formed by sonication of magnetite in aqueous $HAuCl_4$ with added methanol. Dark particles are gold, grey particles are magnetite.

removal of the initially present capping ligand during the sonication process. Figure 3.4 depicts the TEM for gold-magnetite nanocomposite material formed with diethylene glycol as additive, and Figure 3.5 presents the TEM image when oleic acid was used. When diethylene glycol was used, more uniform gold particles were observed.

In addition, the Fe/Au ratio decreased compared to the material prepared using methanol as an additive. With oleic acid added, substantially smaller gold particles were observed, and the Fe/Au ratio also decreased. Therefore, adjusting the identity and amounts of these additives may

provide a mechanism for preparing gold-magnetite nanocomposite materials with a range of selected Fe/Au compositions and particle sizes.

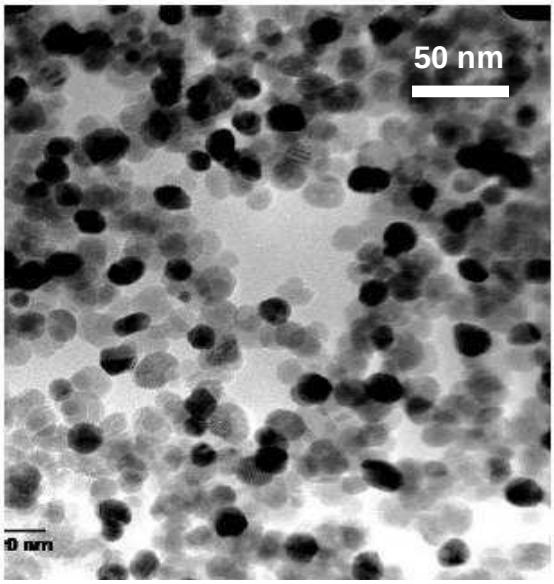

Figure 3.4. TEM image of gold-magnetite nanocomposite formed with diethylene glycol additive

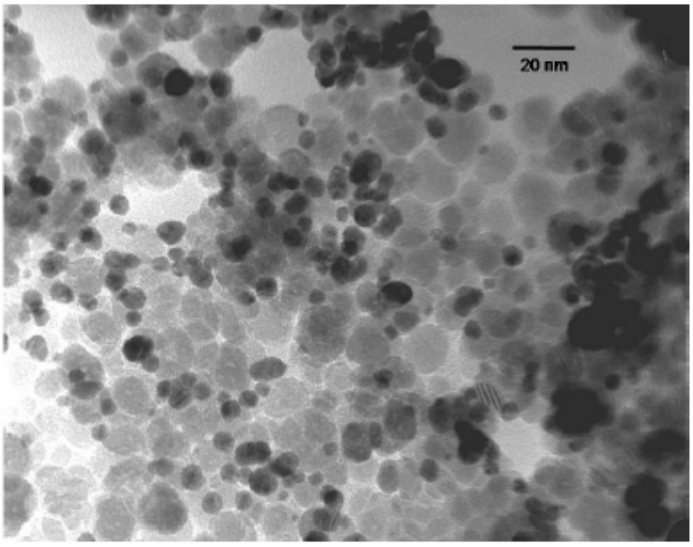

Figure 3.5. TEM image of gold-magnetite nanocomposite formed with oleic acid additive

We did some ICP measurements to verify the respective observations from the TEM images. The ICP results are presented below.

Table 3.1. The ratios of Au and Fe in the samples with MeOH, DEG and Oleic acid. Data obtained from ICP analysis of digested samples.

Sample prepared with	Au weight %	Fe weight %
Methanol	26	74
Diethylene Glycol	57	43
Oleic Acid	50.4	49.6

Mass balance calculations for the ICP results were performed to validate the ICP results. The measured mass of iron (calculated from ICP measurement) was converted to mass of magnetite (assuming all Fe was Fe_3O_4) and this mass was added to the measured mass of gold. For each of the nanocomposites, the resulting sum was within 5% of the weighed mass of the sample prior to digestion.

3.5.3 EDS Data

EDS analysis of the particles indicated the presence of both iron and gold, for all the sets of experiments. The data presented in this EDS spectrum were collected from multiple particles, and is therefore representative of the composite material. Additional EDS spectra collected on single particles verified that the dark particles in the TEM image (Figure 3.3) are in fact gold and the grey particles contain iron as the only metal.

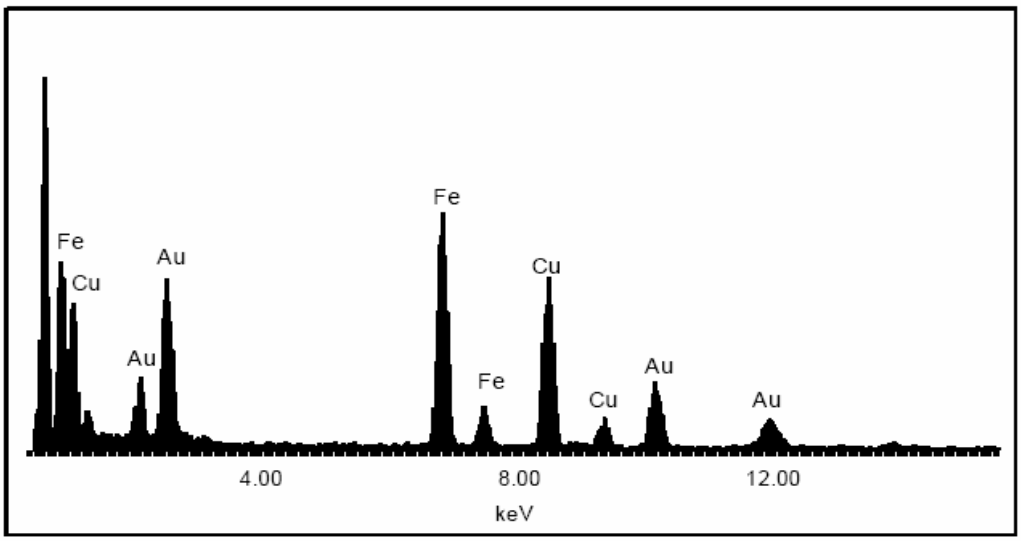

Figure 3.6. EDS spectrum of composite particles depicted in Figure 3.3. Cu and C peaks are from TEM grid

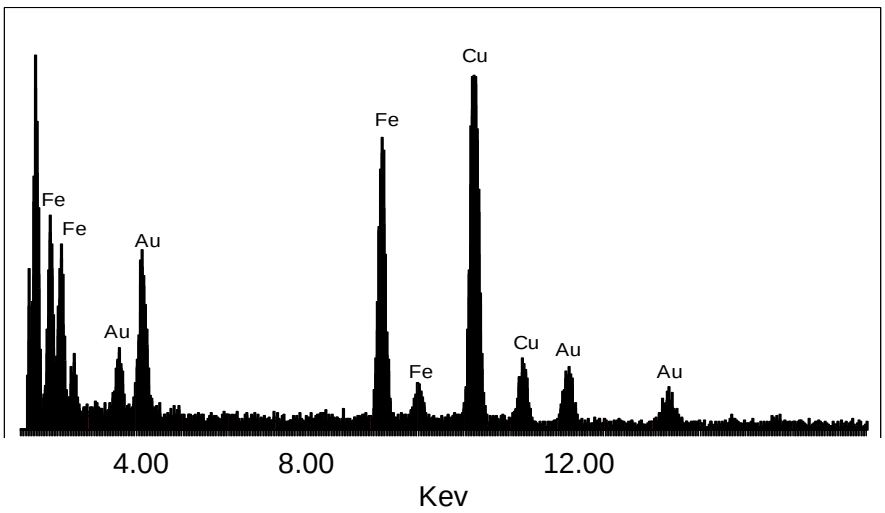

Figure 3.7. EDS Spectra for the Au-magnetite nanocomposites in DEG

3.5.4 Magnetic Measurements

The gold-magnetite nanocomposite material was also characterized to determine its magnetic properties using a SQUID magnetometer. Substantial changes in the magnetic properties of

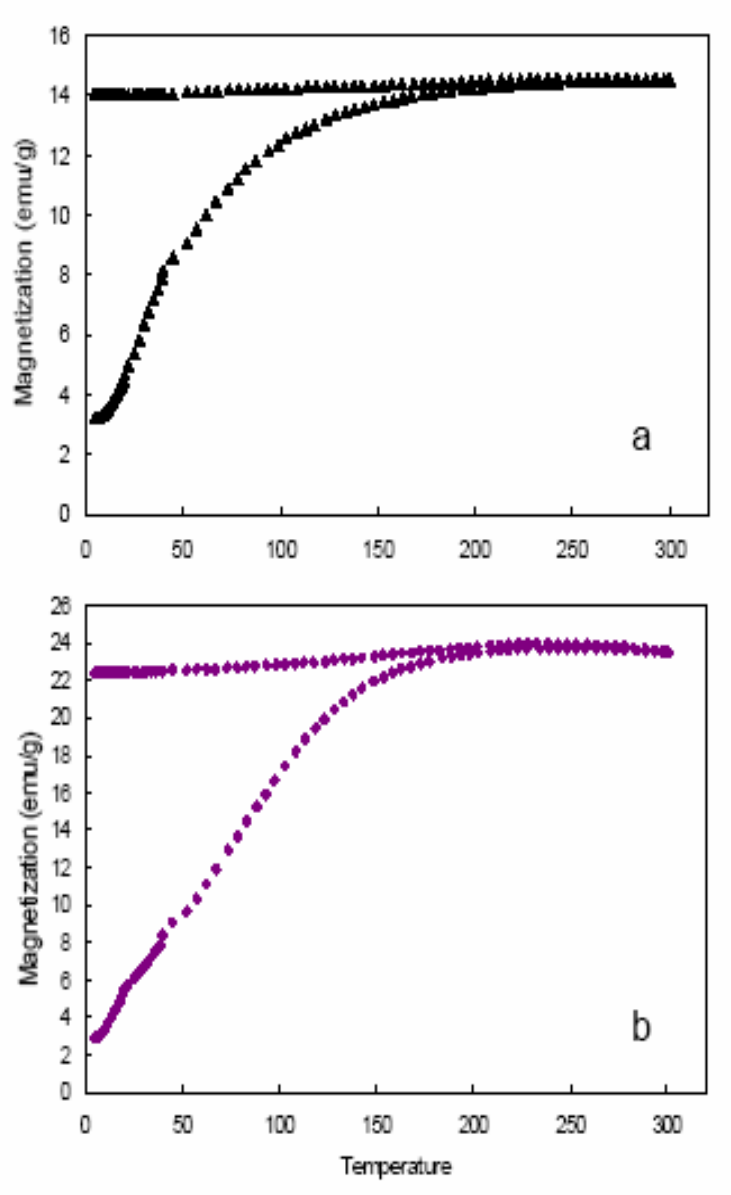

Figure 3.8. Magnetization vs. temperature for magnetite nanoparticles (a) and gold-magnetite nanocomposite material (MeOH) (b). In each panel, the top curve is for the field cooled sample and the bottom curve is for the zero field cooled sample.

these materials were observed compared to the untreated magnetite precursor material. Figure 3.8 compares the magnetization vs. temperature behavior of the untreated magnetite and the gold-magnetite nanocomposite material.

While the general shape of these curves is similar, the gold-magnetite nanocomposite material exhibited a substantially higher magnetization of about 23 emu/g compared to 14 emu/g for the untreated magnetite. The nanocomposites with DEG and oleic acid showed higher magnetization value of ~33 emu/g and 27 emu/g respectively as depicted in Figure 3.9 and 3.10. In all cases, the magnetization was normalized to total mass of magnetite in the sample, so the decrease in magnetization per gram observed for the particles with gold is due to the added mass of the non-magnetic gold.

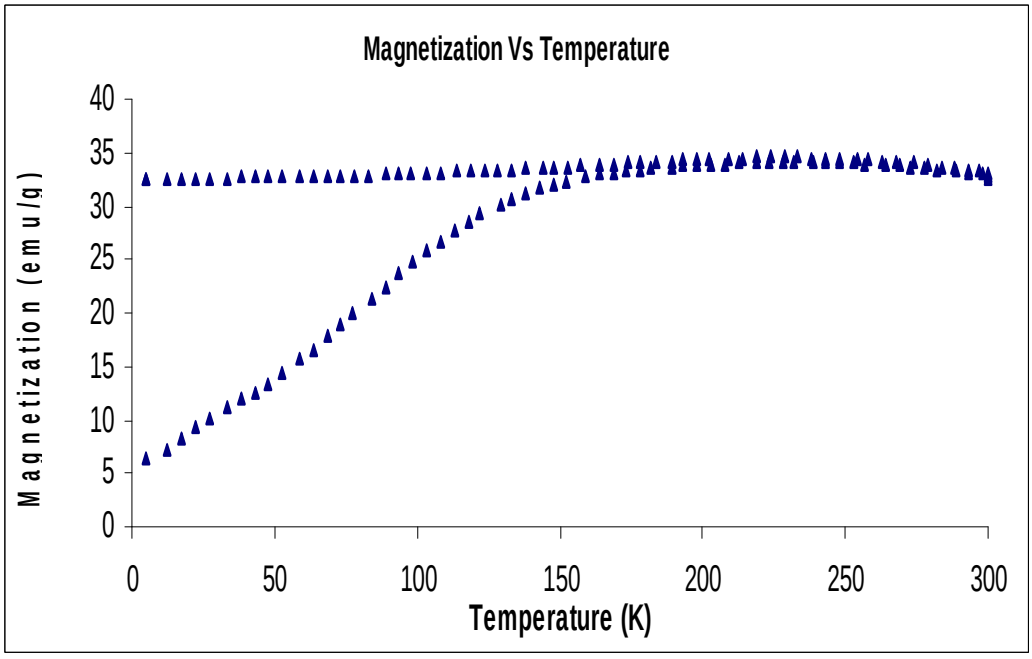

Figure 3.9. Magnetization vs. temperature for gold magnetite nanocomposite material with DEG in 100 Oe

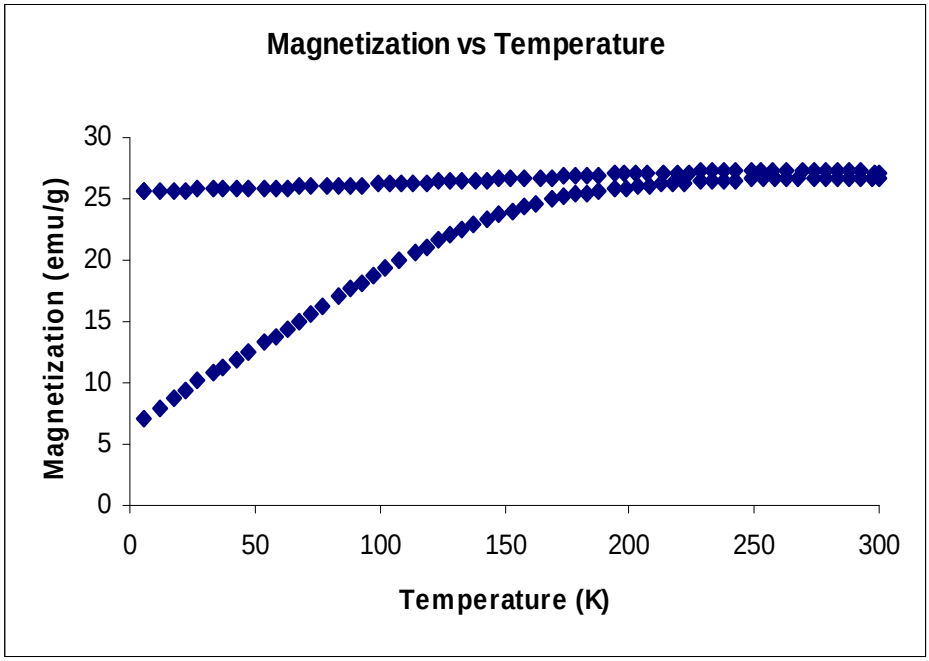

Figure 3.10. Magnetization vs. temperature for gold magnetite nanocomposite material with Oleic Acid in 100 Oe Field.

In addition to the differences in magnetization, the coercivity of the sample changed upon formation of the nanocomposite material. The untreated magnetite had an observed coercivity of 75 Oe, while the gold-magnetite nanocomposite material exhibited a substantially increased coercivity of 200 Oe. These data are depicted in Figure 3.11. Also apparent in this figure, is the significantly larger saturation magnetization (M_s) for the nanocomposite material (M_s ~ 125 emu/g) compared to that of the untreated magnetite (M_s ~ 90 emu/g). The gold-magnetite nanocomposite with DEG as the surfactant had an observed coercivity of 284 Oe, while the gold-magnetite nanocomposite material with Oleic Acid exhibited a coercivity of 155 Oe. These data are depicted in Figure 3.12 and 3.13 respectively. Also apparent from the figures, is the significantly larger saturation magnetization (M_s) for the nanocomposite materials (M_s ~ 186 emu/g) and (M_s ~ 140 emu/g) compared to the untreated magnetite (M_s ~ 90 emu/g).

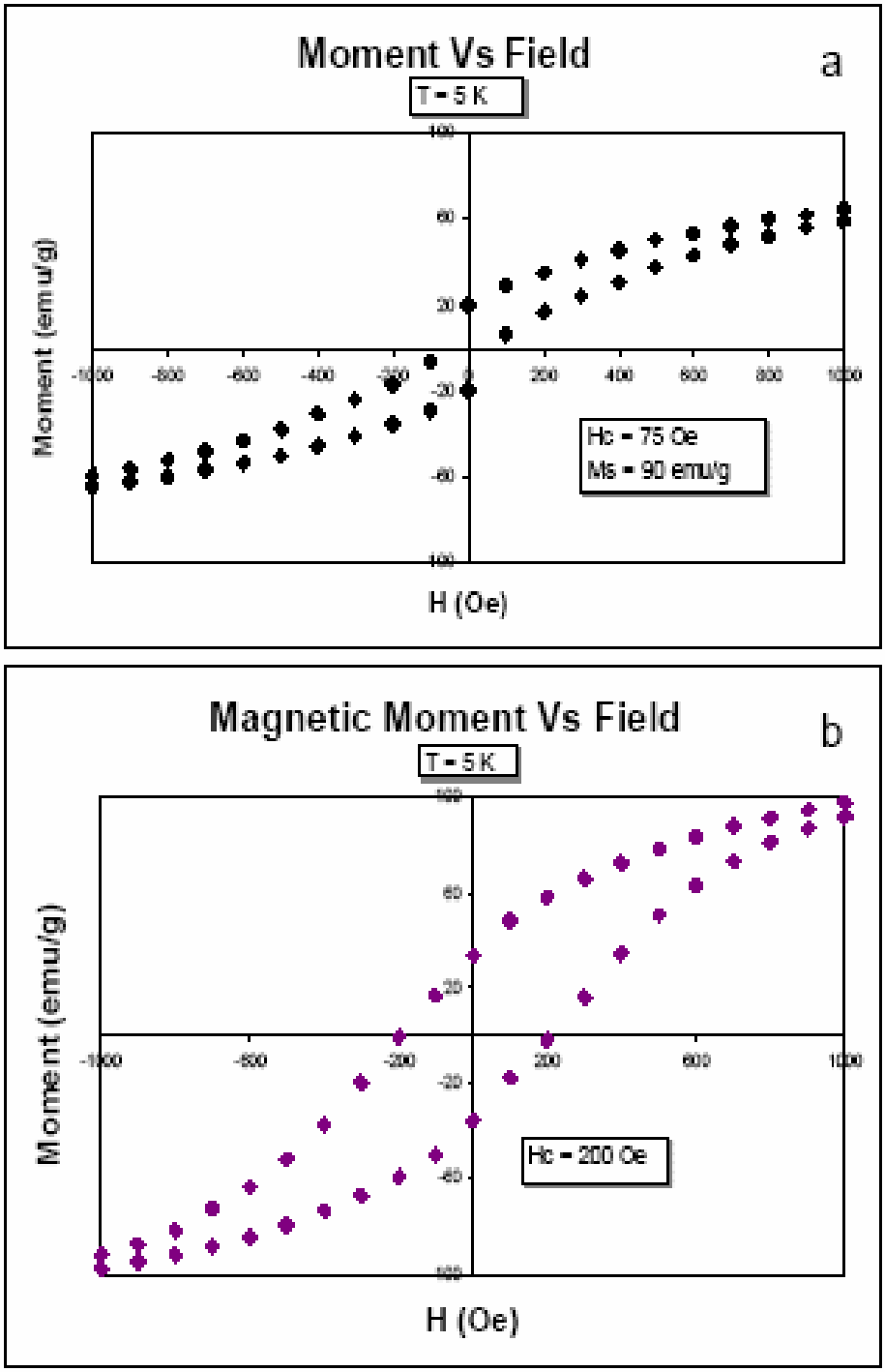

Figure 3.11. Hysteresis loops for untreated magnetite (a) and gold-magnetite nanocomposite material (b).

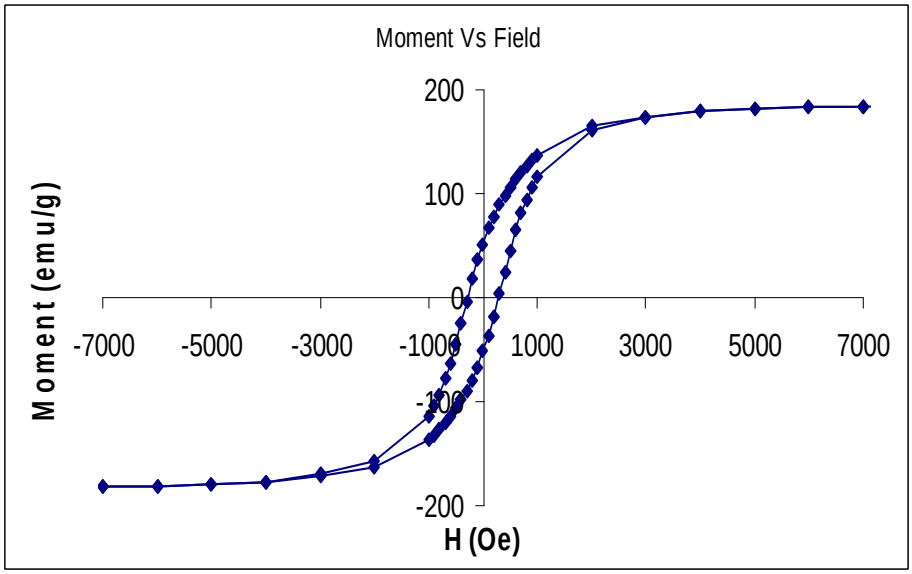

Figure 3.12. Hysteresis loop for gold-magnetite nanocomposite material in DEG at 5K.

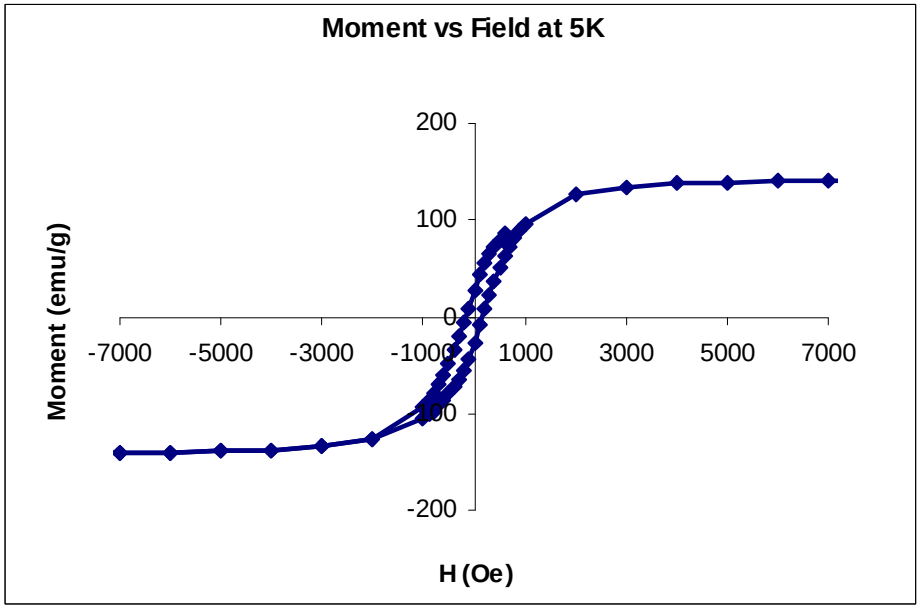

Figure 3.13. Hysteresis loop for gold-magnetite nanocomposite material in Oleic Acid.

The changes in magnetic properties are most likely due to changes in the surface characteristics of the magnetite. During sonication, the capping ligands initially present can be removed. Removal of these capping ligands could cause a change in the surface charge or magnetic domains. Surface modification of the magnetite is also possible under the reactive conditions that occur during sonication. In addition, interactions between magnetite particles could be enhanced by their direct contact, which is not possible with capping ligands present. Finally, interaction of the magnetite surface with gold could contribute to changes in the surface states, yielding altered magnetic properties. A control experiment was performed in which magnetite was sonicated under identical conditions but with no $HAuCl_4$ present. The magnetic properties for these particles showed decreased saturation magnetization (Ms ~ 5 emu/g) compared to untreated magnetite. The fact that magnetite sonicated in the absence of gold exhibited different magnetic properties compared to magnetite sonicated in the presence of gold indicates that the gold plays an important role in controlling the magnetic properties, either through direct gold-magnetite interactions or through alteration of the processes occurring during sonication. Yu, et al. reported that interactions between attached gold and magnetite particles altered the observed magnetic properties of the magnetite through interfacial communication.[12]

3.5.5 Absorbance Data

Figure 3.14 shows the absorbance spectra of the three types of gold magnetite nanocomposites suspended in ethanol. The spectrum of pure gold nanoparticles (30 nm diameter) obtained from a commercial supplier is also included for comparison. The absorbance maximum of the pure gold nanoparticles was observed at 523 nm, while the gold-magnetite nanocomposites showed maxima at longer wavelengths. Gold-magnetite nanocomposites prepared with methanol showed an absorbance peak at 569 nm, and nanocomposites prepared with DEG showed a maximum at 557 nm. The Au-magnetite nanocomposites prepared with oleic acid did not yield a clear absorbance maximum due to excessive scattering by the particles (not shown). The red shift in the gold surface plasmon observed for gold-magnetite nanocomposites is most likely due to interaction of the gold particles with the magnetite to which they are attached. The surface plasmon resonance is highly dependent upon the local microenvironment of the particle,[24] so attachment to magnetite is expected to change the surface plasmon.

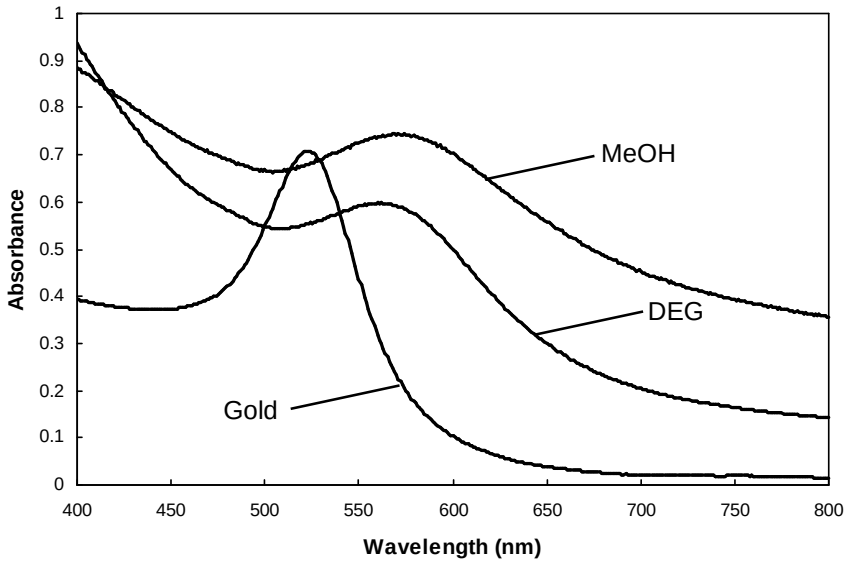

Figure 3.14. The absorbance spectra of gold magnetite nanocomposites suspended in ethanol.

3.6 Experimental Procedure of UV Radiation Synthesis

3.6.1. Time Based Experiment

An aliquot of tetrachloroauric acid solution was placed in a quartz test tube and to it was added 100 µl of preformed magnetite suspended in methanol (~1 mg of magnetite). It was shaken thoroughly so that the magnetite was uniformly dispersed in the aqueous solution. The color of the solution was brown. Then the test tube was inserted in a Rayonet (Southern New England Ultraviolet Company, Branford, CT) merry-go-round photochemical reactor which produced UV radiation in the 254 nm range. Four different time periods of reaction were chosen. The time periods were 15 min, 30 min, 45 min and 60 min. The color of the solution turned from brown to light purple or dark purple according to the respective reaction time periods. The whole solution was transferred into a plastic centrifuge tube and placed in front of a magnet for a day. The purple particles were separated and the solution became colorless. These particles were then collected, washed with water twice and separated in front of the magnet each time. After being washed with water, the particles were washed with ethanol and resuspended in 2 ml of ethanol. The synthesized nanoparticles were characterized by TEM, EDS, ICP and XRD.

3.6.2 Concentration Based Experiment

Different concentrations (0.05mM, 0.01mM, 0.1mM and 0.2mM) of aqueous tetrachloroauric acid solution were prepared from an aqueous stock solution. These were put into different quartz test tubes. 100µl of preformed magnetite suspended in methanol (~1 mg) was added to each of the four different concentrated solutions. They were thoroughly shaken and put

into irradiation apparatus (254 nm) for a reaction time period of 1 hour. The color of the solution was brown before it was irradiated with UV. After an hour the color of the solutions turned light red to dark purple, depending on the concentration of gold in the original solution. A similar procedure from the time based experiment was followed to separate the particles from the solution. The whole solution was transferred into a plastic centrifuge tube and placed in front of a magnet for a day. The purple particles were separated and the solution was colorless. These particles were then collected, washed with water twice and separated in front of the magnet each time. After being washed with water, the particles were washed with ethanol and resuspended in 2 ml of ethanol. The synthesized nanoparticles were characterized by TEM, EDS, ICP and XRD.

3.7 Results and Discussions

3.7.1 TEM IMAGES

The morphology of the magnetite nanoparticles was examined with a JEOL JEM 2010 transmission electron microscope (TEM) at 200KV. TEM samples were prepared by a conventional technique consisting of depositing several drops of the gold magnetite particles suspended in ethanol solution onto carbon coated Cu grids followed by the slow evaporation of the solvent.

Concentration Based Experiment

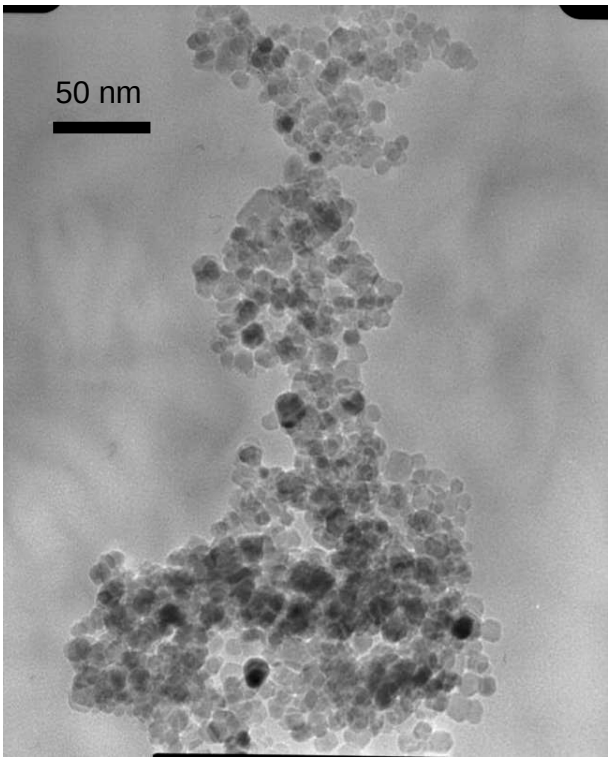

Fig 3.15. TEM image of gold-magnetite nanoparticles irradiated with UV light for 60 min in 0.05 mM $HAuCl_4$. The dark particles are gold and the gray particles are magnetite

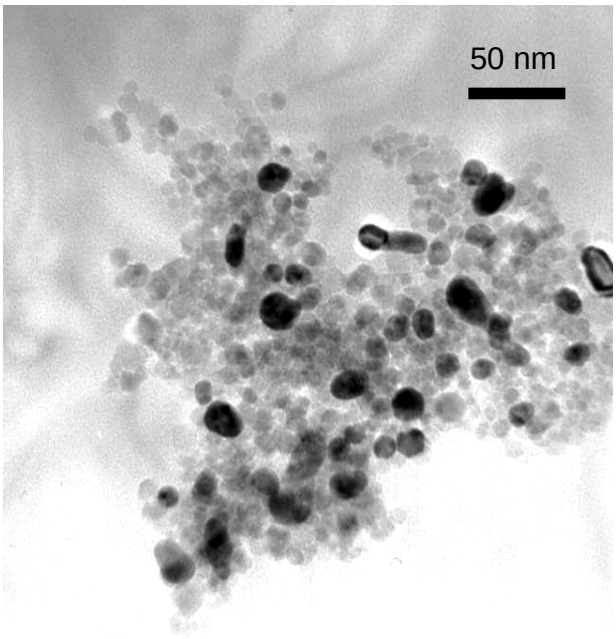

Fig 3.16. TEM image of gold-magnetite nanoparticles irradiated with UV light for 60 min in 0.1 mM $HAuCl_4$.

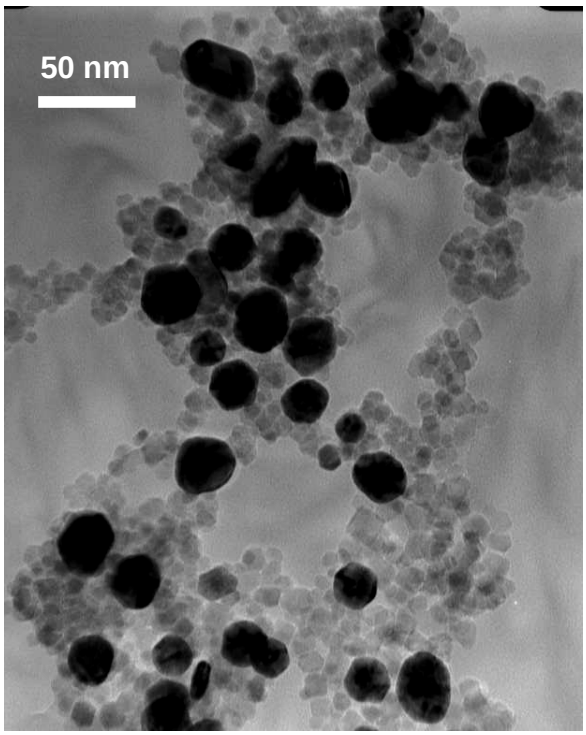

Fig 3.17. TEM image of gold-magnetite nanoparticles irradiated with UV light for 60 min in 0.2 mM $HAuCl_4$. The dark particles are gold and the gray particles are magnetite

Time Based Experiment

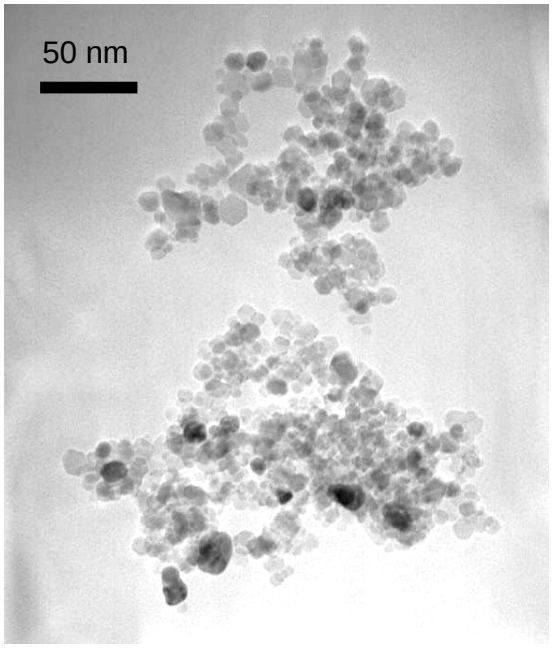

Fig 3.18. TEM image of gold-magnetite nanoparticles irradiated with UV light for 30 min in 0.1 mM $HAuCl_4$.

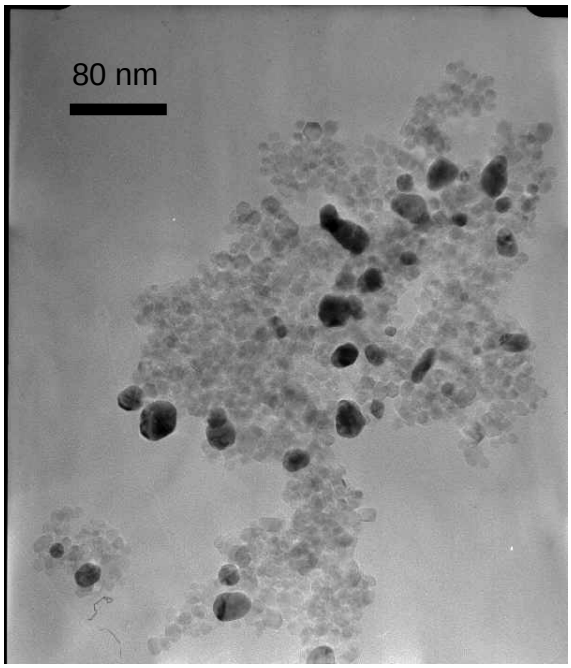

Fig 3.19. TEM image of gold-magnetite nanoparticles irradiated with UV light for 45 min in 0.1 mM $HAuCl_4$. The dark particles are gold and the gray particles are magnetite

In the concentration based experiment from the TEM pictures it is evident that as we increase the concentration of the tetrachloroauric acid solution, the amount of gold nanoparticles as well as their size tended to increase. The number of gold particles, ie. the number of dark dots (gold is seen as dark dots in TEM) increases as we go from Fig 3.15 to Fig 3.17. This result was also supported by the EDS spectra (section 3.7.2) as well as the ICP data. Since the nanocomposites were attracted towards a magnet even after washing it with ethanol and water, it can be concluded that the gold particles were attached to the magnetite nanoparticles.

In the time based experiment we also observed that as we increased the irradiation time from 15 min to 60 min the amount of the gold particles increased. This was also concluded from EDS (section 3.7.2) and the ICP data

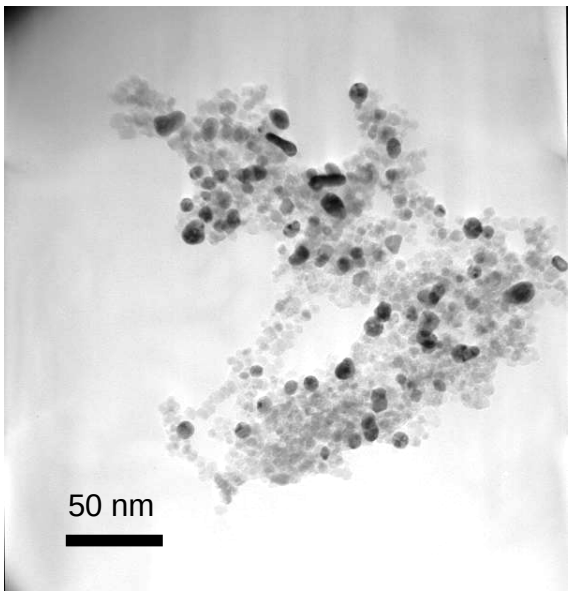

Fig 3.20. TEM image of gold-magnetite nanoparticles irradiated with UV light for 60 min in 0.1 mM $HAuCl_4$. The dark particles are gold and the gray particles are magnetite

3.7.2 EDS Spectra

The EDS spectra for the gold magnetite nanoparticles also show the presence of both Au and Fe. This can be seen in Figures 3.21 and 3.22. The data presented in this EDS spectrum were collected from multiple particles, and is therefore representative of the composite material. Additional EDS spectra collected on single particles verified that the dark particles in the TEM images are in fact gold and the grey particles contain iron as the only metal.

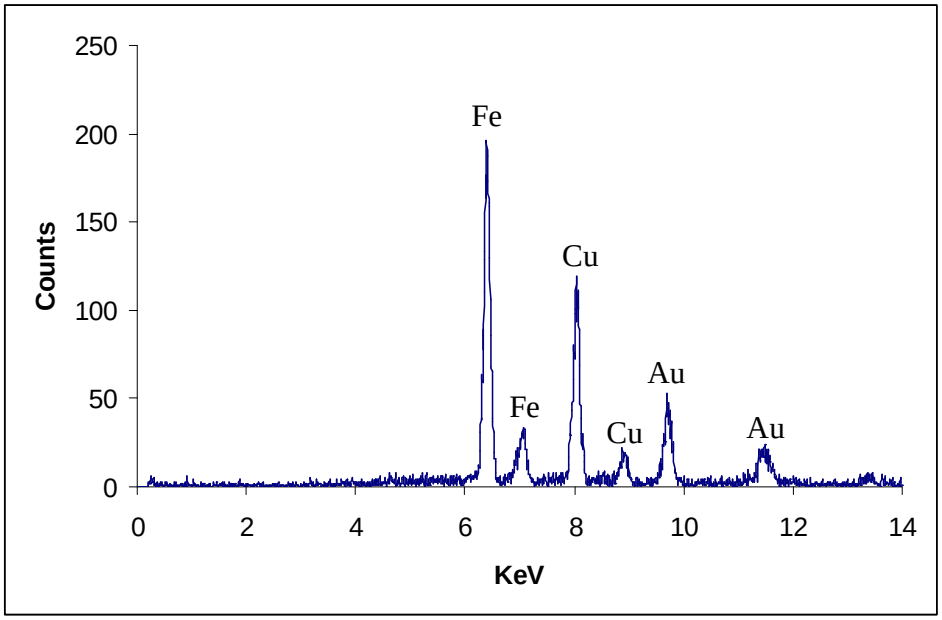

Fig. 3.21. EDS spectrum of composite particles depicted in Figure 3.16. Cu peaks are from TEM grid

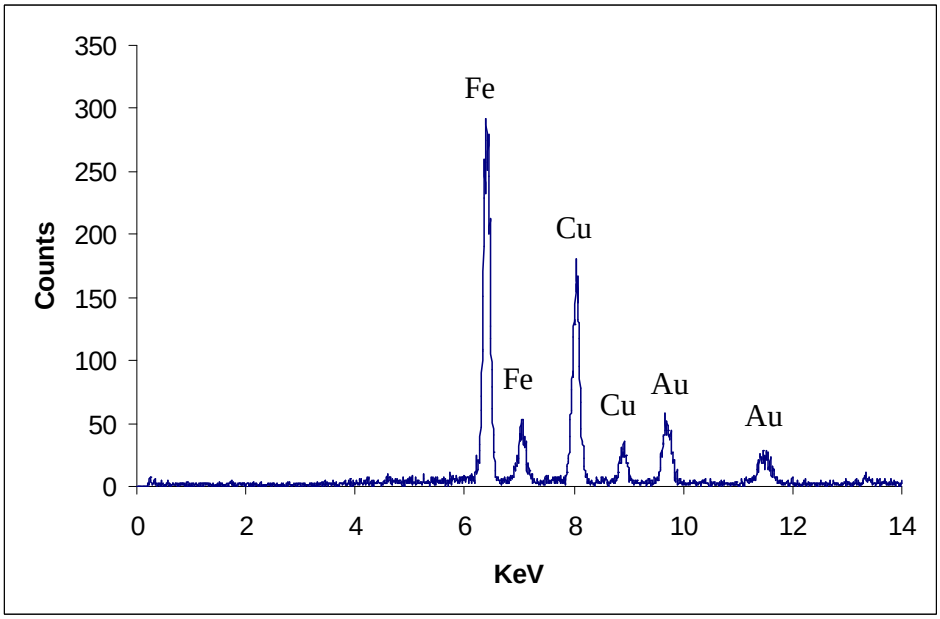

Fig. 3.22. EDS spectrum of composite particles depicted in Figure 3.20. Cu peaks are from TEM grid

3.8 Conclusion

The experiments conducted to date have resulted in a novel method for preparation of gold-magnetite nanocomposite materials. These materials substantially maintain the optical properties of gold. At the same time, the gold can be separated or otherwise manipulated with a magnetic field. The new methodology also includes parameters that can be adjusted to vary the Au/Fe ratio and particle sizes of the gold structures within the nanocomposites. These new particles have potential use in biomedical applications, in sensor applications, and in electronic, optoelectronic, and magneto-optic devices. Furthermore, the fundamental interactions occurring at the gold-magnetite interface are poorly understood. These new nanocomposite materials provide an opportunity to study these interfaces and gain knowledge about interparticle interactions within nanoscale materials.

3.9 References

1. Lyon J. L.; Fleming D. A.; Stone M.B.; Schiffer P.;Williams M.E., *Nanoletters* **2004**, *4*, 719-723.
2. Salata, O.V.; *J. Nanobiotech.* **2004**, 2**:**3 doi:10.1186/1477-3155-2-3
3. Hirsch, L. R.; Jackson, J. B.; Lee, A.; Halas, N. J.; West, J. L., *Anal. Chem.* **2003**, *75*, 2377-2381.
4. Halbreich, A.; Roger, J.; Pons, J. N.; Geldwerth, D.; Da Silva,M. F.; Roudier, M.; Bacri, J. C. *Biochim.* **1998**, *80*, 379-390.
5. Raschke, G.; Brogl, S.; Susha, A.S.; Rogach, A.L.; Klar, T.A.; Feldmann, J., *Nanoletters*, **2004,** *4(10)*, 1853-1857.
6. Templeton, A.C.; Pietron, J.J.; Murray, R.W.; Mulvaney, P., *J. Phys. Chem. B*, **2000**, *104*, 564- 570.
7. Malinsky, M.D.; Kelly, K.L.; Schatz, G.C.; Van Duyne, R.P., *J. Am. Chem. Soc*., **2001**, *123*, 1471-1482.
8. Storhoff, J. J.; Elghanian, R.; Mucic, R. C.; Mirkin, C. A.; Letsinger, R. L. *J. Am. Chem. Soc.* **1998**, *120*, 1959-1964.
9. Brust, M.; Walker, M.; Bethell, D.; Schiffrin, D.; Whyman, R. *J. Chem. Soc. Chem. Commun.* **1994**, 801-802.
10. Templeton, A.; Chen, S.; Gross, S.; Murray, R. W. *Langmuir* **1999**, *15*, 66-76.
11. Zeng, H..; Li, J.; Wang, Z. L.; Liu, J. P.; Sun, S. *Nanoletters*, **2004**, *4*, 187-190.
12. Yu, H.; Chen, M.; Rice, P. M.; Wang, S. X.; White, R. L.; Sun, S. *Nanoletters*, **2005**, *5*, 379-382.

13. Storhoff, J. J.; Elghanian, R.; Mucic, R. C.; Mirkin, C. A.; Letsinger, R. L. *J. Am. Chem. Soc.* **1998**, *120*, 1959-1964.

14. He, B.; Tan, J.J.; Liew, K.Y.; Liu, H., *J. Mol. Catalysis A*, **2004**, *221*, 121-126.

15. Evanoff, D.D.; Chumanov, G., *J. Phys. Chem. B*, **2004** *108*, 13957-13962.

16. Ferrel, G.W.; Crum, L.A., *J. Acoustical Soc. Am.*, **2002**, *112*, 1196-1201.

17. Thompson, L.H.; Doraiswamy, L.K., *Ind. Eng. Chem. Res.*, **1999**, *38*, 1215-1249 .

18. Okitsu, K; Yue, A.; Tanabe, S.; Matsumoto, H.; Yobiko, Y., *Langmuir*, **2001**, *17*, 7717-7720.

19. Su, C.H.; Wu, P.L.; Yeh, C.S., *J. Phys. Chem. B*, **2003**, *107*, 14240-14243.

20. Pradhan, A.; Jones, R.; Tarr, M. A. Novel synthetic routes to formation of magnetic nanocomposites with noble metals. *Abstracts of Papers, 229th ACS National Meeting, San Diego, CA*, **2005**, INOR-151; manuscript submitted.

21. Caruntu, D.; Remond, Y.; Chou, N.H.; Jun, M.; Caruntu, G.; He, J.; Goloverda, G.; O'Connor, C.; Kolesnichenko, V, *Inorg. Chem*, **2002**, *41*, 6137-6146.

22. Daniela Caruntu, Gabriel Caruntu, Charles J O'Connor; J. Phys. D: Appl. Phys., **2007**, 40, 5801–5809

23. Daniela Caruntu, Gabriel Caruntu, Yuxi Chen, Charles J. O'Connor, Galina Goloverda, Vladimir L. Kolesnichenko; *Chem. Mater.*, **2004**, 16 (25), 5527 -5534

24. S. K. Ghosh, T. Pal; Chem. Rev., 107 (2007), 4797-4862.

Chapter 4. Synthesis and Characterization of Gold-Titania-Magnetite Nanoparticles

4.1 Abstract

TiO_2 nanoparticles with embedded magnetite were suspended in aqueous $HAuCl_4$ and ultraviolet irradiated to photodeposit gold on the surface. The degree of gold coating and the wavelength of absorbance could be controlled by adjusting the concentration of $HAuCl_4$. Absorbance maxima were between 540-590 nm. Particles exhibited superparamagnetic properties (blocking temperature ~170 K) whether or not they were coated with gold. These particles have potential applications as drug delivery agents, magnetic imaging contrast agents, and magnetically separable photocatalysts with unique surface properties.

4.2 Introduction

Gold-coated magnetite nanoparticles have become increasingly important in research because their combination of magnetic and chemical properties makes them suitable for biomedical applications.[1–5] Magnetic nanoparticles for cancer treatment or detection are moving to market through testing stages or are already in use.[6,7] Several recent reports have indicated some success in producing gold-magnetite composite particles.[1–3,8] Caruntu and coworkers were able to attach 3-nm gold nanoparticles onto larger magnetite particles by coating the magnetite with a positively charged capping ligand and mixing them with negatively charged gold particles.[9] However, this approach was not able to achieve a complete shell of gold around the magnetite.

Lyon et al. reported the reduction of gold onto the surface of hematite using hydroxylamine as the reducing agent, but they were unable to attach gold to magnetite without first oxidizing the outer surface of the magnetite to hematite.[1] In other work, a microemulsion method was used to coat iron oxide nanoparticles with gold,[10] but it is not clear whether the iron oxide was maghemite or magnetite. Furthermore, no evidence was presented to support the assumption that gold was coated on the surface of the magnetic particles. Another approach to forming magnetic nanocomposite materials containing gold involved coating polystyrene spheres with magnetite and silicon dioxide coated gold particles using a layering method.

Wang et al. reported the formation of gold coated magnetite by initial synthesis of Fe_3O_4 followed by reduction of $Au(OOCCH_3)_3$ in the presence of the magnetite seed particles.[2] While

the data presented in this report indicate the formation of gold-magnetite composite materials, no strong evidence was presented to support the claim of core-shell structures.

Although some success has been achieved, attaching gold to magnetite nanoparticles remains a challenging task. In an alternate approach, we have utilized titanium dioxide as a bridging agent to achieve particles with a magnetite core and a gold surface. Titanium dioxide was chosen as a bridging layer because magnetite and titanium dioxide show good cohesive properties.[12] Furthermore, titanium dioxide is a good photocatalyst, allowing for photoreduction of gold onto its surface with ultraviolet (UV) irradiation.

Previous reports have indicated that noble metals on the surface of semiconductor nanoparticles can improve photocatalytic properties of the semiconductor through charge separation of electron-hole pairs.[13–15] Photocatalytic deposition of noble metals onto TiO_2 powders has been performed previously,[16] and bimetallic nanoparticles of Ag and Au have also been prepared through a photochemical approach.[17] In a two-step process, we have produced three component nanocomposite materials with a magnetite core, a TiO_2 bridging layer, and gold surfaces. These novel particles have potential use for many biomedical applications such as magnetic resonance imaging (MRI) contrast agents and magnetic drug delivery.

In addition, these particles have potential application as novel magnetic photocatalysts, with the magnetic core allowing easy separation of the heterogeneous catalyst after use[12] and the noble metal surface serving to enhance the catalytic activity.[13–15,18–21] For both biomedical and

photocatalytic applications, easy modification of the gold surfaces with chemical or biorecognition molecules can provide the particles with chemical or biological selectivity.[1,2,9,10]

4.3 Experimental Procedure

Magnetite particles were prepared in the process described by Caruntu et al.[3] To coat the magnetite particles with titanium dioxide a sol-gel technique was used.[12] Titanium (IV) tetra-butoxide (TBOT) was hydrolyzed in the presence of magnetite, and thus a layer of titanium dioxide was allowed to form on the surface of magnetite nanoparticles. The experimental procedure involved the dispersion of 100 μl magnetite particles (~1 mg) in 10 ml ethanol followed by sonication for 15 min. Next, 100 μl water and 1 ml TBOT solution (0.26 M in ethanol) were added rapidly.

The final reaction mixture was aged in an ultrasonic bath at a constant temperature of 15 °C for 5 h. The reaction was stopped by immersion in an ice-water bath and dilution with ethanol. The particles were separated by centrifugation and washed two times with ethanol, followed by two rinses with water. Then the particles were separated by a magnet. Once prepared, the particles were stored in ethanol. In this study, Fe_3O_4–TiO_2 nanoparticles were not annealed after formation.

Previous work has indicated that crystalline TiO_2 can degrade the core magnetite material.[12] Consequently, we chose to leave the titania in its amorphous state for this study. Once Fe_3O_4–TiO_2 nanoparticles were obtained, gold was added in a photochemical step. An aliquot (100–300 μl) of Fe_3O_4–TiO_2 particles (1.3 μg/μl in ethanol suspension) was added to 5 ml aqueous $HAuCl_4$ (0.05–0.5 mM) in a 1.4-cm (inner diameter) quartz test tube; this solution appeared colorless. After mixing, the samples were subjected to UV irradiation with 254 nm lamps in a Rayonet (Southern New England Ultraviolet Company, Branford, CT) merry-go-

round photochemical reactor for 15-45 min. After UV irradiation, the solution appeared purple in color, but there was no observable precipitate. The contents of the test tube were then placed next to a strong magnet to allow magnetic separation.

Within a few hours, the particles were attracted to the magnet and separated from the clear, colorless supernatant. After removing the supernatant, the particles were washed with water and then resuspended in 1.5 ml ethanol. The resulting suspension was typically dark purple and was stored in the dark. Magnetic characterization was performed with a Quantum Design (San Diego, CA) MPMS-5S superconducting quantum interference device (SQUID) magnetometer. For these measurements, multiple batches (~20) of particles were prepared as described above, combined, and then dried in air over several days.

The dried particles were then weighed and sent for measurement. To obtain transmission electron microscope (TEM) images, about 10–20 μl ethanol suspension was dried on a copper grid prior to analysis with a JEOL (Peabody, MA) Model 2010 TEM. For ultraviolet–visible (UV-vis) absorbance measurements, aliquots of ethanol suspensions were diluted 10-fold in ethanol and analyzed with a Cary 5E absorbance spectrometer (Varian, Inc., Palo Alto, CA). X-ray diffraction (XRD) data were collected by drying multiple aliquots (40μl each) of an ethanol suspension on a small section of a 1 cm^2 glass slide. Once deposited, the dried sample was analyzed with a Philips (Eindhoven, The Netherlands) X'pert-MPD x-ray powder diffraction system.

4.4 Results and Discussion

Irradiation of the TiO_2–Fe_3O_4 particles in aqueous tetrachloroauric acid resulted in the formation of a purple product indicating the presence of nanoscale gold particles. Because these colored particles were completely separated from the supernatant using magnetic means, it is clear that the gold was physically attached to the magnetic core particles. Previous studies on photodeposition of noble metals onto titania have indicated that the metal forms at the surface of the titania and remains attached at the site of formation.[16] The mechanism of formation most likely involves formation of an isolated free electron at the surface of the titania, stepwise reduction of the metal to the zero valent state, and then repeated metal reduction steps at the metal nucleation site.[16] Growth of the metal particle after nucleation occurs because the metal site accepts electrons from the titania and serves as a site for easy electron transfer.[14–16]

4.4.1 TEM IMAGES

Figure 4.1 presents a representative TEM image of the particles made with 5 ml 0.1 mM $HAuCl_4$, 100 μl TiO_2–Fe_3O_4 suspension (1.3 μg/μl in ethanol suspension), and 30 min UV irradiation. In this image, approximately 10 nm-diameter magnetite particles can be seen embedded in the titanium dioxide, and gold particles can be seen attached to the surface of the TiO_2. A complete coating of gold around the TiO_2–Fe_3O_4 was not formed under these conditions. However, particles prepared with 0.5 mM $HAuCl_4$ (aq), 100 μl TiO_2–Fe_3O_4 suspension (1.3 μg/μL in ethanol suspension), and 45 min UV irradiation showed more complete coating with gold. A representative TEM image for these conditions is presented in Fig. 4.2. In this image, only gold is clearly visible except for a small amount of TiO_2 in the upper right section of the image.

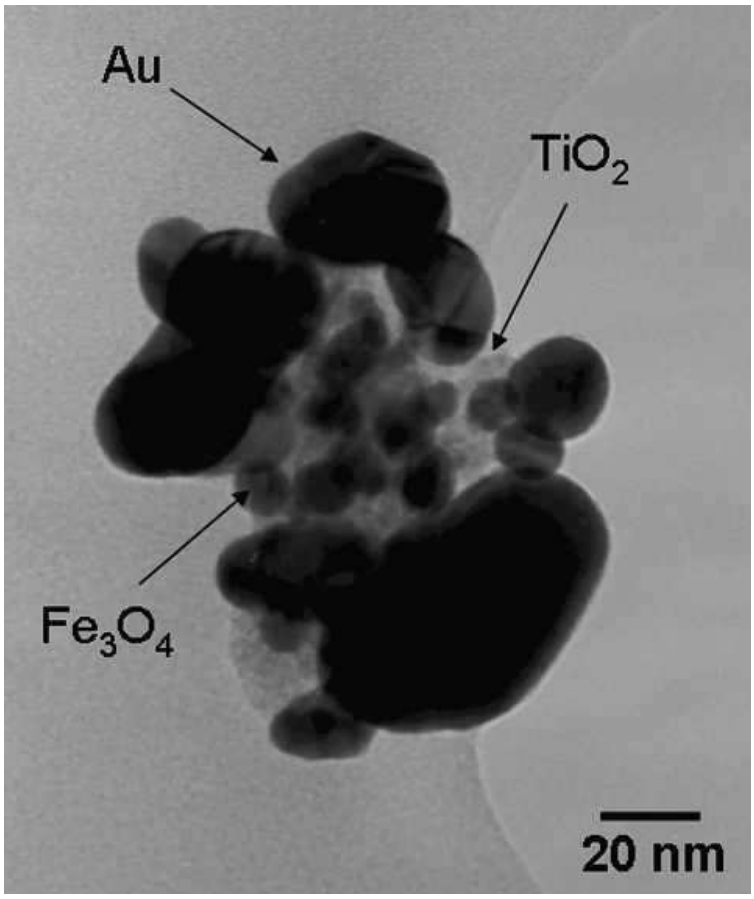

Fig 4.1. TEM image of Fe_3O_4–TiO_2–Au nanocomposite formed by irradiating Fe_3O_4–TiO_2 suspended in 0.1 mM $HAuCl_4$ (aq with 2% EtOH); irradiated with 254 nm lamps for 30 min.

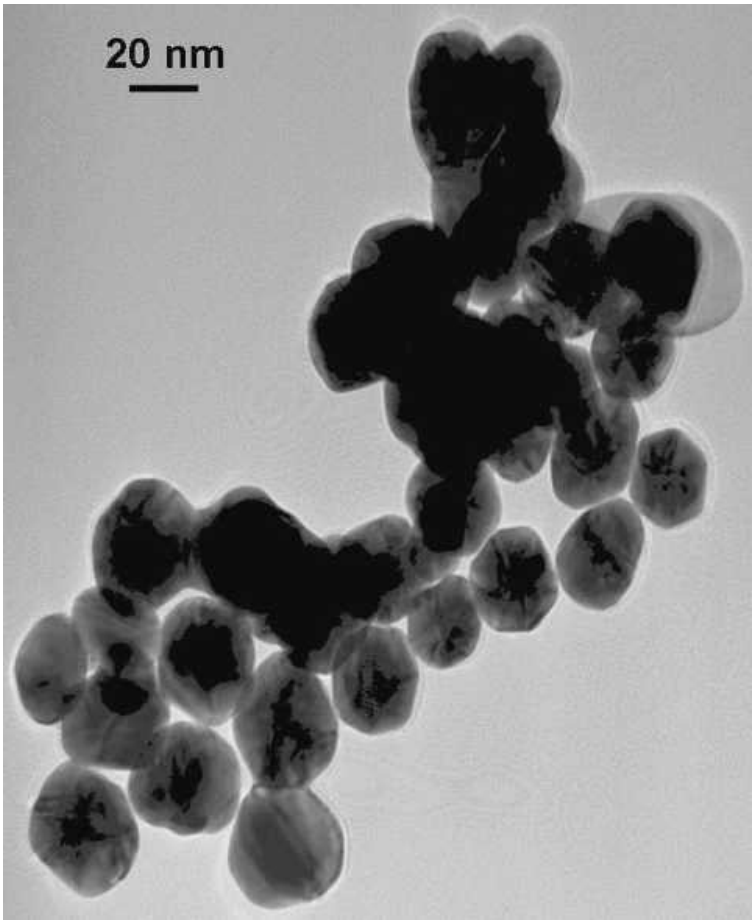

Fig 4.2. TEM image of Fe_3O_4–TiO_2–Au nanocomposite formed by irradiating Fe_3O_4–TiO_2 suspended in 0.5 mM HAuCl4 (aq with 2% EtOH); irradiated with 254 nm lamps for 45 min.

4.4.2 EDS SPECTRA

Energy dispersive spectroscopy (EDS) verified the identity of the different components of this nanocomposite material; this spectrum is presented in Fig. 4.2. EDS spectra of these particles clearly indicated the presence of gold, titanium, and iron. Furthermore, these particles were collected with magnetic separation and therefore must contain magnetic material.

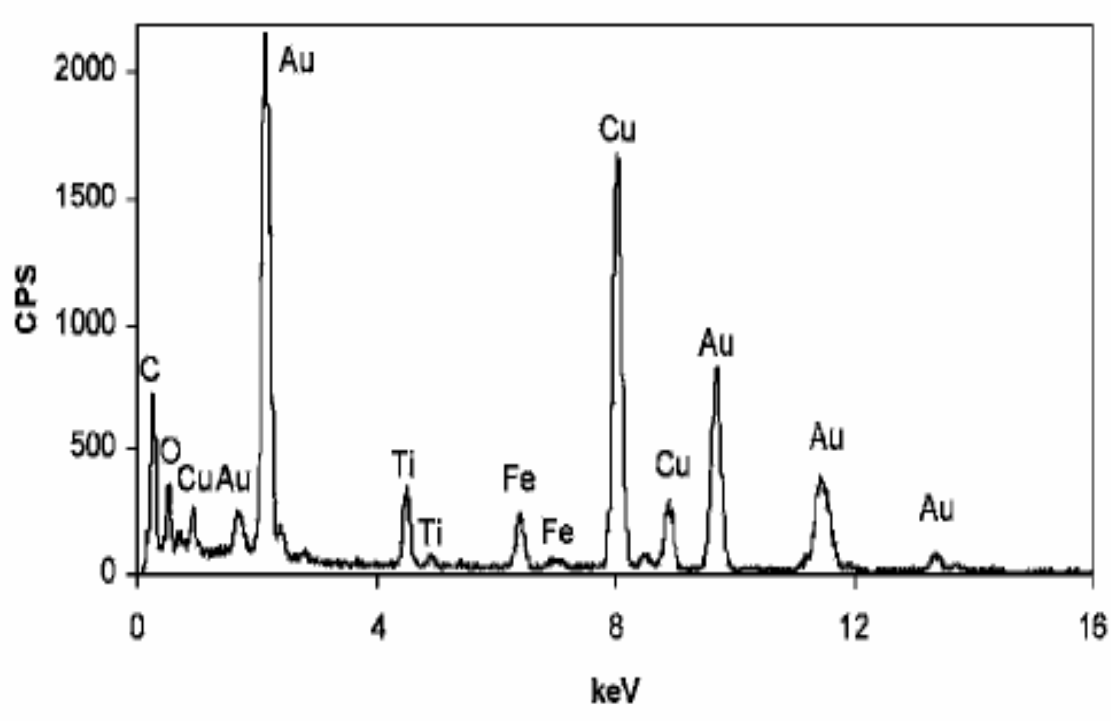

Fig 4.3. EDS spectrum from particles in Fig. 4.1. Copper and carbon peaks are from the TEM grid.

4.4.3. ABSORBANCE DATA

UV-vis absorbance measurements (Fig. 4.4) show that these particles have absorbance maxima between 540 and 590 nm, which is within the expected range for the gold surface plasmon resonance. Altering the concentration of $HAuCl_4$ used in particle formation resulted in shifts in the peak wavelength of the surface plasmon resonance (SPR).

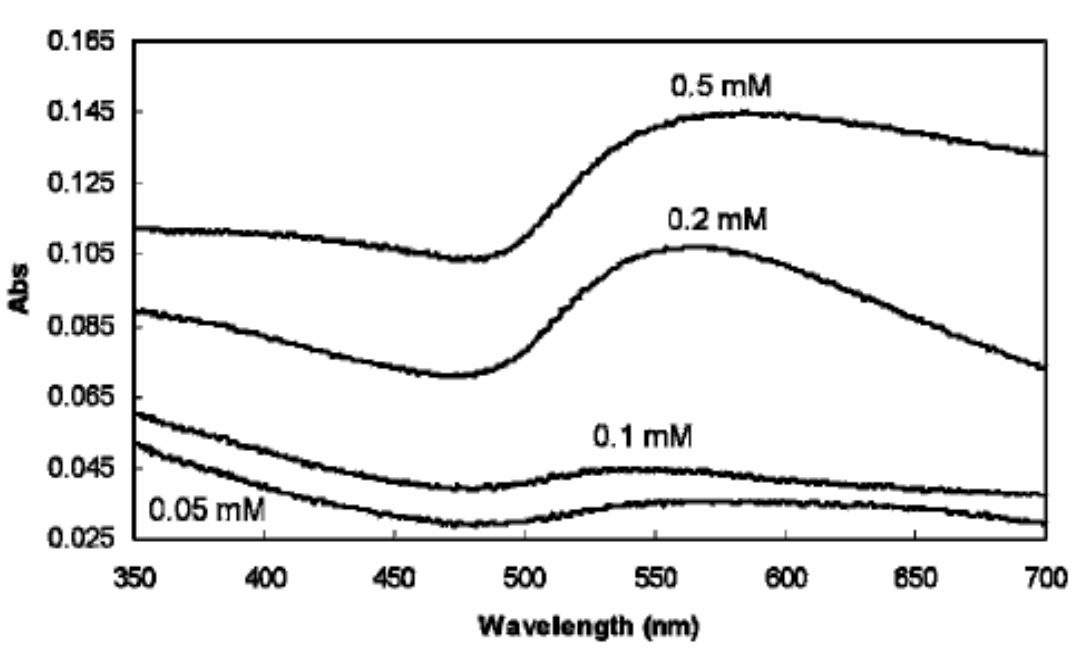

Fig 4.4. Absorbance spectra of particles made with varying concentrations of $HAuCl_4$ as indicated on the graph. $Fe3O_4$–TiO_2–Au formed by irradiating Fe_3O_4–TiO_2 suspended in aqueous $HAuCl_4$ with 2% EtOH; irradiated with 254 nm lamps for 45 min.

The bar chart in Fig. 4.5 shows the average peak wavelength for triplicate samples as a function of $HAuCl_4$ concentration used during synthesis. The change in surface plasmon resonance wavelength may be due to changes in gold particle size or shape, or could be due to interactions between the gold and TiO_2.[8,11] Several studies have reported that electronic interactions between gold and semiconductors can shift the SPR wavelength. [1,2,8,11] Our results indicate that the SPR peak wavelength for these composite materials can be tuned to a desired

wavelength by adjusting the conditions used during particle synthesis. Such control is an important tool needed to prepare nanomaterials with desired physical, optical, and chemical properties.

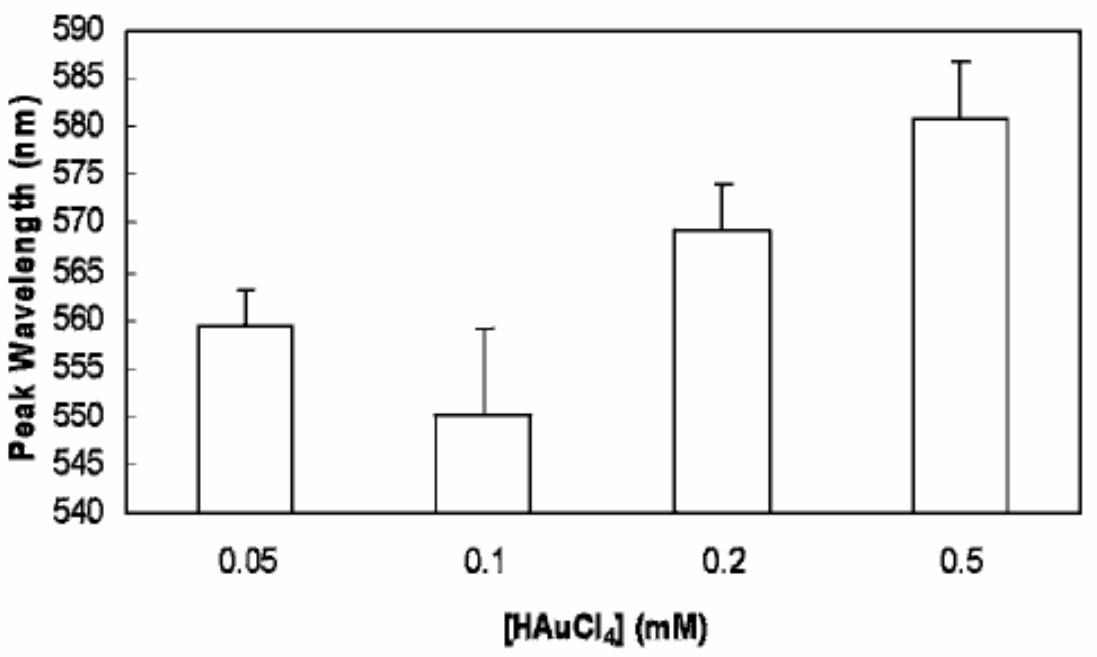

Fig 4.5 Wavelength of maximum absorbance versus [$HAuCl_4$] used in preparation of particles. Error bars represent standard deviation for triplicate measurements.

4.4.4 MAGNETIC MEASUREMENTS

Magnetic measurements (SQUID) of the composite, presented in Fig. 6, showed that the Fe_3O_4–TiO_2–Au nanocomposite material was superparamagnetic with a blocking temperature of

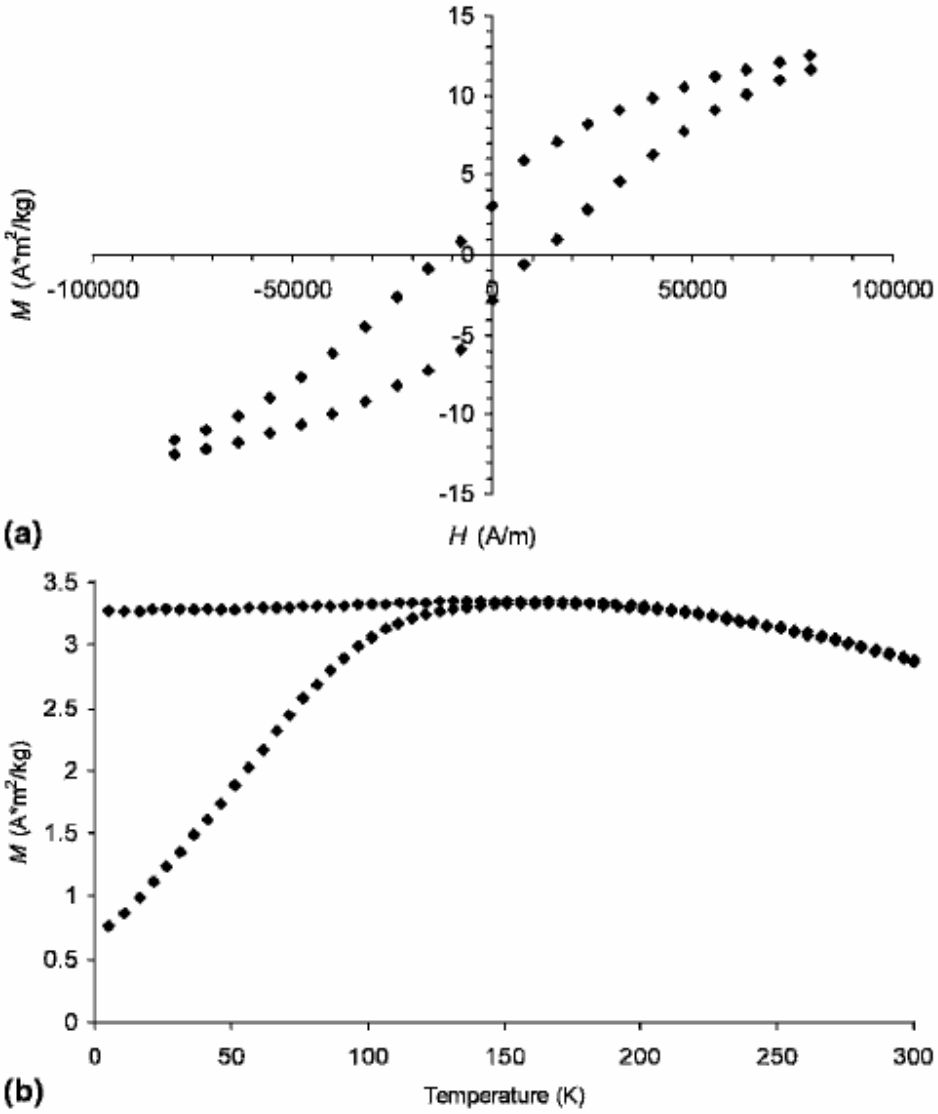

Fig 4.6. Fe_3O_4–TiO_2–Au nanocomposite magnetic properties: (a) hysteresis loop at 5 K and (b) ZFC/FC curves at an applied field strength of 7960 A/m (1 A/m = 4π/103 Oe; 1 A.m2/kg = 1 emu/g). Magnetization (*M*) relative to total mass of composite material.

about 170 K. The coercivity at 5 K was approximately 11,940 A/m (150 Oe). These magnetic properties were similar to those of pure TiO_2–Fe_3O_4 particles, but the blocking temperature was considerably lower than that for the untreated Fe_3O_4 particles (blocking temperature at or above room temperature). These results indicate that magnetite interactions with TiO_2 caused changes in the magnetic properties, but the magnetite was effectively isolated from the gold, preventing surface communication between these materials. Such communication has been observed in other studies in which direct gold-magnetite contact exists.[1,8,10,22]

4.4.5 XRD DATA

To verify that the magnetite was not oxidized during the nancomposite formation process, XRD data were collected for the nanocomposite material. Only peaks from gold and magnetite were observed in the XRD spectrum (see Fig. 4.7), indicating that the iron oxide is predominantly, if not completely, in the form of magnetite. Titanium dioxide peaks were not observed because this material was amorphous.

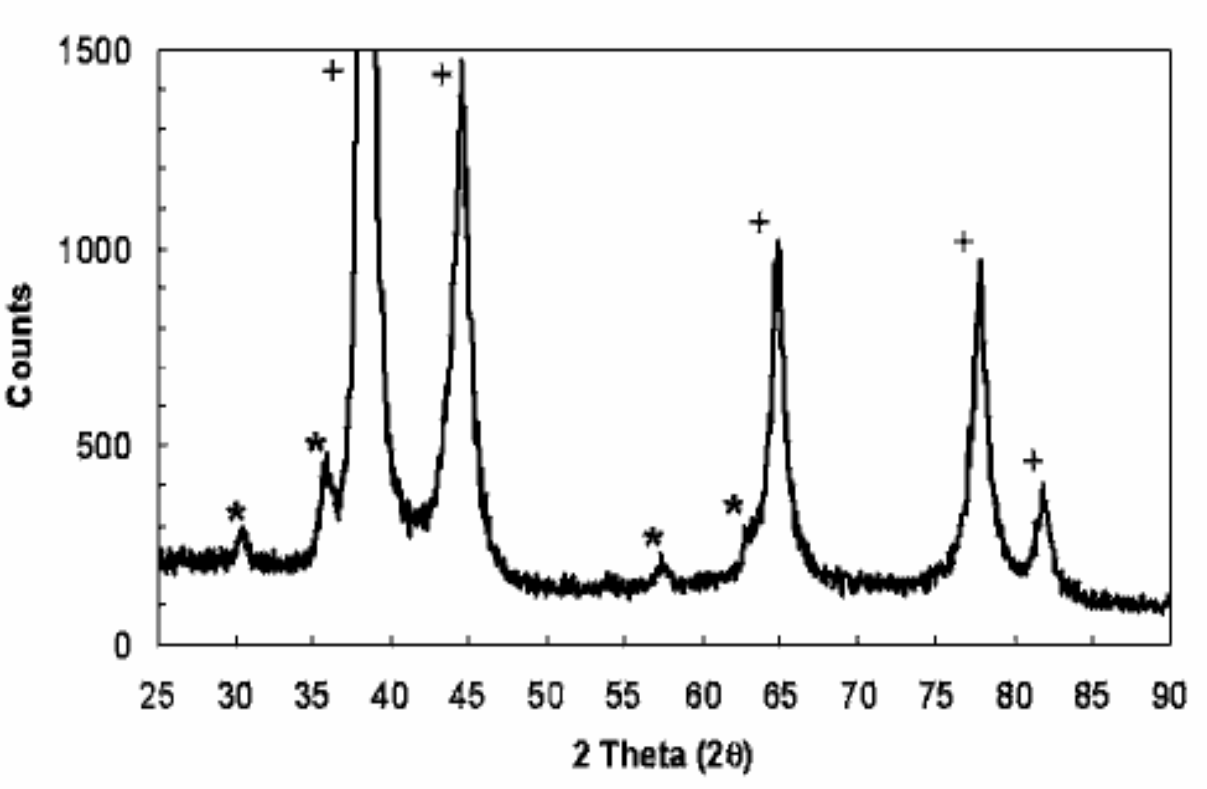

Fig 4.7. XRD data for Fe_3O_4–TiO_2–Au nanocomposite pictured in Fig. 4.1: (*) Fe_3O_4 and (+) Au.

4.5 Conclusion

Nanocomposite particles made with lower concentrations of $HAuCl_4$ were not fully coated with gold. These particles may be well suited for photocatalytic applications as the TiO_2 surface can still be exposed to UV radiation. The photocatalytic properties of these materials will likely be different from that of pure titania due to increased charge separation and enhanced electron transfer rates that result from the presence of gold surface sites.[14,15] Because the particles have a magnetic core, they can be readily separated from solutions by use of magnetic fields. These partially gold-coated particles may also be useful in biomedical applications in which the magnetic core can serve as a magnetic contrast agent or as a means of focusing particles in diseased tissue. The gold surface will allow for biofunctionalization for drug delivery or immunorecognition applications. A partial coating of gold may be sufficient for such applications.

The widespread use of titanium for medical implants and titanium dioxide in consumer products (paints, sunscreens) suggest that titanium dioxide will have little toxicity for these applications. However, in tissues that can be irradiated, these particles may serve as photoactivated materials that can destroy diseased cells. Digestive tract, urinary tract, uterine, and cervical tissues accessible to fiber optic probes may fall in this category.

Nanocomposites made with higher concentrations of $HAuCl_4$ are fully or almost fully coated with gold. These particles may be beneficial for applications in which exposed TiO_2 is undesirable. The ability to tune both the degree of gold coverage as well as the optical properties of these materials allows design of magnetic nanomaterials that can be used in a wide range of

applications. While these potential biomedical applications require extensive testing and trials, applications of other magnetic nanoparticles are well on their way to real world application. [6,7]

4.6 References

1. J.L. Lyon, D.A. Fleming, B.B. Stone, P. Schiffer, and M.E. Williams: Synthesis of Fe oxide core/Au shell nanoparticles by iterative hydroxylamine seeding. *Nano Lett.,* **2004,** 4**,** 719.

2. L. Wang, J. Luo, M.M. Maye, Q. Fan, Q. Rendeng, M.H. Engelhard, C. Wang, Y. Lin, and C-J. Zhong: Iron oxide-gold core-shell nanoparticles and thin film assembly. *J. Mater. Chem.,* **2005,** 15**,** 1821

3. D. Caruntu, G. Caruntu, Y. Chen, C.J. O'Connor, G. Goloverda, and V.L. Kolesnichenko: Synthesis of variable-sized nanocrystals of Fe3O4 with high surface reactivity. *Chem. Mater.,* **2004**, 16**,** 5527.

4. D. Caruntu, Y. Remond, N.H. Chou, M-J. Jun, G. Caruntu, J. He, G. Goloverda, C. O'Connor, and V. Kolesnichenko: Reactivity of 3D transition metal cations in diethylene glycol solutions. Synthesis of transition metal ferrites with the structure of discrete nanoparticles complexed with long-chain carboxylate anions. *Inorg.Chem.* **2002**, 41**,** 6137.

5. C-M. Fu, Y-F. Wang, Y-C. Chao, S-H. Hung, and M-D. Yang: Directly labeling ferrite nanoparticles with Tc-99m radioisotope for diagnostic applications. *IEEE Trans. Magn.* **2004,** 40**,** 3003.

6. R.F. Service: Nanotechnology takes aim at cancer. *Science;* **2005,** 310**,** 1132.

7. X. Gao, Y. Cui, R.M. Levenson, L.W.K. Chung, and S. Nie: In vivo cancer targeting and imaging with semiconductor quantum dots. *Nat. Biotechnol;.***2004**, 22**,** 969.

8. H. Yu, M. Chen, P.M. Rice, S.X. Wang, R.L. White, and S. Sun: Dumbbell-like bifunctional Au–Fe3O4 nanoparticles. *Nano Lett.,* **2005**, 5**,** 379.

9. D. Caruntu, B.L. Cushing, G. Caruntu, and C.J. O'Connor: Attachment of gold nanograins onto colloidal magnetite nanocrystals. *Chem. Mater.,* **2005**, 17, 3398.

10. M. Mikhaylova, D.K. Kim, N. Bobrysheva, M. Osmolowsky, V. Semenov, T. Tsakalakos, and M. Muhammed: Superparamagnetism of magnetite nanoparticles: Dependence on surface modification. *Langmuir,* **2004**, 20**,** 2472.

11. M. Spasova, V. Salgueiriño-Maceira, A. Schlachter, M. Hilgendorff, M. Giersig, L.M. Liz-Marzán, and M. Farle: Magnetite and optical tunable microsphere with a magnetic/gold nanoparticle shell. *J. Mater. Chem.*, **2005**, 15, 2095.

12. D. Beydoun, R. Amal, G.K-C. Low, and S. McEvoy: Novel photocatalyst: Titania-coated magnetite. Activity and photodissolution. *J. Phys. Chem. B,* **2000**, 104, 4387.

13. M. Jakob and H. Levanon: Charge distribution between UV irradiated TiO2 and gold nanoparticles: Determination of shift in the fermi level. *Nano Lett.,* **2003**, 3, 353.

14. H. Haick and Y. Paz: Long-range effects of noble metals on the photocatalytic properties of titanium dioxide. *J. Phys. Chem. B,* **2003**, 107**,** 2319.

15. I.M. Arabatzis, T. Stergiopoulos, D. Andreeva, S. Kitova, S.G. Neophytides, and P. Falaras: Characterization and photocatalytic activity of Au/TiO2 thin films for azo-dye degradation. *J. Catal.*, **2003**, 220, 127.

16. M. Jakob and H. Levanon: Charge distribution between UV irradiated TiO2 and gold nanoparticles: Determination of shift in the Fermi level. *Nano Lett.,* **2003**, 3, 353.

17. K. Malik, M. Mandal, N. Pradhan, and T. Pal: Seed mediated formation of bimetallic nanoparticles by UV irradiation: A photochemical approach for the preparation of “core-shell” type structures. *Nano Lett.*, **2001**, 1, 319.

18. J. Rodriguez, G. Liu, R. Jirsak, J. Hrbek, Z. Chang, J. Dvorak, and A. Maiti: Activation of gold on titania: Adsorption and reaction of SO2 on Au/TiO2(110). *J. Am. Chem. Soc.*, **2002**, 124, 5242.

19. Y. Iizuka, T. Tode, T. Takao, K. Yatsu, T. Takeuchi, S. Tsubota, and M. Haruta: A kinetic and adsorption study of CO oxidation over unsupported fine gold powder and over gold supported on titanium dioxide. *J. Catal.*, **1999**, 187, 50.

20. T.V. Choudhary, C. Sivadinarayana, C.C. Chusuei, A.K. Datye, J.P. Fackler, Jr., and D.W. Goodman: CO oxidation on supported nano-Au catalysts synthesized from a [Au6(PPh3)6](BF4)2 complex. *J. Catal.*, **2002**, 207, 247.

21. H. Kominami, T. Nakaseko, Y. Shimida, A. Furusho, H. Inoue, S. Murakami, Y. Kera, and B. Ohtani: Selective photocatalytic reduction of nitrate to nitrogen molecules in an aqueous suspension of metal-loaded titanium(IV) oxide particles. *Chem. Commun.*, **2005**, 2933.

22. G. Shemer and G. Markovich: Enhancement of magneto-optical effects in magnetite nanocrystals near gold surfaces. *J. Phys.Chem. B*, **2002**, 106**,** 9195.

Chapter 5: Photocatalytic Activity of Nanoparticles

5.1 Abstract

In this study, the photocatalytic activity of magnetite-titania-gold nanocomposite material has been investigated. Magnetite particles were first coated with titanium dioxide. Resulting particles were then irradiated with UV light in the presence of tetrachloroauric acid to deposit gold on the surface. Magnetite-titania-gold nanocomposites prepared in this manner were characterized by TEM, EDS, UV-Vis absorbance, SQUID magnetometry, XRD, and ICP. These nanocomposite materials have potential applications for drug delivery, magnetic imaging, and photocatalysis. In this work, the influence of gold deposition on photocatalytic activity was studied.

5.2 Introduction

Titanium dioxide (TiO_2) is well known as chemically stable and harmless material, and has been applied widely in various fields.[1-5] For example, it is used for surface coating, photoelectrodes, high-k dielectrics, paints, cosmetics, and so on. In recent years, it has been received a great deal of attention especially as a photocatalytic material.[5-7] TiO_2 which shows specific photocatalytic properties, such as photo-induced decomposition of organic compounds and photo-induced hydrophilicity,[5,8,9] is expected to apply in the environmental fields. Various utilizations such as antibacterial, antipollution and deodorization have been attained.[6] Because of these unique photocatalytic properties, application of the TiO_2 will spread increasingly from now on.

Doping of various transition metal ions or rare earth ions in TiO_2 have been intensively investigated for photocatalytic decomposition of organic compounds.[10-13] Very recently, Asahi et al. reported that nitrogen (N) doping in TiO_2 shifted its optical absorption and enhanced the photocatalytic activity such as photodegradation of methylene blue and gaseous acetaldehyde in the visible region.[14]

Primarily, the role of photocatalysts is the same with that of common catalysts in that they promote the reaction by lowering the activation energy. Based on the content of several review articles,[15-17] it seems essential to suppress the recombination process and to increases the lifetime of separated electron-hole pairs for the achievement of high photocatalytic activity, so that electron transfer can occur from the surface of TiO_2 to adsorbed reactants. From the report of M. Hagfeldt *et al.*[18], doping of transition metals or precious metals on the surface of TiO_2 could function as a trap in the process of recombination of photo-excited electron-hole pairs. On

the other hand, M. M. Rahman *et al.*[19] reported that UV-VIS transmittance pattern of TiO_2 could be an index of band gap energy.

Chen and his coworkers have deposited platinum on TiO_2 films and degraded o-cresol to see the improvement of photocatalytic activity of the new nanocomposites. The degradation of o-cresol was found to increase in the Pt deposited TiO_2 nanocomposites. From their results they have concluded that the deposition of platinum on TiO_2 promoted the optical absorption in the visible region and made it possible to be excited by visible light.[20] Same types of results were also observed during oxidation of resorcinol[21].

McEvoy *et al.*[22] have been able to deposit silver particles on TiO_2 nanoparticles and were able to oxidize organic compounds like salicylic acid and sucrose. For high loadings of sucrose Ag-TiO_2 really improved the oxidation compared to its low loading. They have concluded that nanosize silver deposits on TiO_2 particles acted as sites of electron accumulation where the reduction of adsorbed species such as oxygen occurred. The enhanced reduction of oxygen through better electron–hole separation in Ag/TiO_2 particles compared to pure TiO_2 particles increased the rate of sucrose mineralization. Similar results were observed during reduction of nitrates[23] also.

Bisphenol A is the building block for plastic bottles and gum resins. However, recent research has shown it to be an estrogen receptor agonist which can activate estrogen inside the body.[24-26] Some hormone disrupting effects in studies on animals and human cancer cells have been shown to occur at very low levels. It has been claimed that these effects lead to health problems such as lower sperm count, obesity, or triggering early puberty. Recent studies have confirmed that bisphenol A exposure during development has carcinogenic effects and produces precursors of breast cancer. As an environmental contaminant this compound has been in debate

for quite a long time. It has already been proven to be toxic in nature and having carcinogenic effects for humans as well as the plant world.

Being a toxic contaminant scientists have tried to degrade this compound using different methods. Therefore, we also wanted to degrade bisphenol A with our synthesized nanoparticles in order to develop new methods that can be easier and less costly.

5.3 Experimental Procedure

5.3.1 Degradation Study of bisphenol A

3 ml of 0.5mM bisphenol A was put into 1.4-cm (inner diameter) quartz test tubes. The solution was irradiated with different UV lamps (wavelength: 254 nm, 300 nm and 350 nm) in a Rayonet (Southern New England Ultraviolet Company, Branford, CT) merry-go-round photochemical reactor with

- No particles
- With $TiO_2@Fe_3O_4$ particles
- With $Au@TiO_2@Fe_3O_4$ particles

For each reaction set there was a control experiment conducted. Three test tubes were covered with aluminum foil. In these test tubes 3 ml of 0.5mM bisphenol A was added. To one of the test tube no particles were added, in the second one $TiO_2@Fe_3O_4$ particles and in the third one $Au@TiO_2@Fe_3O_4$ nanocomposites were added. This control experiment was done so that we know what effect bisphenol A has when introduced into a photochemical reactor with out the radiation. The control test tube for each experiment was kept for the longest reaction time period for that particular experiment. The irradiation time also was varied 15 min to 300 min depending on the experiment. Once the reaction completed for the desired time, the whole solution was placed in front of a magnet. Once the particles separated out, the solution was taken out and evaluated by an Agilent HPLC instrument. The column used for this analysis was a Econosphere C-18 reversed phase column with the mobile phase being water and acetonitrile (60:40) mixture throughout the analysis time period. The flow rate was kept constant at 1ml per minute and a 100µl loop was used. The signal was captured by a diode array detector (DAD).

In another set of experiments, different amounts of $Au@TiO_2@Fe_3O_4$ particles were put into the aqueous solution of bisphenol A to monitor the amounts of degradation for Bisphenol A. In this study we used 3 ml of 0.5mM Bisphenol A and irradiated it under UV light for 30 min in the presence of 100µl, 200µl, 300µl and 400µl aliquots of $Au@TiO_2@Fe_3O_4$ nanoparticle suspensions (100µl suspension = 0.13mg nanoparticles). Similar separation technique was used and the solutions were examined by the Agilent HPLC keeping the previous analysis procedure.

5.3.2 Reuse of the photocatalytic $Au@TiO_2@Fe_3O_4$ particles

In this experimental procedure we wanted to see whether the nanoparticles can be reused or not. We exposed 3ml of 0.5 mM Bisphenol A under UV radiation (254 nm) in the presence of 100µl (1.3µg/µl) of $Au@TiO_2@Fe_3O_4$ particles for 30 min. After exposure, the whole solution was placed in front of a magnet for 1 hour for complete separation. Once the particles separated and the solution was colorless, the solution was taken out carefully and examined by HPLC. Then to the test tube containing the separated particles we added fresh 0.5 mM Bisphenol A and irradiated it under UV light to see whether Bisphenol A degraded or not. After 30 min of exposure, the sample was kept beside a magnet to separate the particles again. This recycling procedure was carried four times and each time the solution was evaluated with HPLC to determine the amount of degradation of Bisphenol A.

5.4 Results and Discussion

Bisphenol A was irradiated at three different wavelengths 254 nm, 300 nm and 350 nm. Different amounts of degradation were observed in the three sets of experiments. In the 254 nm, 300 nm wavelengths we observed the same trend of degradation of bisphenol A without the presence of particles, with $TiO_2@Fe_3O_4$ particles and Au@ $TiO_2@Fe_3O_4$ particles. In the presence of the Au@ $TiO_2@Fe_3O_4$ particles the degradation was the most followed by the

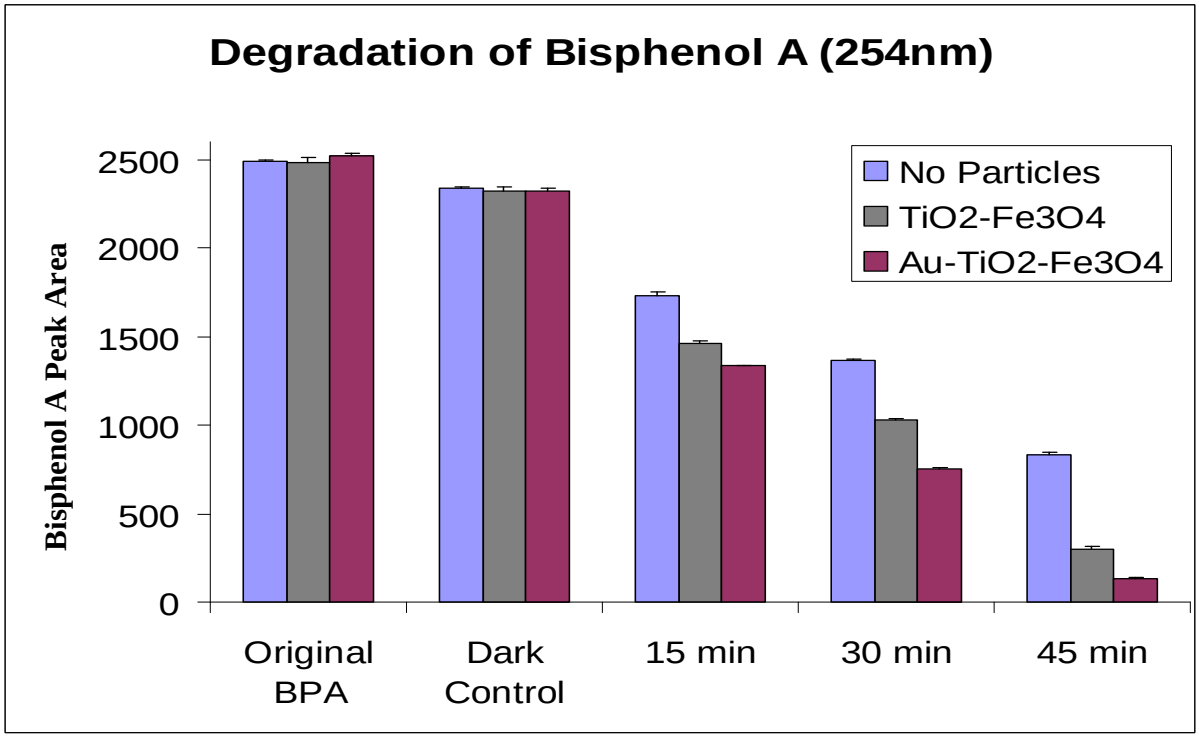

Figure 5.1. Degradation of 0.5 mM Bisphenol A solution for different amounts of time in presence of 254 nm lamps

$TiO_2@Fe_3O_4$ particles and the least was with no particles present in the reaction. For the dark control in all the sets of experiments there was very minimal degradation of the aqueous solution of bisphenol A. This was because we prevented the radiation process by covering the test tubes with aluminum foil. The small amount of degradation observed for the dark control occurred because of the increase in temperature in the exposure chamber for a time period of 45 min or

120 min or 300 min depending on the experiment. With the 254 nm lamps, degradation of bisphenol A without particles was more than that at 300 nm. This was true for all the time periods the target compound was exposed to.

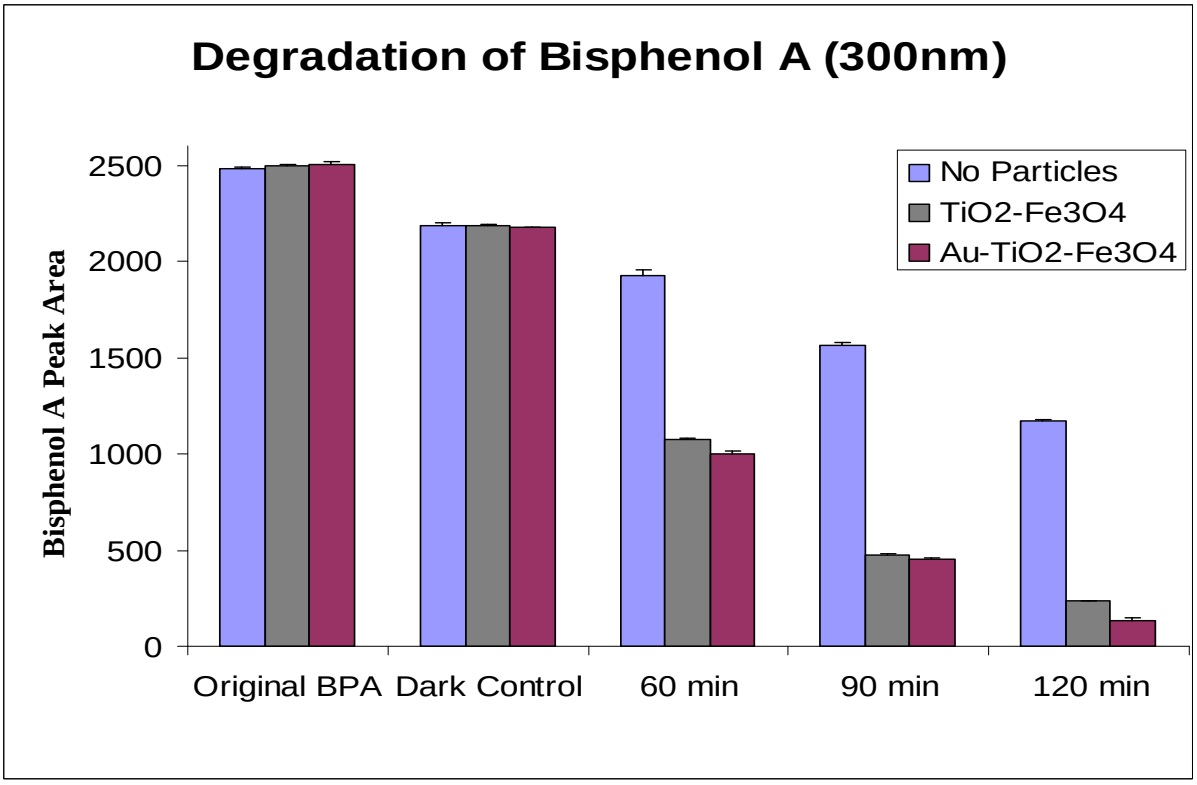

Figure 5.2. Degradation of 0.5 mM Bisphenol A solution for different amounts of time in presence of 300 nm lamps

The degradation in presence of $TiO_2@Fe_3O_4$ particles and $Au@TiO_2@Fe_3O_4$ particles was similar for 254 nm and 300nm wavelength experiments. The presence of gold on the surface of the $TiO_2@Fe_3O_4$ particles helped in degrade the bisphenol A compared to the $TiO_2@Fe_3O_4$ particles. For the 254 nm experiment, the rate of degradation was faster than the other sets. The only difference was the time periods. For the 254 nm lamps and 300 nm lamps the reaction times were 45 min and 120 min respectively. In both cases for the longest reaction time, bisphenol degraded more than 90% in the presence of $Au@TiO_2@Fe_3O_4$ particles.

From the above data it can be concluded that in the presence of $TiO_2@Fe_3O_4$ particles with gold attached to it, the degradation was most effective at 254 nm irradiation. The advantage of adding gold was less evident at the 300 and 350 nm wavelengths. This confirms the theoretical approach that doping with transition metals or precious metals on the surface of TiO_2 could function as a trap in the process of recombination of photo excited electron-hole pairs. So the photoexcited electron-hole pairs have more time to react with the pollutants and thus helps increase degradation of the compounds.

When we did the same type of reaction but only changed the wavelength of the irradiation light to 350 nm we did not find much degradation of bisphenol A in the presence of $TiO_2@Fe_3O_4$ particles or $Au@TiO_2@Fe_3O_4$ particles as seen in Fig 5.3. This can attributed to the fact that the titanium dioxide absorbs much more weakly at 350 than at the lower wavelengths used. Compared to the dark control for the different time periods, we observed only minimal

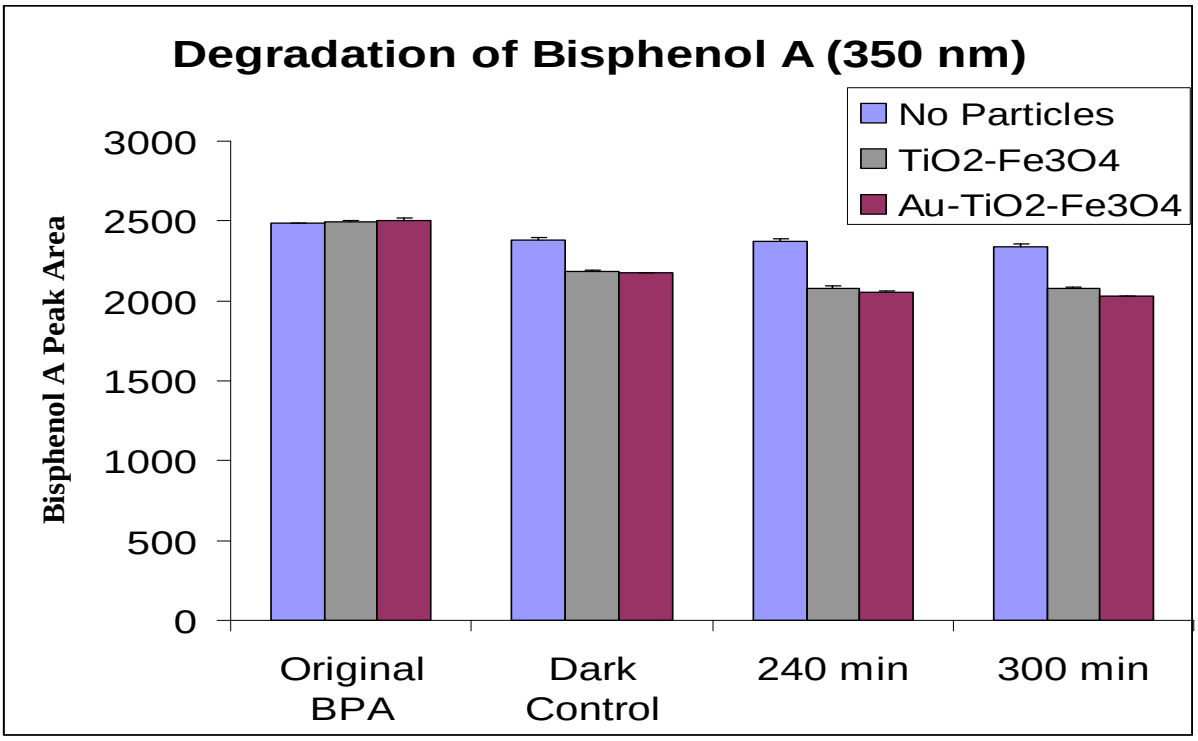

Figure 5.3. Degradation of 0.5 mM Bisphenol A solution for different amounts of time in presence of 350 nm lamps

degradation of the bisphenol A in the absence or presence of the nanocomposites even though the reaction was allowed to happen for 240 min and 300 min respectively. Since the $Au@TiO_2@Fe_3O_4$ particles or $TiO_2@Fe_3O_4$ particles absorb weakly at this particular wavelength the amount of degradation is very hard to see but the same trends seem to be present at 350 nm if we would have irradiated the solution of bisphenol A for a much much longer time period.

When we irradiated bisphenol A with different amounts of $Fe_3O_4@TiO_2@Au$ nanoparticles, from Figure 5.4 it can be inferred that the presence of more particles degraded the pollutant more. The increase in extent of degradation was small compared to the increase in the

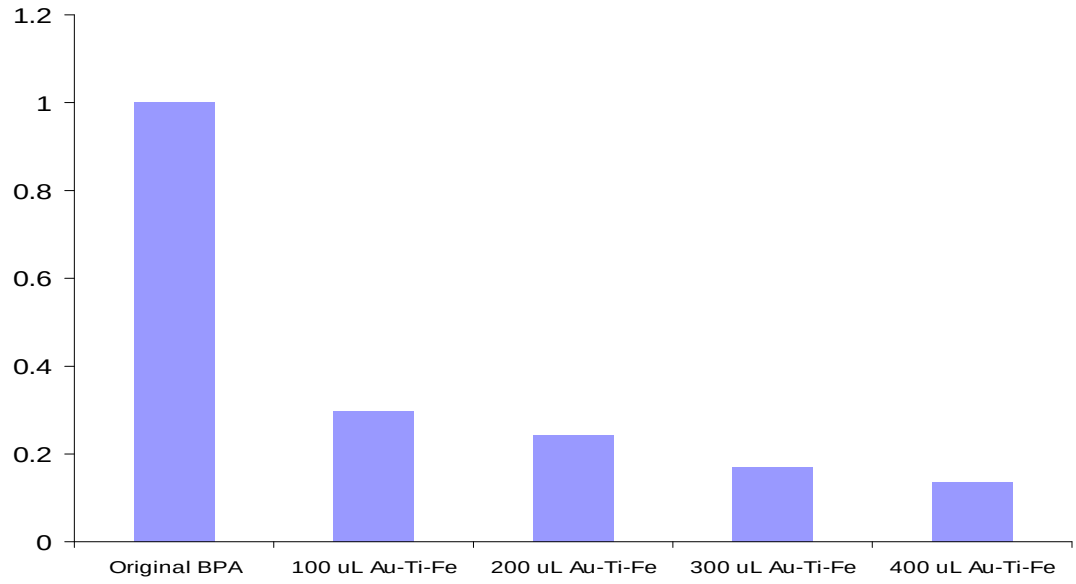

Figure 5.4. Different amounts of $Fe_3O_4@TiO_2@Au$ nanoparticles used to degrade of 0.5 mM Bisphenol A solution for 30 min.

concentration of the particles. Consequently it can be concluded that lower particles loadings can be effectively used for pollutants degradation.

In the case of reuse of the magnetic nanoparticles, we were able to confirm that they can be repeatedly used as photocatalysts. Even after the use for the fourth time, we observed no substantial loss in the ability to degrade bisphenol A. This was evident from figure 5.5. Moreover there was very minimal loss of the nanoparticles which can prove this method to be quite cost effective.

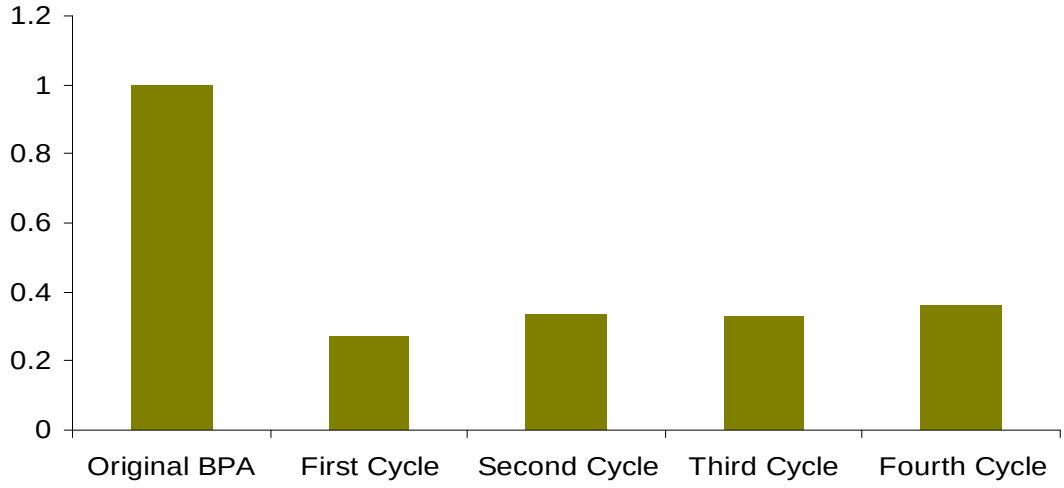

Figure 5.5. Separate Bisphenol A samples were degraded for 30 min using 100µL of Fe_3O_4@TiO_2@Au nanoparticles with magnetic separation between exposures

5.5 Conclusions

We were able to produce photocatalyst nanoparticles which can be eventually used for degradation of pollutants in the environment. Easy modification of the gold surfaces with chemical or biorecognition molecules can provide chemical or biological selectivity for the particles. Catalytic activity of particles is maintained through several degradation cycles. Magnetic recovery and re-use is feasible which will make this process less costly and more effective.

5.6 References

1. http://www.teamenviroclean.com/titanium_dioxide
2. http://energy.caeds.eng.uml.edu/peru-07/173a.pdf
3. Maurizio Addamo, Vincenzo Augugliaro, Elisa García-López, Vittorio Loddo, Giuseppe Marcì and Leonardo Palmisano; *Catalysis Today*, **1995**, 6(12), 107-108
4. T Matsunaga, R Tomoda, T Nakajima, N Nakamura, and T Komine; Appl *Environ Microbiol.*, **1988**, 54(6), 1330
5. http://www.ozonelite.com/faq-other-uses-TiO2.shtml
6. Sopyan I, Murasawa S, Hashimoto K and Fujishima A; *Chem. Lett*., **1994**, 8, 723
7. Maeda M and Watanabe T; *Thin Solid Films*, **2005**, 489, 320
8. Wang R, Hashimoto K and Fujishima A; *Nature*, **1997**, 388, 431
9. Maeda M and Yamasaki S; *Thin Solid Films*, **2005**, 483, 102
10. Choi, W.; Termin, A.; Hoffmann, M. R.; *J. Phys. Chem*., **1994**, 98, 13669.
11. Di Paola, A.; Garcı´a-Lo´pez, E.; Ikeda, S.; Marcı`, G.; Ohtani, B.;Palmisano, L.; *Catal. Today*, **2002**, 75, 87.
12. Xu, A.-W.; Gao, Y.; Liu, H.-Q.; *J. Catal.*, **2002**, 207, 151.
13. Kato, H.; Kudo, A.; *J. Phys. Chem. B*, **2002**, 106, 5029.
14. Asahi, R.; Morikawa, T.; Ohwaki, T.; Aoki, K.; Taga, Y.; *Science*, **2001**, 293, 269.
15. Michael R. Hoffman, Scott T. Martin, Wonyong Choi, Detlef W. Bahnemann; *Chem. Rev.*, **1995**, 95, 69.
16. Marta I Litter; *Applied Catal. B; Environmental*, **1999**, 23, 89.
17. José Peral, Xavier Domènech, David F. Ollis; *J. Chem. Technol. Biotechnol*, **1997**, 70, 117.
18. A. Hagfeldt , M. Grätzel; *Chem. Rev*., **1995**, 95, 49.

19. Md. Mosaddeq-ur-Rahman, Tekeshi Miki, Murali Krishna, Tetsuto Soga, Kazuo Igarashi, Sakae Tanemura, Masayoshi Umeno; *Material Science and Engineering B*, **1996**, 41, 67.

20. Hua-Wei Chen, Young Ku and Yu-Lin Kuo; *Water Research*, **2007**, 41(10), 2069-2078

21. Sai Wei Lam, Ken Chiang, Tuti M. Lim, Rose Amal and Gary K-C. Low; *Applied Catalysis B: Environmental*, **2007**, 72(3-4), 363-372

22. Veronica Vamathevan, Rose Amal, Donia Beydoun, Gary Low and Stephen McEvoy; *Journal of Photochemistry and Photobiology A: Chemistry*, **2002**, 148,(1-3), 233-245

23. Fuxiang Zhang, Ruicai Jin, Jixin Chen, Changzhun Shao, Wenliang Gao, Landong Li and Naijia Guan; *Journal of Catalysis*, **2005**, 232(2), 424-431

24. Sayaka Takayanagi, Takatoshi Tokunaga, Xiaohui Liu, Hiroyuki Okada, Ayami Matsushima and Yasuyuki Shimohigashi; *Toxicology Letters*, **2006**, 167(2), 95-105

25. Yelena B. Wetherill, Benson T. Akingbemi, Jun Kanno, John A. McLachlan, Angel Nadal, Carlos Sonnenschein, Cheryl S. Watson, R. Thomas Zoeller and Scott M. Belcher; *Reproductive Toxicology*, **2007**, 24,(2), 178-198

26. Renée M. Bergeron, Tommy B. Thompson, Linda S. Leonard, Linda Pluta and Kevin W. Gaido; *Molecular and Cellular Endocrinology*, **1999**, 150(1-2), 179-187

Chapter 6: Synthesis of Indium Doped Magnetite Nanoparticles for Radiotracer Studies

6.1 Abstract

The overall goal of this project is to synthesize and characterize indium doped magnetite nanoparticles for application as radiotracers for *in vivo* fate studies. The labeled particles will be useful for determination of pharmacological behavior in biological systems. Indium (cold) doped magnetite particles with varying size and surface chemistry were synthesized using wet chemical techniques. The synthesized nanoparticles were characterized in terms of size and shape by TEM, elemental composition by ICP and EDS, crystal structure by XRD, and magnetic properties by SQUID measurements. It was found that the indium loading could be controlled even though the magnetic properties were similar. These particles when synthesized with radioisotope In^{111} could be used as radiotracers.

6.2 Introduction

Nanoparticles are being extensively studied for potential application in medicine,[1-12] and this application has been termed nanomedicine. However, the fate of nanoparticles in biological systems is still poorly understood. Given the large future growth of the role of nanoparticles in biomedical applications, it is essential that the behavior of these materials be understood in biological systems. Nanoparticles are currently being developed for a wide variety of applications including drug delivery, medical imaging, sensing, catalysis, nanocircuitry, and information storage. Applications of these materials include imaging and disease detection,[7, 13-16] drug delivery[17-21] and other novel disease treatment methods (eg. Photothermal therapy[9-12]). However, the environmental and biological impacts of these new materials are poorly understood. Although much data is available for inhalation of ultrafine particles,[22-25] and some data is available for nanotoxicology,[26,27] information is lacking for the fate and transport of nanoparticles, especially for novel materials.[28,29] Biodistribution studies for magnetite nanoparticles have been carried out,[30-33] but these studies have relied on magnetic resonance, histological, or X-ray imaging techniques to follow the nanoparticles. These approaches are substantially limited by their poor detection limits. For example, histological methods can only detect large, micron-scale aggregates of nanoparticles. Furthermore, quantitative measurement of nanoparticle loading using magnetic resonance, histology, or X-ray imaging is difficult.

An understanding of the biological fate and transport of nanoparticles is critically needed in order to ensure safe and environmentally sound development of nanotechnology.[34] For both environmental and biological fate, new approaches are needed that will allow both short term and long term studies. Indium has been previously incorporated into spinel structures, including

ferrites.[35,36] Researchers were able to incorporate various other metals as can be seen in previous reports.[37-39] In related research, Lu *et al.*[40] prepared Sn doped magnetite particles. Nanoparticles that are integrally labeled with a radiotracer would provide an excellent solution to this important problem due to several advantages: 1) the integral radiotracer is part of the nanoparticle crystal lattice and cannot be lost through simple surface modifications, 2) the radiotracer selected for this study has a sufficient lifetime to allow studies over several days, 3) gamma imaging of the particles will allow mapping of particle locations within experimental subjects (e.g. mice), 4) the excellent detectability of radiotracers will allow detection of labeled nanoparticles even in tissues with low loading, and 5) pharmacological fate and excretion can be measured by radiotracer detection in tissue, blood, urine, and feces.

6.3 Chemicals and Instruments Used

The chemicals used for all sets of reaction mentioned below are:

Ferrous Chloride Tetrahydrate ($FeCl_2.4H_2O$), Ferric Chloride Hexahydrate ($FeCl_3.6H_2O$), Indium Chloride Tetrahydrate ($InCl_3.4H_2O$), Diethylene Glycol (DEG), Sodium Hydroxide (NaOH), Ethanol, Ethyl Acetate and Oleic Acid was obtained from Aldrich

To obtain transmission electron microscope (TEM) images, about 10–20 μl ethanol suspension containing the indium doped magnetite nanoparticles was dried on a copper grid prior to analysis with a JEOL (Peabody, MA) Model 2010 TEM. X-ray diffraction (XRD) data were collected by drying multiple aliquots (40μl each) of an ethanol suspension on a small section of a 1 cm^2 plastic slide. Once deposited, the dried sample was analyzed with a Philips (Eindhoven, The Netherlands) X'pert-MPD x-ray powder diffraction system. The elemental analysis was done by a Varian Simultaneous CCD ICP-OES.

6.4 Experimental Procedure

1mmol of $FeCl_2.4H_2O$ was dissolved in 20g of diethylene glycol (DEG) under argon atmosphere. It was allowed to dissolve overnight. 32g of sodium hydroxide (NaOH) was also dissolved under argon in another separate 20g of DEG for over 12 hours. In another 20g DEG, $FeCl_3.6H_2O$ and $InCl_3.4H_2O$ were dissolved together and the mixture was let to stay for 4 hours under argon. The color of the solution was yellow-orange. Once the above solution dissolved completely it was allowed to react with the solution of $FeCl_2.4H_2O$ for 2 hours at room temperature. The color of the solution turned yellow-brown. Then the NaOH solution is introduced to the above mixture dropwise and allowed to react under argon for 3 hours at room temperature. Eventually the color of the whole solution turned black.

Then the temperature of the solution was raised to 140^oC over a period of 50 minutes and then to 210^oC over 40 min. Then the temperature was kept constant at 210^oC for 3 hours. Once the reaction was complete, 2mmol of oleic acid dissolved in DEG was put into the reaction vessel and allowed to mix well. Within a few minutes the black nanoparticles separated and settled at the bottom. The mixture was allowed to cool to room temperature and centrifuged. The particles were washed twice with 50:50 by volume of ethanol:ethyl acetate mixture. The black nanoparticles were washed in ethanol twice and separated magnetically. Then the particles were resuspended in 5 ml of ethanol.

Table 6.1. Different amounts of $FeCl_3.6H_2O$ and $InCl_3.4H_2O$ used for different reactions.

Experiment	mmol of $FeCl_2.4H_2O$	mmol of $FeCl_3.6H_2O$	mmol of $InCl_3.4H_2O$
2%	1.0	1.96	0.04
5 %	1.0	1.9	0.1
10%	1.0	1.8	0.2
15%	1.0	1.7	0.3
50%	1.0	1.0	1.0

6.5 Results and Discussions

6.5.1 TEM Images

The nanoparticles synthesized following the above procedure were characterized for their shape and size by transmission electron microscopy. The particles observed by TEM had similar appearances for all the procedures. These images are presented in Figures 6.1-6.5.

2% Indium magnetite

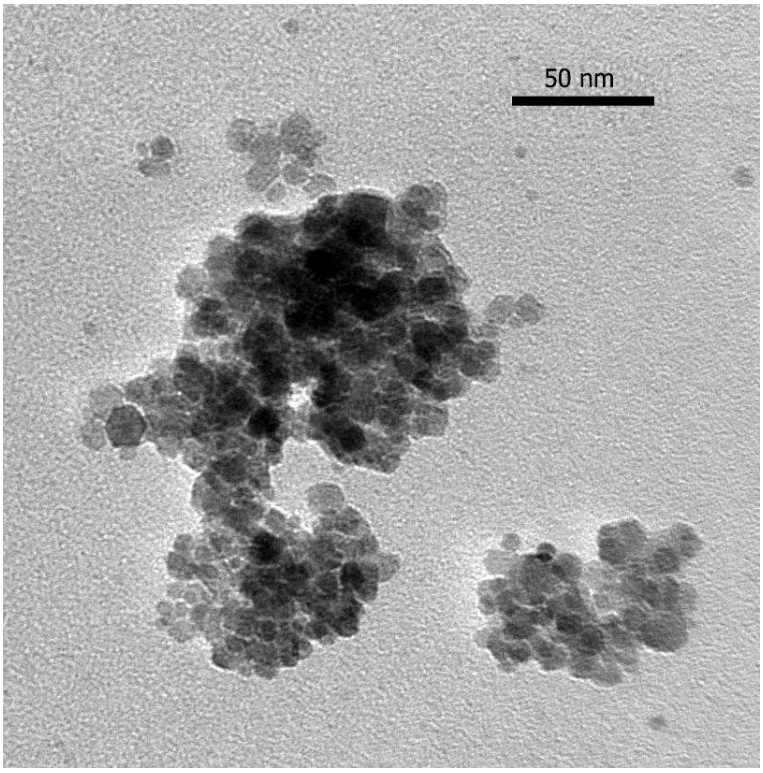

Figure 6.1. TEM image of 2% indium doped magnetite nanoparticles after magnetic separation and washing.

5% Indium Magnetite

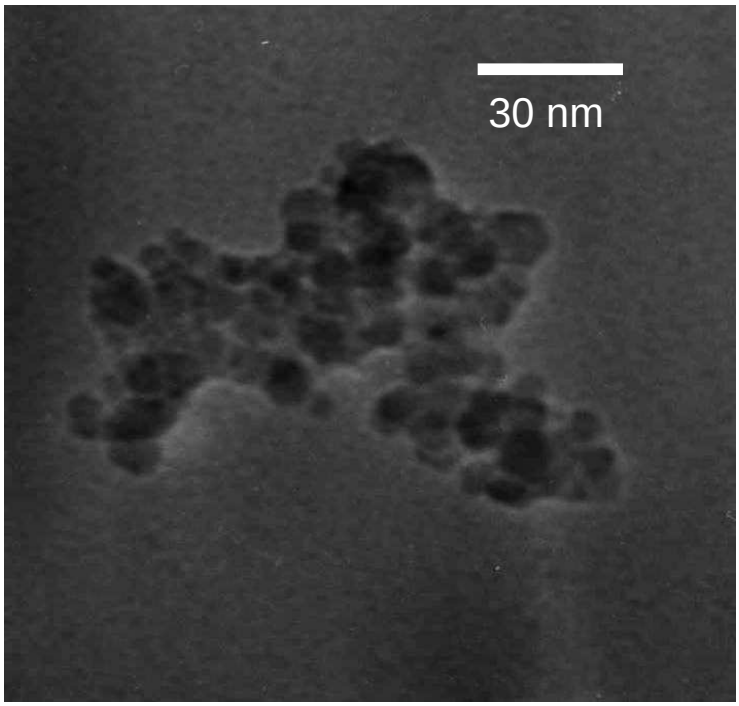

Figure 6.2. TEM image of 5% indium doped magnetite nanoparticles after magnetic separation and washing.

10% Indium Magnetite

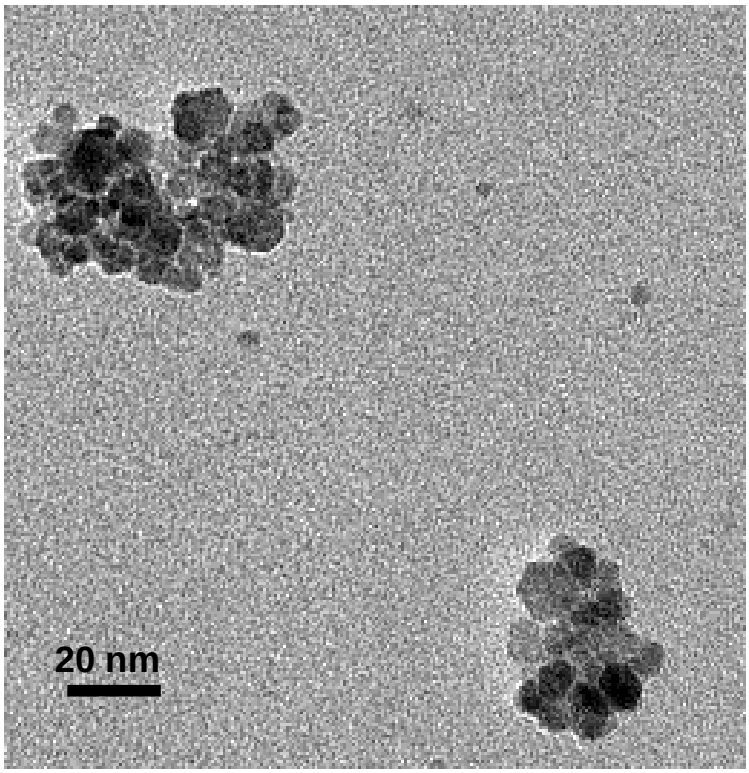

Figure 6.3. TEM image of 10% indium doped magnetite nanoparticles after magnetic separation and washing.

15% Indium Magnetite

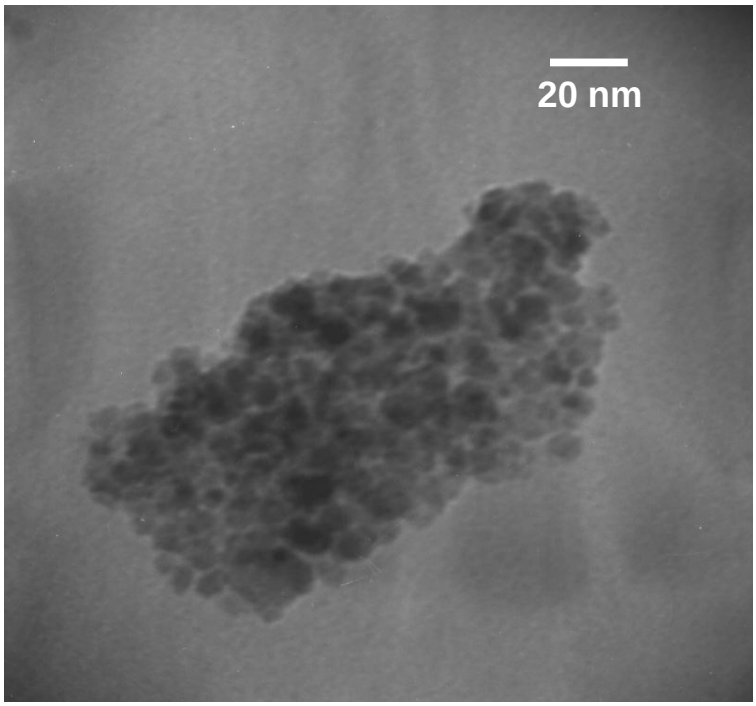

Figure 6.4. TEM image of 15% indium doped magnetite nanoparticles after magnetic separation and washing.

50% Indium Magnetite

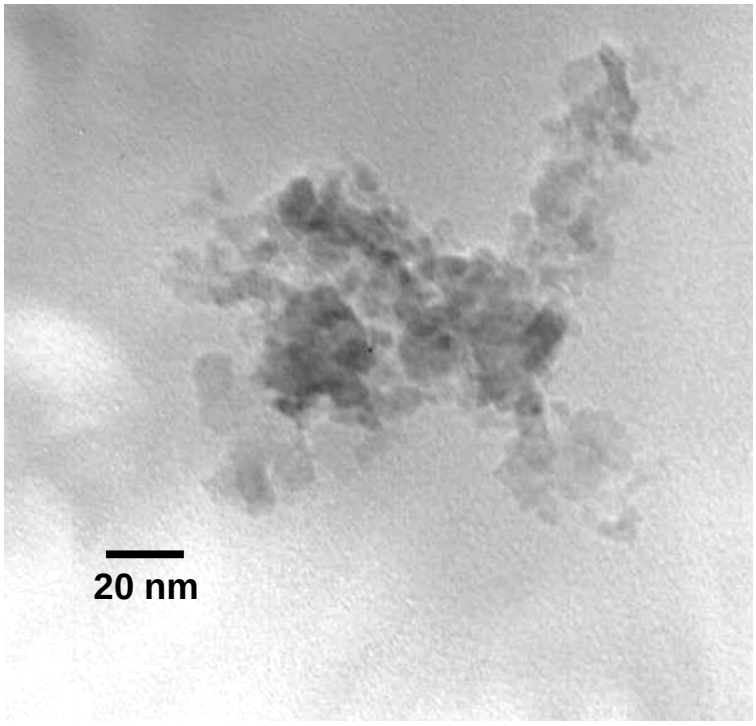

Figure 6.5. TEM image of 50% indium doped magnetite nanoparticles after magnetic separation and washing.

The TEM pictures show that the particles are agglomerated as no capping ligands were used in the final reaction step. But the particle shape and size was very much similar to one another. Even though the ICP and the EDS results confirmed that there was increase in indium loading from Figure 6.1 to Figure 6.5 but the shape of the particles remained the same. So by adjusting the amount of starting materials even though we could change the indium loading but we were able to produce particles of similar shapes.

6.5.2 EDS Data

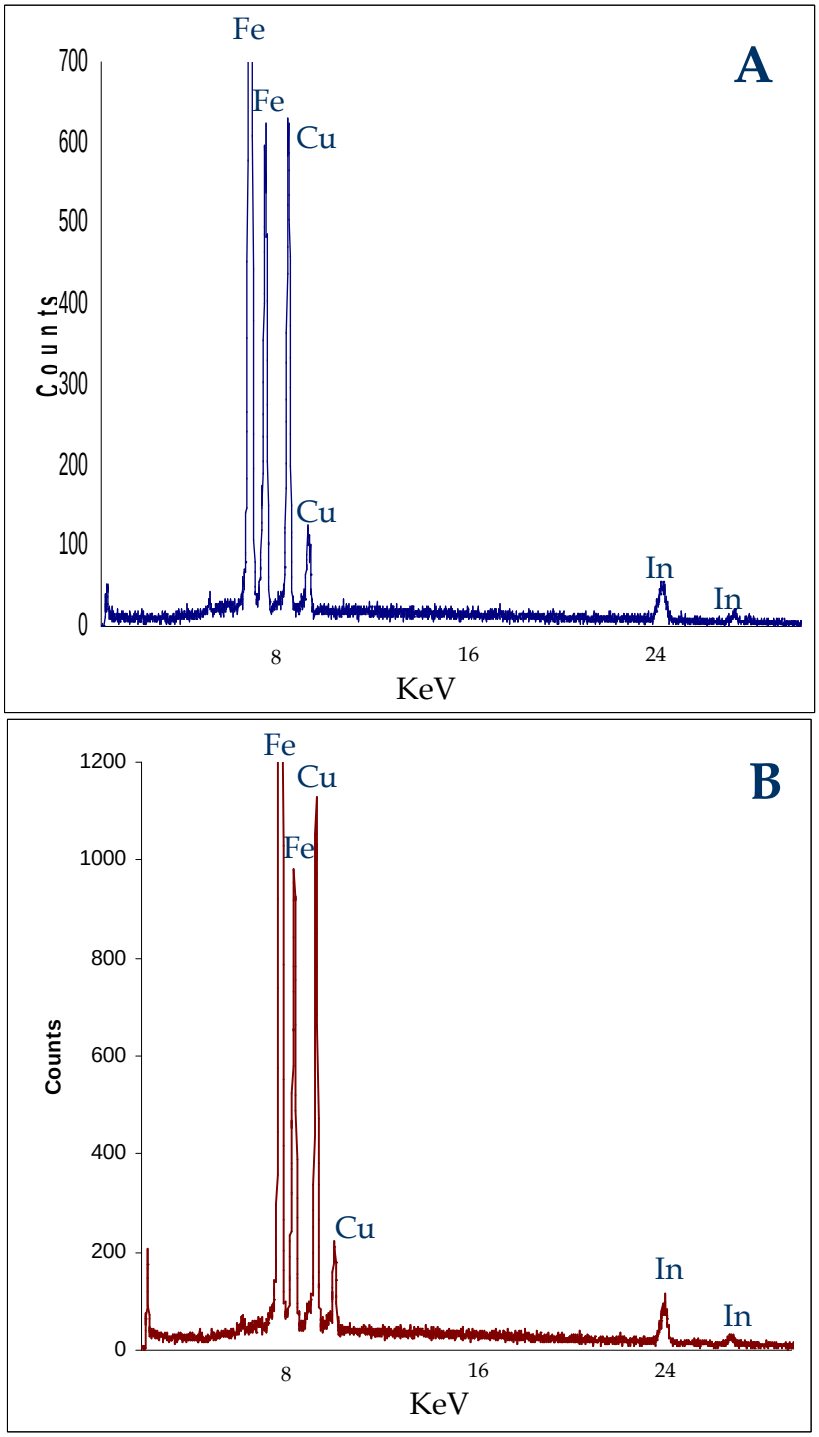

Figure 6.6. EDS pattern for water dispersible indium doped magnetite nanoparticles (5 mol % [A] and 15 mol % [B]).

The EDS spectrum for all the nanoparticles showed the presence of respective peaks of indium and iron confirming the incorporation of indium within the magnetic nanoparticles. The intensity of the indium peak for the 15% loading of the indium was higher than that of the 5% loading which verifies the presence of more indium in the first set of particles compared to the second one. From the EDS data (all not shown) it was seen that as we increased the amount of indium loading in the starting material the peak intensity of indium for the synthesized materials increased indicating the fact that more amount of indium was incorporated within the magnetite nanoparticles. For the 2% indium magnetite particles we were not able to see the respective peak of indium as it was below the detection limit. But its presence was confirmed from the ICP data.

6.5.3 Indium Loading in Particles

To 100 ml of the indium magnetite particles (~ 1 mg), 1 ml of aqua regia was added and the particles were allowed to dissolve for more than an hour. At first the solution was cloudy and then it became transparent yellow eventually after an hour. The volume of the solution was made upto 25 ml with nanopure water and then it was analyzed to find out the composition of the metal loading by inductively coupled plasma (ICP). The following observations were made.

Table 6.2. Indium loading of the magnetic nanoparticles

Indium loading in starting material (mass %)	**Observed indium loading in synthesized particles (mass %)**
2.7	2.4
6.8	3.9
13.7	8.2
22.9	14.7

With the increase in the $InCl_3.4H_2O$ for the respective reactions the amount of indium loading increased which suggests that the indium loading in the particles could be controlled. This result was also concluded by the EDS data which has been shown previously.

6.5.4 XRD Data

To characterize the morphology of the particles the X-ray diffraction data was obtained. The XRD data was analyzed with a Philips (Eindhoven, The Netherlands) X'pert-MPD x-ray powder diffraction system.

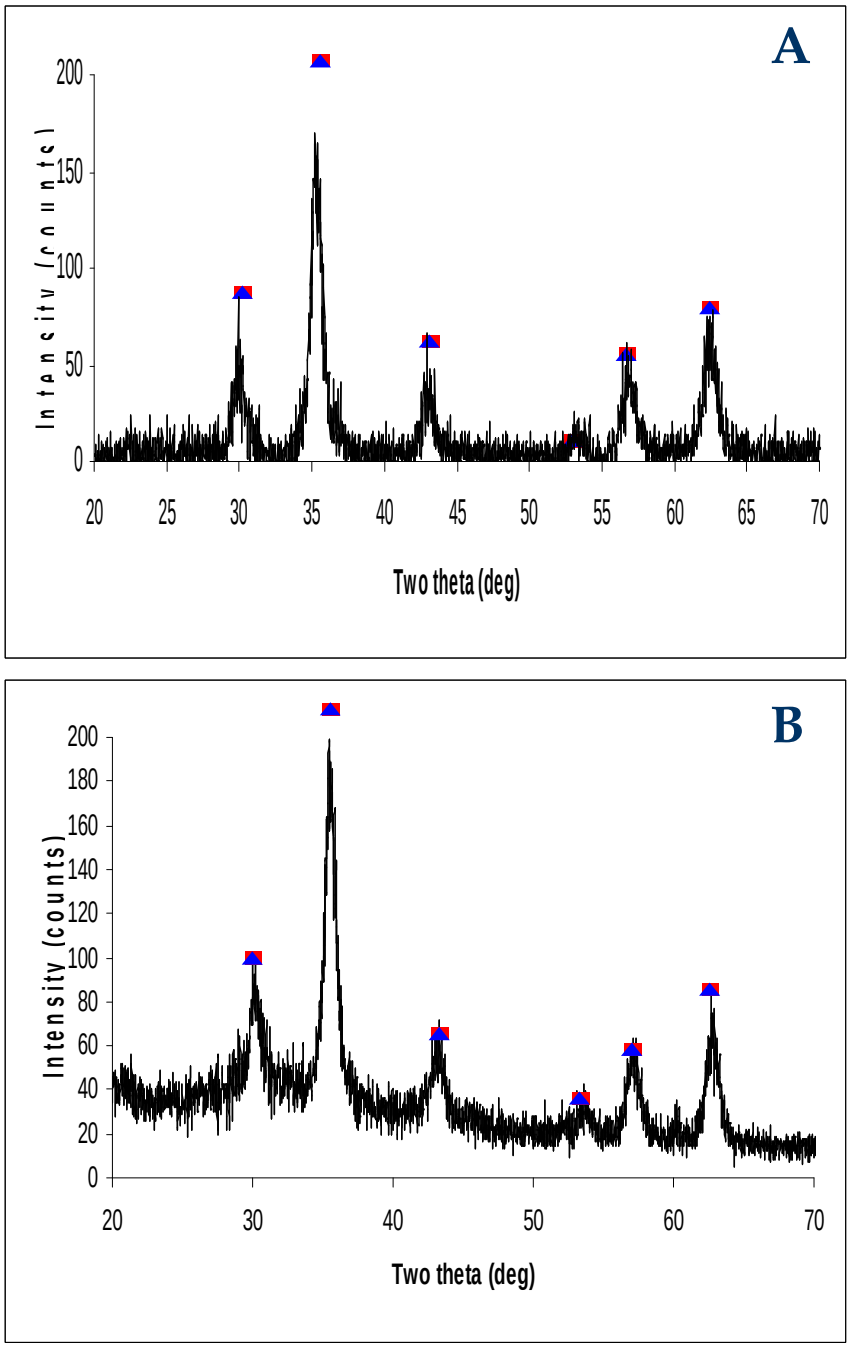

Figure 6.7. X-ray powder diffraction pattern for water dispersible indium doped (2 mol % [A] and 5 mol % [B]) magnetite nanoparticles (black line). Theoretical peak positions are shown for magnetite (■) and indium iron oxide (▲).

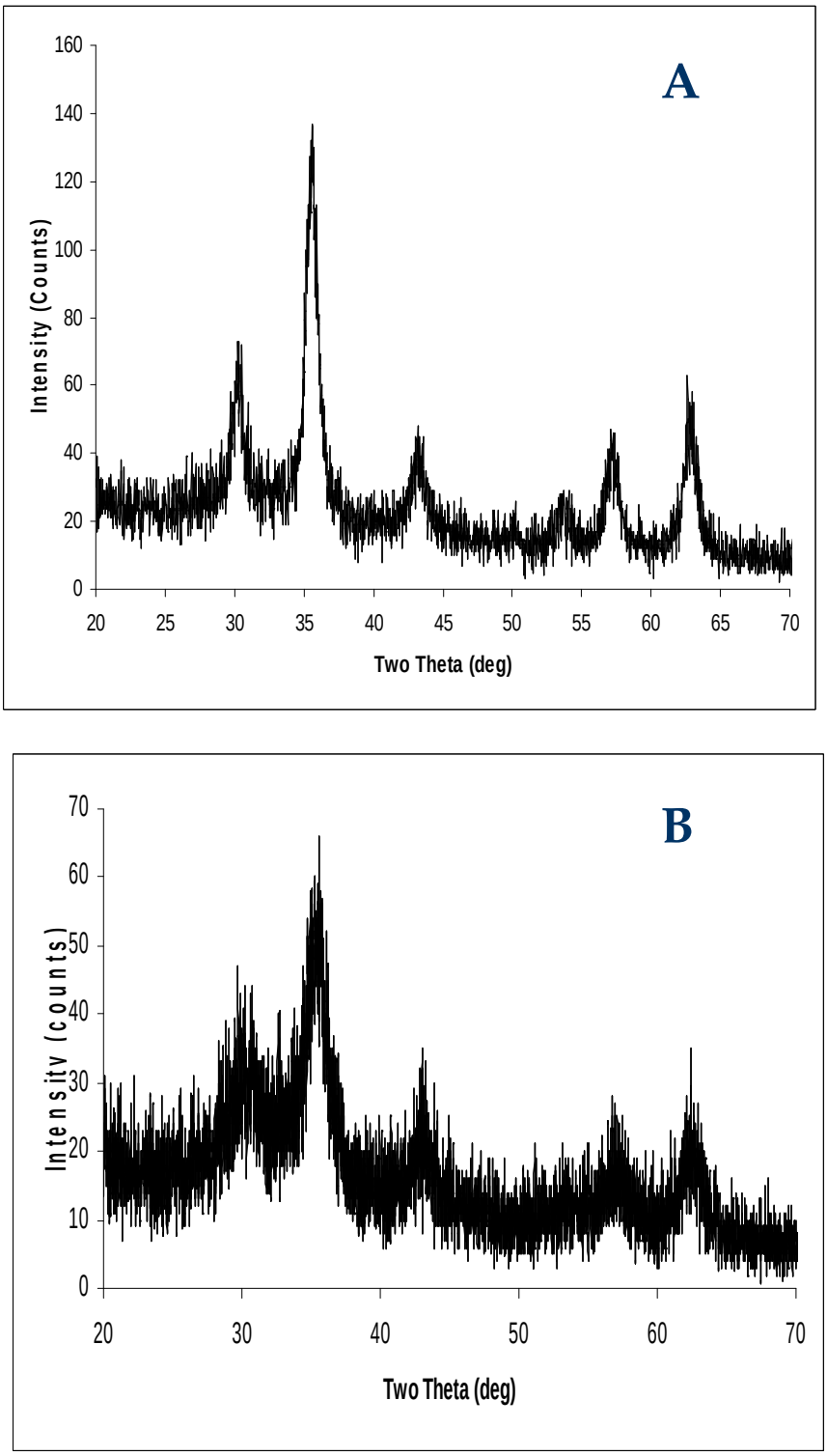

Figure 6.8. X-ray powder diffraction pattern for water dispersible indium doped (10 mol % [A] and 15 mol % [B]) magnetite nanoparticles.

In all the percentages of indium loading except that for 50% loading, the crystalline structure of the nanoparticles corresponded well with the pure magnetite nanoparticles structure. Only for the 50% indium loading in the magnetite particles there was a visible change in the XRD spectra. We saw new peaks emerging at different two theta values than the magnetite particles. The cell value (a) has been calculated for the 2% to 15% indium doped magnetite particles and they are very close to the calculated value of pure magnetite. Moreover from the XRD data it can also be concluded that the particles are crystalline in nature and they showed only the respective peaks for magnetite and no separate peak for indium.

6.5.5 Magnetic Measurements

6.5.5.1 Hysterisis Loop

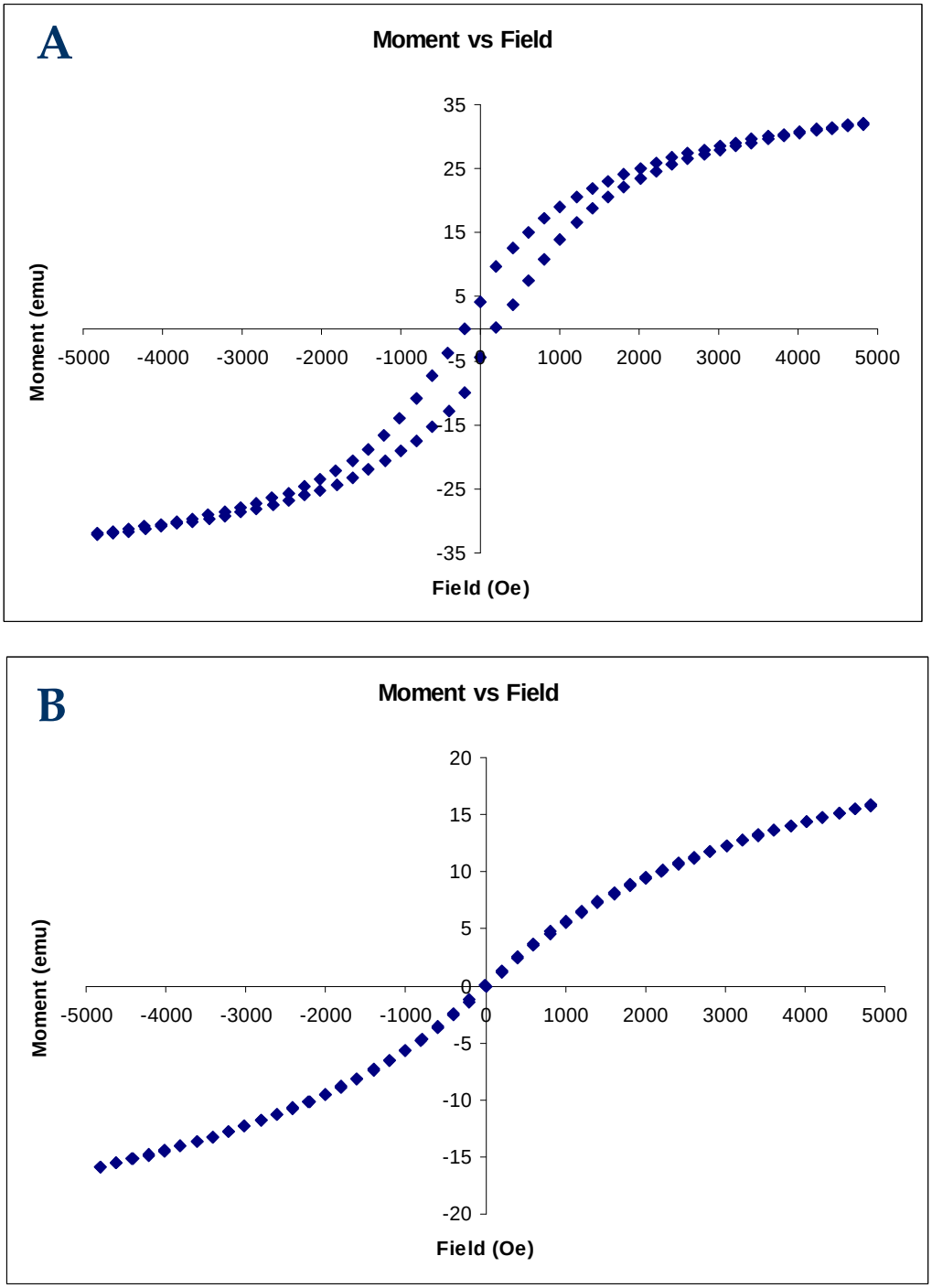

Figure 6.9. SQUID measurements for 5% Indium doped magnetite particles. Magnetic moment vs Field at 5 K (FIGURE A) and 300 K (FIGURE B).

10% Indium magnetite

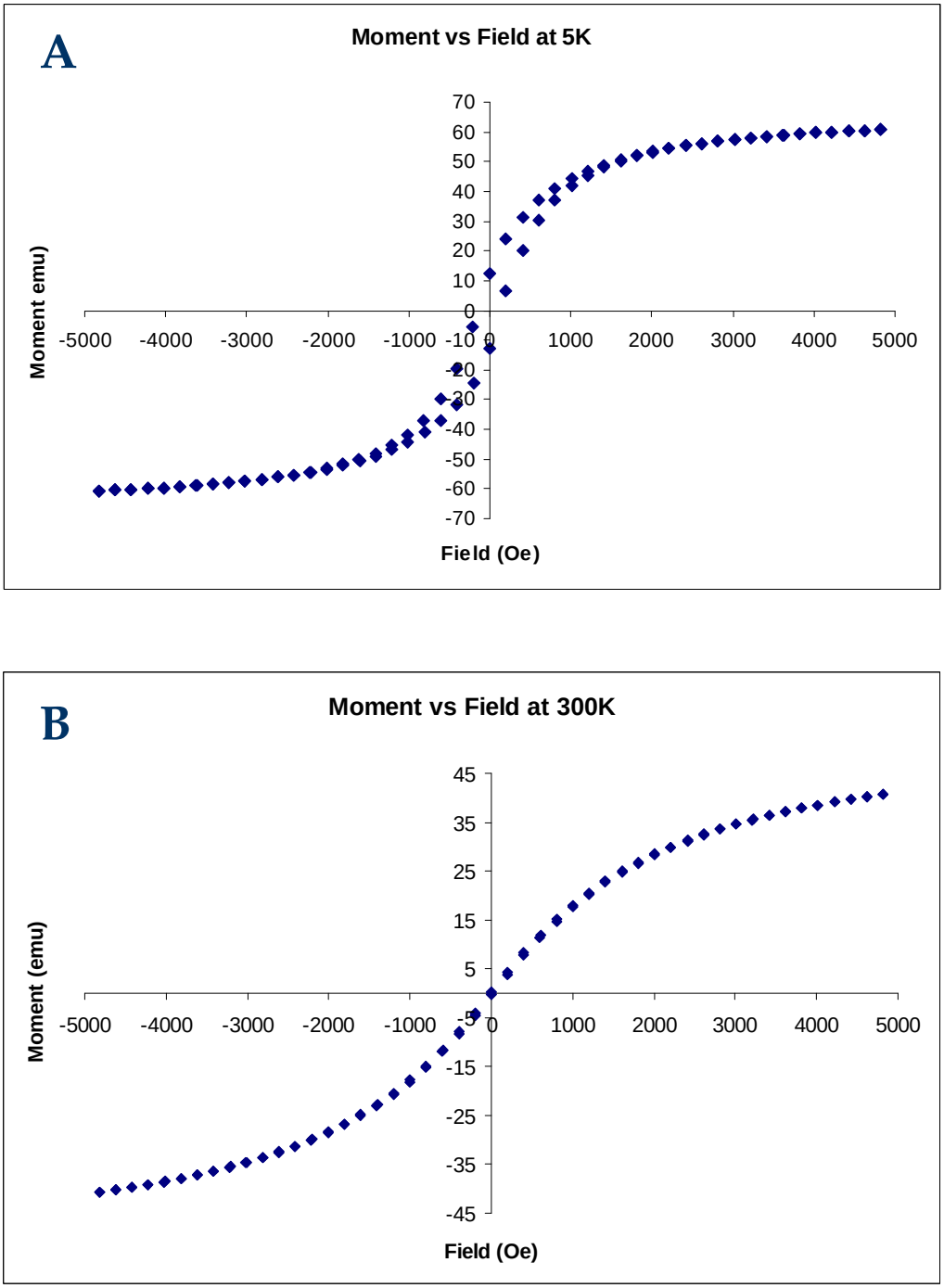

Figure 6.10. SQUID measurements for 10% Indium doped magnetite particles. Magnetic moment vs Field at 5 K (FIGURE A) and 300 K (FIGURE B).

15% Indium magnetite

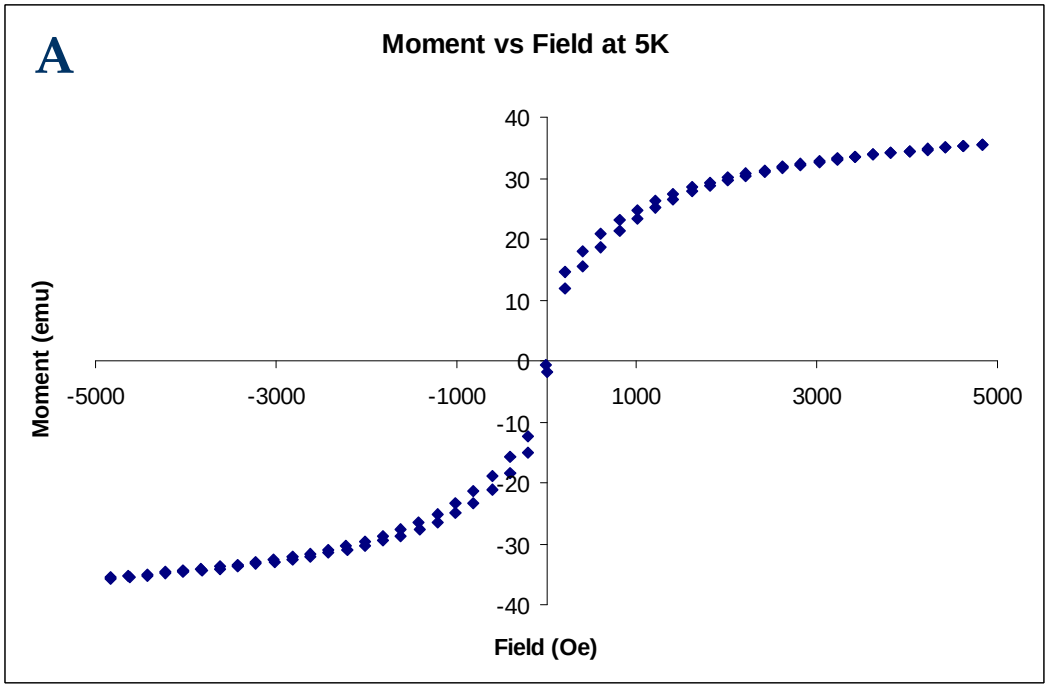

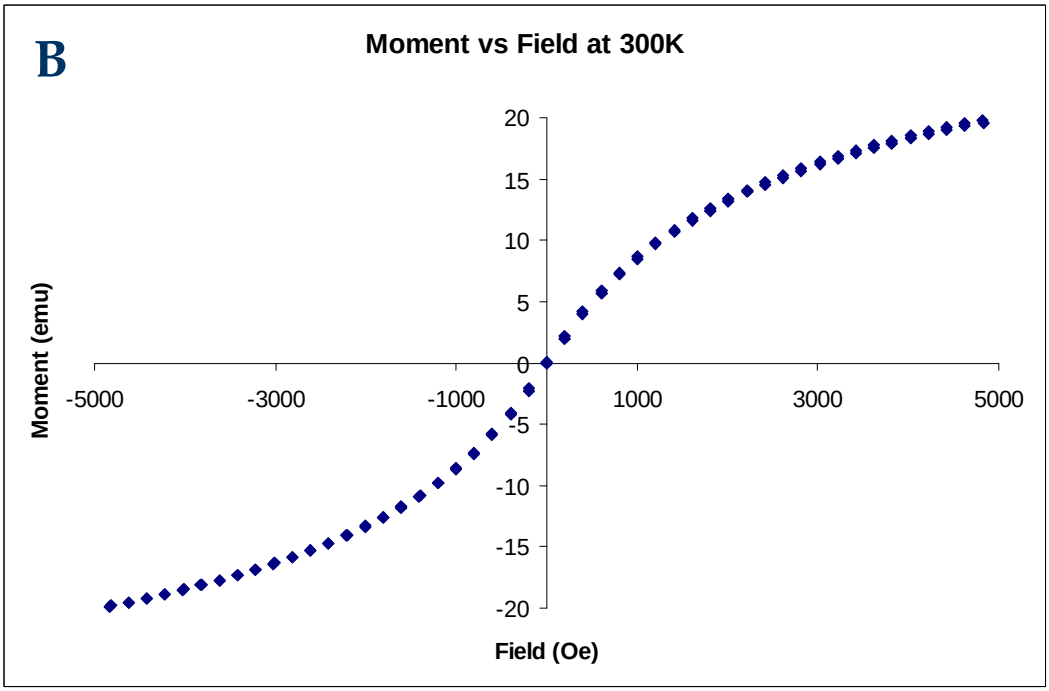

Figure 6.11. SQUID measurements for 15% Indium doped magnetite particles. Magnetic moment vs Field at 5 K (FIGURE A) and 300 K (FIGURE B).

The indium-magnetite nanocomposite material was characterized to determine its magnetic properties using a SQUID magnetometer. There were no substantial changes observed in the magnetic properties of these materials compared to the magnetite nanoparticles. Figures 6.9-6.11 shows the magnetization versus temperature plot or hysterisis plot of the indium-magnetite nanocomposites at 5K and 300K. The general shape of the graphs remained almost similar. The particles showed superparamagnetic behavior. At 5K they showed a hysterisis loop and the coercivity was found to change with the different loading of indium in magnetite. But at 300 K there was no coercivity observed in case of all the different sets of indium magnetite nanocomposite materials. The coercivity change of the different sets of particles are shown in the table below.

Table 6.3. Coercivity change for 5%, 10% and 15% Indium magnetite particles

Particles	Coercivity (Oe)
5% Indium magnetite	200
10% Indium magnetite	140
15% Indium magnetite	20

6.5.5.2 ZFC-FC Graph

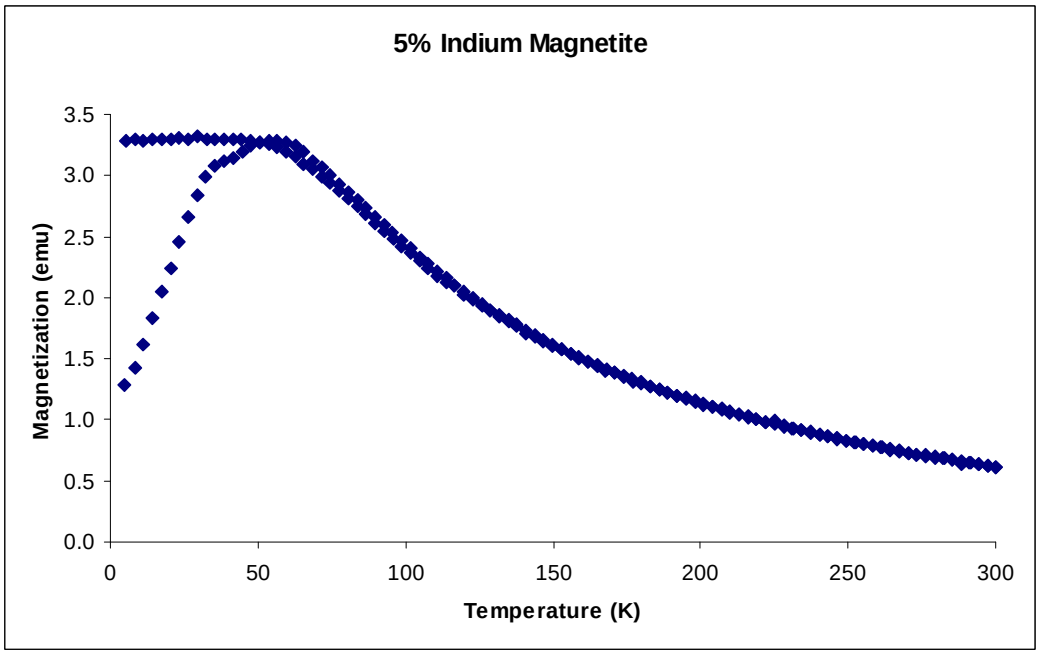

Figure 6.12. Zero Field Cooled – Field Cooled graph for 5% Indium doped magnetite particles

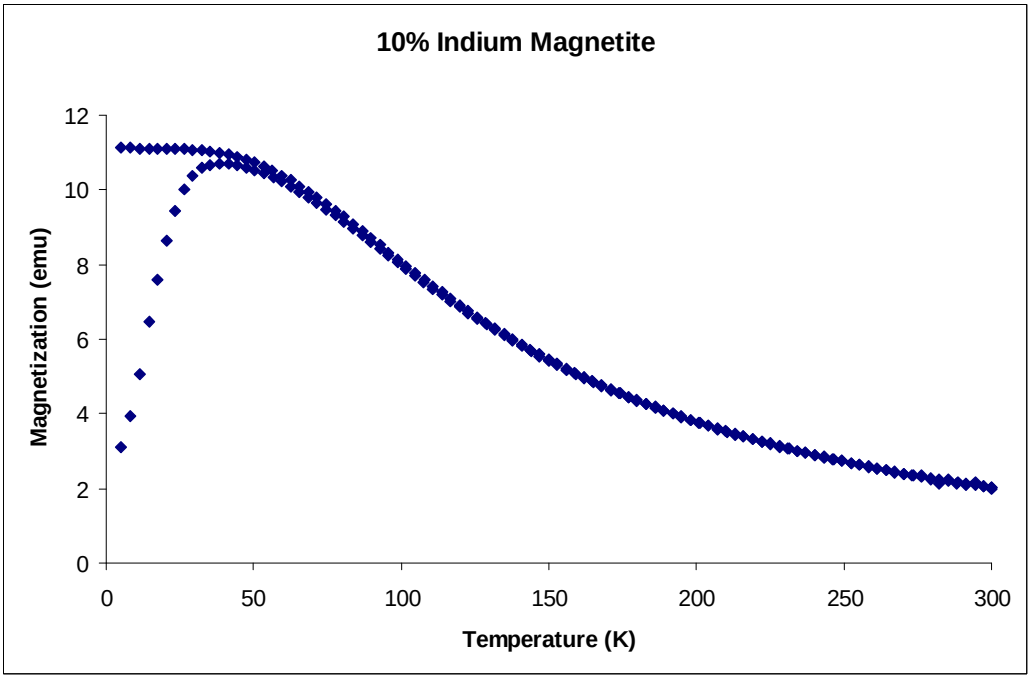

Figure 6.13. Zero Field Cooled – Field Cooled graph for 10% Indium doped magnetite particles

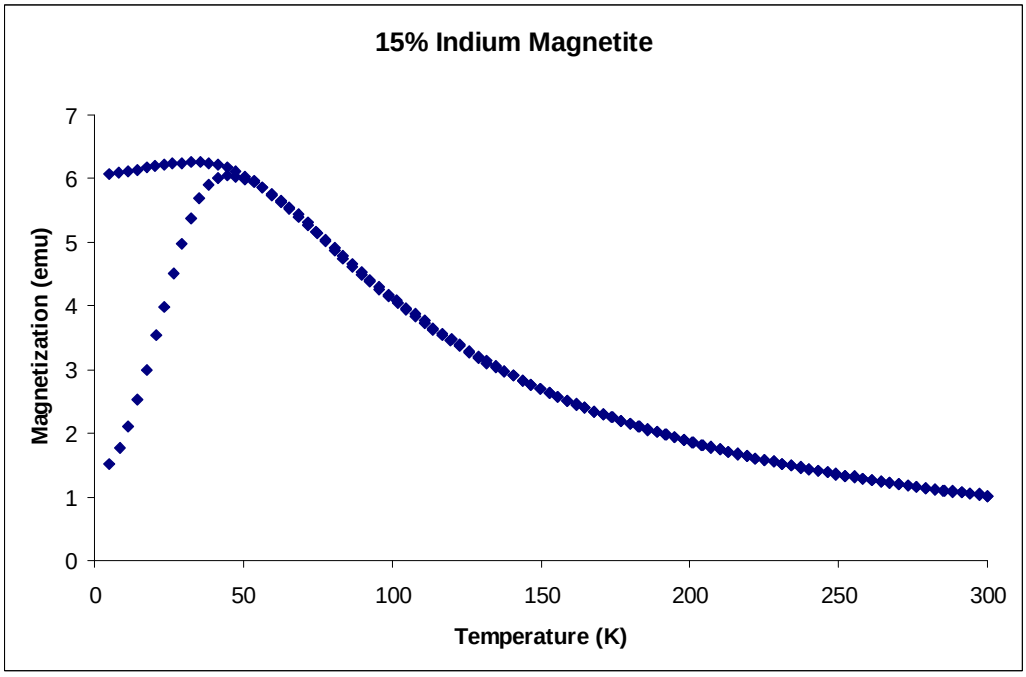

Figure 6.14. Zero Field Cooled – Field Cooled graph for 15% Indium doped magnetite particles

It has been seen from previous researches that as the particle size decreases below 100 nm there is significant change in the magnetic properties as compared to the bulk material. As the particle size reduces, the bulk magnetic domain is replaced by single domain structure which is characteristic of individual particles and this gives rise to a new event like superparamagnetism. The magnetic susceptibility of these particles is generally between that of ferromagnetic and paramagnetic materials. For these nanoparticles, the magnetization is oriented in the direction of easy axes which minimizes the energy of the particles at low temperatures. So in Figures 6.12 – 6.14 we see that for the zero field cooled (ZFC) curve at low temperatures the magnetization of the particles are very low. Since the easy axes are oriented randomly the magnetization tends to be near zero value. But as the temperature is increased from 5 K to 300K, at round 156K the thermal energy overcomes the anisotropy energy and the magnetization of the

particles begin to fluctuate between the two easy axes. This particular temperature is known as blocking temperature (T_B) or Curie temperature. After this point the particles tend to behave as a classical magnet. So in other words the maximum in the ZFC curve is the representation of blocking temperature.

The gap between the filed cooled (FC) and the ZFC curves can be implied as a fact that the nanocomposites are agglomerated with each other and that they are not evenly dispersed. In the FC curve, as the temperature is decreased from 300K to 5k we find that the magnetization increases and then levels off. This shape is the contribution of the dipole dipole interaction of the nanocomposite material. The dissimilarity between the ZFC and the FC curve is a common indication that the particles behave superparamagnetically between these temperatures.

6.6 Conclusion

From the above studies it can be concluded that indium was incorporated into the particles. The magnetic separation provides the proof that for all the loadings of the indium the nanoparticles still remain magnetic in nature. Also one can readily control the loading of indium in the particles by varying the amount of indium chloride during the starting of the reaction. Because of the moderately short half life of ^{111}In, its commercial availability, its easily achievable radiation protocol, and its ability to be incorporated into magnetite, this isotope makes an excellent starting point for radiotracer studies with magnetic nanoparticles. Once preliminary expectations are proven, a multitude of future radiotracer studies with ^{111}In and longer lived species will follow in both the biomedical field and the environmental field.

Completion of this study will lead to additional studies for development of treatment technologies. Radiolabeled nanoparticles that bind to disease cells can be used to selectively kill the disease cells via gamma irradiation. Results of this study will be directly applicable to future studies on design of particles that can bind to diseased tissue and rapidly clear other tissues. Such particles will selectively expose the diseased tissue to lethal doses of gamma irradiation while not harming healthy tissue.

6.7 Reference

1. Traykova, T.; Aparicio, C.; Ginebra, M. P.; Planell, J. A. Bioceramics as nanomaterials. *Nanomed.* **2006**, *1*, 91-106.
2. Emerich, D. F.; Thanos, C. G. The pinpoint promise of nanoparticle-based drug delivery and molecular diagnosis. *Biomol. Eng.* **2006**, *23*, 171-184.
3. Nijhara, R.; Balakrishnan, K. Bringing nanomedicines to market: regulatory challenges, opportunities, and uncertainties. *Nanomed.* **2006**, *2*, 127-136.
4. Garnett, M. Nanomedicines: delivering drugs using bottom up nanotechnology. *Int. J. Nanoscience* **2005**, *4*, 855-861.
5. Pison, U.; Welte, T.; Giersig, M.; Groneberg, D. A. Nanomedicine for respiratory diseases. *Eur. J. Pharmacol.* **2006**, *533*, 341-350.
6. Kawasaki, E. S.; Player, A. Nanotechnology, nanomedicine, and the development of new, effective therapies for cancer. *Nanomed.* **2005**, *1*, 101-109.
7. Lin, A. W. H.; Lewinski, N. A.; West, J. L.; Halas, N. J.; Drezek, R. A. Optically tunable nanoparticle contrast agents for early cancer detection: model-based analysis of gold nanoshells. *J. Biomed. Opt.* **2005**, *10*, 064035/1-064035/10.
8. Hirsch, L. R.; Halas, N. J.; West, J. L. Whole-blood immunoassay facilitated by gold nanoshell-conjugate antibodies. *Methods Mol. Biol.* **2005**, *303*(NanoBiotechnology Protocols), 101-111.
9. O'Neal, D. P.; Hirsch, L. R.; Halas, N. J.; Payne, J. D.; West, J. L. Photothermal cancer therapy using intravenously injected near-infrared-absorbing nanoparticles. *Proc. SPIE* **2005**, *5689*(Optical Methods for Tumor Treatment and Detection: Mechanisms and Techniques in Photodynamic Therapy XIV), 149-157.

10. O'Neal, D. P.; Hirsch, L. R.; Halas, N. J.; Payne, J. D.; West, J. L. Photo-thermal tumor ablation in mice using near infrared-absorbing nanoparticles. *Cancer Lett.* **2004**, *209*, 171-176.
11. Loo, C.; Lowery, A.; Halas, N.; West, J.; Drezek, R. Immunotargeted Nanoshells for Integrated Cancer Imaging and Therapy. *Nano Lett.* **2005**, *5*, 709-711.
12. El-Sayed, I. H.; Huang, X.; El-Sayed, M. A. *Nano Lett.* **2005,** *5*, 829-834.
13. Sokolov, K.; Follen, Mi.; Aaron, J.; Pavlova, I.; Malpica, A.; Lotan, R.; Richards-Kortum, R. *Cancer Res.* **2004,** *63*, 1999-2004.
14. Arbab, A. S.; Liu, W.; Frank, J. A. Cellular magnetic resonance imaging: current status and future prospects. *Expert Rev. Med. Devices* **2006**, *3*, 427-439.
15. Sun, C.; Sze, R.; Zhang, M. Folic acid-PEG conjugated superparamagnetic nanoparticles for targeted cellular uptake and detection by MRI. *J. Biomed. Mat. Res., Part A* **2006**, *78A*, 550-557.
16. Frias, J. C.; Ma, Y.; Williams, K. J.; Fayad, Z. A.; Fisher, E. A. Properties of a Versatile Nanoparticle Platform Contrast Agent To Image and Characterize Atherosclerotic Plaques by Magnetic Resonance Imaging. *Nano Lett.* **2006**, *6*, 1752-1756.
17. Niidome, T.; Yamagata, M.; Okamoto, Y.; Akiyama, Y.; Takahashi, H.; Kawano, T.; Katayama, Y.; Niidome, Y. PEG-modified gold nanorods with a stealth character for in vivo applications. *J. Controlled Release* **2006**, *114*, 343-347.
18. Astete, C. E.; Sabliov, C. M. Synthesis of poly(DL-lactide-Co-glycolide) nanoparticles with entrapped magnetite by emulsion evaporation method. *Particulate Sci. Technol.* **2006**, *24*, 321-328.

19. Bertram, J. MATra - magnet assisted transfection: combining nanotechnology and magnetic forces to improve intracellular delivery of nucleic acids. *Curr. Pharm. Biotechnol.* **2006**, *7*, 277-285.
20. Wu, W.; DeCoster, M. A.; Daniel, B. M.; Chen, J. F.; Yu, M. H.; Cruntu, D.; O'Connor, C. J.; Zhou, W. L. One-step synthesis of magnetic hollow silica and their application for nanomedicine. *J. Appl. Phys.* **2006**, *99*, 08H104/1-08H104/3.
21. Zhou, W.; Gao, P.; Shao, L.; Caruntu, D.; Yu, M.; Chen, J.; O'Connor, C. J. Drug-loaded, magnetic, hollow silica nanocomposites for nanomedicine. *Nanomed.* **2005**, *1*, 233-237.
22. Oberdoerster, G. Effects and fate of inhaled ultrafine particles. *ACS Symposium Series* **2005**, *890*(Nanotechnology and the Environment), 37-59.
23. Hahn, F. F.; Barr, E. B.; Menache, M. G.; Seagrave, J-C.; Particle size and composition related to adverse health effects in aged, sensitive rats. *Research Report - Health Effects Institute* **2005**, *129*, i-iv, 1-73.
24. Schulz, H.; Harder, V.; Ibald-Mulli, A.; Khandoga, A.; Koenig, W.; Krombach, F.; Radykewicz, R.; Stampfl, A.; Thorand, B.; Peters, A. Cardiovascular Effects of Fine and Ultrafine Particles. *J. Aerosol Med.* **2005**, *18*, 1-22.
25. Donaldson, K.; Brown, D.; Clouter, A.; Duffin, R.; MacNee, W.; Renwick, L.; Tran, L.; Stone, V. The pulmonary toxicology of ultrafine particles. *J. Aerosol Med.* **2002**, *15*, 13-220.
26. Lam, C-W.; James, J. T.; McCluskey, R.; Arepalli, S.; Hunter, R. L. A Review of Carbon Nanotube Toxicity and Assessment of Potential Occupational and Environmental Health Risks. *Crit. Rev. Toxicol.* **2006**, *36*, 189-217.

27. Garibaldi, S.; Brunelli, C.; Bavastrello, V.; Ghigliotti, G.; Nicolini, C. Carbon nanotube biocompatibility with cardiac muscle cells. *Nanotechnol.* **2006**, *17*, 391-397.

28. Oberdorster, G. ; Oberdorster, E. ; Oberdorster, J. Nanotoxicology: an emerging discipline evolving from studies of ultrafine particles. *Environ. Health Perspec.* **2005**, *113*, 823-839.

29. Rushton, E. K.; Oberdorster, G.; Finkelstein, J. N. Toxicological profiles of nanomaterials. *Mat. Res. Soc. Symp. Proc.* **2006**, *895*(Life-Cycle Analysis Tools for "Green" Materials and Process Selection), 167-171.

30. Sadeghiani, N.; Barbosa, L. S.; Guedes, M. H. A.; Chaves, S. B.; Santos, J. G.; Silva, O.; Pelegrini, F.; Azevedo, R. B.; Morais, P. C.; Lacava, Z. G. M. Magnetic resonance of polyaspartic acid-coated magnetite nanoparticles administered in mice. *IEEE Trans. Magn.* **2005**, *41*, 4108-4110.

31. Kim, D-H.; Lee, S-H.; Im, K-H.; Kim, K-N.; Kim, K-M.; Kim, K-D.; Park, H.; Shim, I-B.; Lee, Y-K. Biodistribution of chitosan-based magnetite suspensions for targeted hyperthermia in ICR mice. *IEEE Trans. Magn.* **2005**, *41*, 4158-4160.

32. Chaves, S. B.; Lacava, L. M.; Lacava, Z. G. M.; Silva, O.; Pelegrini, F.; Buske, N.; Gansau, C.; Morais, P. C.; Azevedo, R. B. Light microscopy and magnetic resonance characterization of a DMSA-coated magnetic fluid in mice. *IEEE Trans. Magn.* **2002**, *38*, 3231-3233.

33. Hasegawa, M.; Hanaichi, T.; Shoji, H.; Kawaguchi, T.; Maruno, S. Biological behavior of dextran-iron oxide magnetic fluid injected intravenously in rats. *Jap. J. Appl. Phys.*, Part 1 **1998**, *37*, 1029-1032.

34. Service, R. F. Nanotechnology grows up. *Science* **2004**, *304*, 1732-1734.

35. Okudera, H.; Toyara, H. Crystal structure refinements of $In_xFe_{3-x}O_4$ ($x \leq 0.3$) spinels by the Rietveld method. *Zeitschrift fuer Kristallographie* **1998**, *213*, 461-465.

36. Gerardin, R.; Alebouyeh, A.; Brice, J. F.; Evrard, O.; Sanchez, J. P. Cation distribution in indium ferrites of spinel type $InMFeO_4$ (M = nickel, manganese, cobalt, magnesium). *J. Solid State Chem.* **1988**, *76*, 398-406.

37. Caruntu, D.; Remond, Y.; Chou, N. H.; Jun, M-J.; Caruntu, G.; He, J.; Goloverda, G.; O'Connor, C.; Kolesnichenko, V. Reactivity of 3d Tranisition Metal Cation in Diethylene Glycol Solutions. Synthesis of Tranisition Metal Ferrites with the Structure of Discrete Nanoparticles Complexed with Long-Chain Carboxylate Anions. *Inorg. Chem.* **2002**, *41*, 6137-6146.

38. D. Caruntu, G. Caruntu, Y. Chen, C. J. O'Connor, G. Goloverda, and V. L. Kolesnichenko: Synthesis of Variable-Sized Nanocrystals of Fe_3O_4 with High Surface Reactivity. *Chem. Mater.* **2004**, *16*, 5527-5534.

39. Oliva, B. L.; Pradhan, A.; Caruntu, D.; O'Connor, C. J.; Tarr, M. A. Formation of Gold Coated Magnetic Nanoparticles Using TiO_2 as a Bridging Material. *J. Mat. Res.* **2006**, *21*, 1312-1316.

40. Lu, Yan-Wu; Zhu, Qin-Sheng; Liu, Fang-Xin. Magnetic properties of tin-doped magnetite nanoparticles. *Phys. Lett. A* **2006**, *359*, 66-69.

VITA

Anindya Pradhan was born in Calcutta, India on September 28, 1976. He did his schooling from South Point High School and then went on to join Ramakrishna Mission School for his Class XI and XII. He continued his studies at Ramakrishna Mission Residential College (Calcutta University) working on his Bachelor of Science degree, majoring in Chemistry. After that he pursued a Master of Business Administration in Systems from Institute of Modern Management, Calcutta under Viswabharati University. He completed his MBA degree in 2001. In Fall 2002, he started his Ph.D. degree at University of New Orleans and joined Dr. Matthew A. Tarr's group to follow his interest in analytical chemistry. He received a M.S. degree in Chemistry from University of New Orleans in 2006.